AUTOCRINE AND PARACRINE EFFECTS OF BRAF INHIBITOR INDUCED SENESCENCE IN MELANOMA
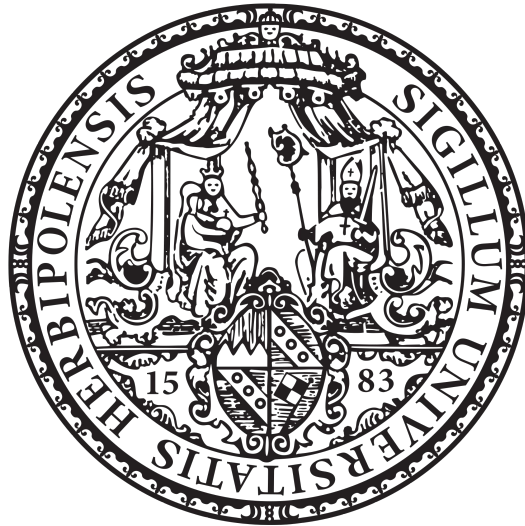
DISSERTATION ZUR ERLANGUNG DES

NATURWISSENSCHAFTLICHEN DOKTORGRADES

DER JULIUS-MAXIMILIANS-UNIVERSITÄT WÜRZBURG

VORGELEGT VON

JOHANNES GRIMM

GEBOREN IN BAD NEUSTADT AN DER SAALE

WÜRZBURG 2019

EINGEREICHT AM: _____

MITGLIEDER DER PROMOTIONSKOMMISSION:

VORSITZENDER: _____

1. GUTACHTER: Prof. Dr. rer. nat. S. Meierjohann

2. GUTACHTER: Prof. Dr. rer. nat. M. Alsheimer

TAG DES PROMOTIONSKOLLOQUIUMS: _____

DOKTORURKUNDE AUSGEHÄNDIGT AM: _____

Content

1. Summary

The FDA approval of targeted therapy with BRAFV600E inhibitors like vemurafenib and dabrafenib in 2011 has been the first major breakthrough in the treatment of metastatic melanoma since almost three decades. Despite increased progression free survival and elevated overall survival rates, complete responses are scarce due to resistance development approximately six months after the initial drug treatment. It was previously shown in our group that melanoma cells under vemurafenib pressure *in vitro* and *in vivo* exhibit features of drug-induced senescence. It is known that some cell types, which undergo this cell cycle arrest, develop a so-called senescence associated secretome and it has been reported that melanoma cell lines also upregulate the expression of different factors after senescence induction. This work describes the effect of the vemurafenib-induced secretome on cells. Conditioned supernatants of vemurafenib-treated cells increased the viability of naive fibroblast and melanoma cell lines. RNA analysis of donor melanoma cells revealed elevated transcriptional levels of *FGF1*, *MMP2* and *CCL2* in the majority of tested cell lines under vemurafenib pressure, and I could confirm the secretion of functional proteins. Similar observations were also done after MEK inhibition as well as in a combined BRAF and MEK inhibitor treatment situation. Interestingly, the transcription of other FGF ligands (FGF7, FGF17) was also elevated after MEK/ERK1/2 inhibition. As FGF receptors are therapeutically relevant, I focused on the analysis of FGFR-dependent processes in response to BRAF inhibition. Recombinant FGF1 increased the survival rate of melanoma cells under vemurafenib pressure, while inhibition of the FGFR pathway diminished the viability of melanoma cells in combination with vemurafenib and blocked the stimulatory effect of vemurafenib conditioned medium. The BRAF inhibitor induced secretome is regulated by active PI3K/AKT signaling, and the joint inhibition of mTor and BRAFV600E led to decreased senescence induction and to a diminished induction of the secretome-associated genes. In parallel, combined inhibition of MEK and PI3K also drastically decreased mRNA levels of the relevant secretome components back to basal levels.

In summary, I could demonstrate that BRAF inhibitor treated melanoma cell lines acquire a specific PI3K/AKT dependent secretome, which is characterized by FGF1, CCL2 and MMP2. This secretome is able to stimulate other cells such as naive melanoma cells and fibroblasts and contributes to a better survival under drug pressure. These data are therapeutically highly relevant, as they imply the usage of novel drug combinations, especially specific FGFR inhibitors, with BRAF inhibitors in the clinic.

2. Zusammenfassung

Die Zulassung der spezifischen BRAFV600E Inhibitoren Vemurafenib und Dabrafenib im Jahr 2011 war der erste wirksame Schritt nach Jahrzehnten der Stagnation in der Behandlung des metastasierenden Melanoms. Allerdings zeigte sich, dass trotz erhöhter Gesamtüberlebensrate und gestiegenem progressionsfreien Überleben komplette Remissionen selten waren. Wir konnten in vorangegangenen Versuchen zeigen, dass eine Behandlung BRAFV600E-mutierter Melanom Zelllinien mit Vemurafenib mit der Induktion von Seneszenz-assoziierten Merkmalen einhergeht. Da bekannt ist, dass seneszente Zellen, darunter auch Melanom Zellen, ein sogenanntes Sekretom ausbilden können, welches andere Zellen beeinflussen kann, war die Identifizierung und Charakterisierung von Vemurafenib-induzierten sezernierten Faktoren das Ziel meiner Arbeit. Initiale Versuche zeigten, dass konditionierter Überstand von Vemurafenib behandelten Zellen das Wachstum naiver Zelllinien erhöhen kann. Ich konnte in weiteren Versuchen zeigen, dass sich die Transkription und Expression des Cytokins *CCL2*, der Matrixmetalloprotease *MMP2* und des Wachstumsfaktors *FGF1* nach Vemurafenib Behandlung erhöht. Darüber hinaus konnte ich interessanterweise auch eine gesteigerte Transkription anderer FGF Liganden (FGF7, FGF17) feststellen, was meinen Fokus auf die Analyse von FGFR abhängigen Prozessen als Antwort auf die BRAF Inhibition gelenkt hat. Es zeigte sich, dass sich Melanomzellen mittels Zugabe von FGF1 besser gegen die Vemurafenib-induzierte MEK/ERK1/2 Hemmung behaupten können. Darüber hinaus konnte durch den Einsatz eines spezifischen FGFR Inhibitors die Viabilität von Melanomzellen unter Vemurafenib Behandlung vermindert werden. Auch der stimulierende Effekt des Vemurafenib konditionierten Überstandes konnte dadurch teilweise aufgehoben werden. Die Induktion des BRAF Inhibitor assoziierten Sekretoms ist auf einen aktiven PI3K/AKT Signalweg angewiesen. So führt eine gleichzeitige Hemmung des MEK/ERK1/2 und PI3K/AKT Signalwegs zu einer verminderten Seneszenzinduktion und einer niedrigeren Transkription der Seneszenz-assoziierten Gene. Zudem konnte ich feststellen, dass auch eine gemeinsame Hemmung von BRAF und MEK Seneszenz und das damit einhergehende Sekretom unter Beteiligung von CCL2, MMP2 und den FGFs induziert.

Zusammenfassend zeigen meine Daten, dass BRAFV600E-mutierte Melanomzellen nach Vemurafenib Behandlung ein Sekretom ausbilden, welches potentiell wachstumsfördernde und matrix-modellierende Faktoren beinhaltet. Dies ist abhängig vom PI3K/AKT Signalweg und charakterisiert durch die Sekretion von FGF1, CCL2 und MMP2. Klinische Relevanz erlangen diese Erkenntnisse durch die Möglichkeit, diese Faktoren im Rahmen einer Kombinationstherapie, z.B. mit einem spezifischen FGFR Inhibitor, zu inaktivieren.

3. Introduction

3.1. Malignant Melanoma

Melanoma is a highly aggressive type of cancer, which arises from transformed melanocytes, e.g. from the skin, the uvea and mucosal tissues. With 91,2%, cutaneous melanoma is the most common form of melanoma, while acral melanoma (2,3%), mucosal melanoma (1,3%) and ocular/uveal melanomas (5,2%) are less prevalent (Vultur and Herlyn, 2013). Melanoma is among the least common skin cancer types, but it is the cause of most skin cancer related deaths (75%) (Schadendorf and Hauschild, 2014). Its incidence rate has risen during the last 50 years on all continents inhabited by a predominantly fair skinned population (Linos *et al.*, 2009) (de Vries and Coebergh, 2004) (Baade *et al.*, 2012) (Bulliard and Cox, 2000) (Sneyd and Cox, 2009). In Germany 25,4 men and 23,4 women per 100,000 individuals were diagnosed with this so called deadliest form of skin cancers in 2014 (Zentrum für Krebsregisterdaten, 2019) (Vultur and Herlyn, 2013). The average age of melanoma diagnosis in Germany is 58 years for women and 66 years for men (Zentrum für Krebsregisterdaten, 2019). These numbers show that this tumor entity is a cancer mostly occurring in aged patients. Melanoma is easy to treat if detected and excised during the first steps of tumorigenesis. In patients, where the primary tumor was detected before metastasis, the 5-year overall survival rates are very high (91,5%) (American Cancer Society, 2017). However, when the tumor has started to metastasize, treatment options are limited and the survival rate drops significantly. If the primary melanoma has spread to a regional lymph node, 5-year survival rates drop to 63% (stage 3) and even as low as 16,6% (stage 4) if the cancer has metastasized (American Cancer Society, 2017).

3.1.1. Melanocytes - Development, function and important genes

Melanocytes as melanin producing cells are ubiquitous across vertebrates. In humans, they are located in the bottom layer of the epidermis and are required to produce melanin via a process called melanogenesis. During development, melanocytes are highly migratory and originate from the neural crest (Mayor and Theveneau, 2013). The first step in their development from undifferentiated cells to progenitor cells called melanoblasts is triggered by the transcription factor SOX10, which initiates the expression of the melanocyte transcription factor MITF in the differentiating precursor neural crest cells (Mort, Jackson and Patton, 2015). The microphthalmia-associated transcription factor (MITF) as the lineage commitment factor for melanocytes plays an important role in melanocyte as well as in melanoma development (Wellbrock and Arozarena, 2015). It regulates genes involved in melanocyte development, proliferation and survival, but also governs the expression of enzymes and structural proteins involved in melanin production (Liu and Fisher, 2010). During development, some of the

melanoblasts reduce their MITF expression and dedifferentiate to form a stem cell pool, which replenishes cells, while the rest become melanin-producing melanocytes. The mature melanocyte is marked by an expression profile mostly characterized by tyrosine-related protein 1 (TYRP1) and 2 (DCT), the melanosomal matrix proteins PMEL and MART-1 as well as MITF (Cichorek *et al.*, 2013). The migratory potential of melanocytes as well as their ability to self-renew from a stem cell pool is discussed to enhance the highly aggressive and metastatic phenotype of their malignant counterpart, the melanoma tumors.

There are two forms of melanocyte pigment in the human skin: eumelanin and pheomelanin. Eumelanin is black or light brown, while pheomelanin has a red or yellowish color (Mort, Jackson and Patton, 2015). Especially eumelanin is important for protecting cells against UVA light and UVB light in scattering and absorbing UV radiation (Brenner and Hearing, 2008).

To convey this protective effect, mature melanocytes reside in the basal layer of the epidermis, where one melanocyte is usually associated with 30-40 keratinocytes and one Langerhans cell (Cichorek *et al.*, 2013) (Brenner and Hearing, 2008). They supply the surrounding keratinocytes with melanin, which is transported in melanosomes to the keratinocytes. Physiologically, UV exposure can trigger the pigmentation by the following pathway: UV-triggered DNA damage causes an activation of p53 in keratinocytes and is followed by α melanocyte stimulating hormone (α-MSH) secretion. α-MSH binds to the melanocortin receptor 1 (MC1R) on the melanocyte membrane, which initiates MITF expression via cAMP upregulation (Liu and Fisher, 2010). The second messenger cAMP is produced by MCR1 receptor driven activation of adenylate cyclase and triggers transcriptional activation of MITF. This leads in turn to an enhanced melanin synthesis by melanocytes and an enhanced transfer of melanin pigments to the epidermal keratinocytes (D'Orazio and Fisher, 2011).

3.1.2. Melanomagenesis and associated pathways

Melanocytes on sun-exposed areas encounter an increased UV light exposure over time leading to a high mutation rate, which eventually can trigger melanoma development. The risk of intense UV light exposure is shown in the three to four times higher incidence rate in Queensland, Australia compared to the rate in the UK (Bataille and de Vries, 2008). Cutaneous melanoma exhibits an unique characteristic mutation profile caused by chronic sun exposure (Vultur and Herlyn, 2013) (Lawrence *et al.*, 2013). Other phenotypic risk factors for developing melanoma are pale skin pigmentation, an increased amount of nevi and red hair color. The risk of developing melanoma increases with a decrease in the eumelanin pigmentation. Individuals with red hair and white skin who bear polymorphisms in the MC1R gene therefore have the highest risk to develop melanoma (Palmer *et al.*, 2000).
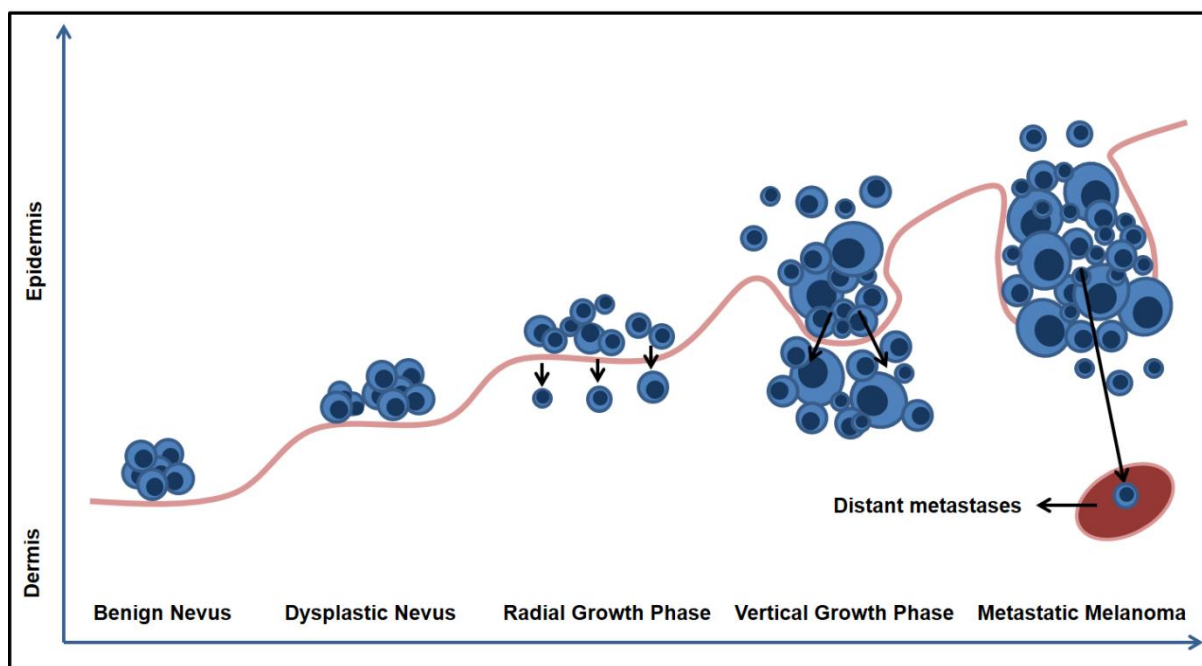
Figure 1: Melanoma tumor progression according to the Clarke model. Progression from normal melanocytes can start with the formation of a benign nevus, which can start to proliferate to a dysplastic nevus characterized by its approximately 5mm size and irregular borders. In the radial growth phase, the melanocytes proliferate into the epidermis, followed by vertical proliferation and invasion of the basement membrane in the vertical growth phase. In the next step the now formed metastatic melanoma spreads its malignant melanocytes to distant parts of the body, most of the time at first to the lymph nodes, skin, subcutaneous soft tissue, lungs and brain.

Melanomagenesis, the progression from melanocytes to metastatic melanoma, was first described in a model in 1970s by Clarke as a process that gradually progresses through different histopathological stages of increasing proliferative as well as invasive potential (Takata, Murata and Saida, 2010). In the model, he proposed melanomagenesis starts with a transformed melanocyte that has acquired different growth promoting tumorigenic mutations (Fig.1). Tumor development thereafter advances from the formation of benign nevi to dysplastic nevi. In the next step, the primary tumor spreads in a radial manner, followed by a vertical growth phase, in which cells invade the dermis. Eventually, the tumor cells leave the site of their primary lesion, encounter adjacent blood vessels and start to metastasize. Due to rapid mutations and tumor heterogeneity, different steps during this process can be skipped leading to an even faster onset of metastasis (Damsky, Theodosakis and Bosenberg, 2013). Melanoma tumors are very heterogeneous with around 16,8 mutations per Mbp of DNA (Cancer Genome Atlas Network, 2015). Despite the high number of mutations, it is believed that only a small subset of driver mutations is needed to start and maintain melanomagenesis (Abildgaard and Guldberg, 2015).
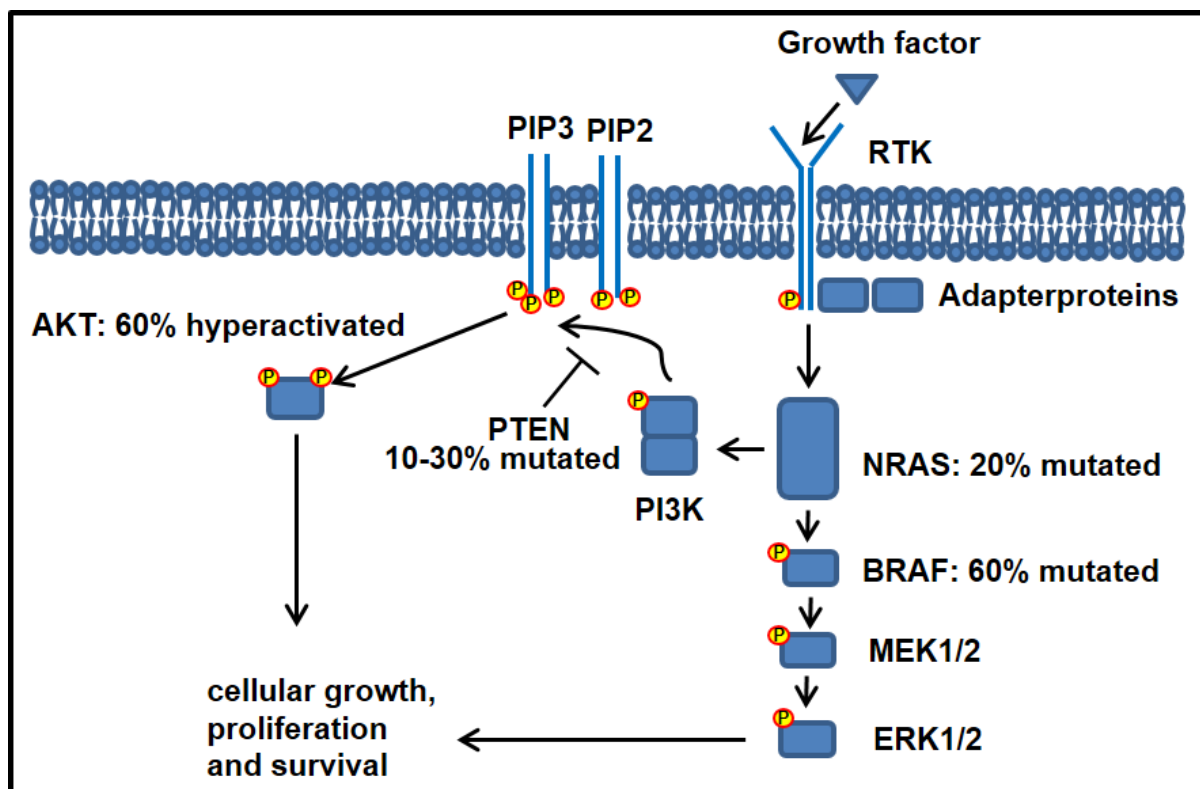
Figure 2: Signaling in melanoma. Simplified diagram of the two major pathways involved in melanoma development and maintenance. The MEK/ERK1/2 pathway is triggered by an array of different receptor tyrosine kinases (RTKs). Signaling is propagated via the adapter proteins SHC, GRB2 and SOS (not shown here) to the RAS family members (HRAS, KRAS, NRAS, only NRAS shown). Via the RAF proteins (ARAF, BRAF, CRAF, only BRAF shown), MEK1/2 and ERK1/2 the pathway influences cellular growth, proliferation and expression. The PI3K/AKT pathway is predominantly activated by RTKs and signaling is then conducted through RAS over phosphoinositide 3-kinase (PI3K) and phosphatidylinositol 4,5-bisphosphate (PIP2 → PIP3) to AKT, which activates an array of different proteins which influence cellular growth, proliferation and survival. 60% of all melanoma tumors harbor a mutation in BRAF and 20% are NRAS mutated. AKT is hyperactivated in approximately 60% of all melanomas, in approximately a third of all specimen due to loss of PTEN function (10-30%).

Most of them affect the MEK/ERK1/2 pathway, which regulates under normal physiological conditions cellular proliferation, growth and survival and which is activated in 90% of all melanoma tumors (Niault and Baccarini, 2010) (Lopez-Bergami, 2011). The pathway is triggered through an array of different receptors on the plasma membrane that can fine-tune the cellular behavior according to the ligand abundancy (Fig.2) (McCubrey *et al.*, 2012). Via the proteins SHC, GRB2 and SOS signaling is then transduced to the small G protein RAS. The activated RAS isoforms HRAS, KRAS and NRAS subsequently phosphorylate monomers of the three isoforms of the serine/threonine kinase RAF (ARAF, BRAF, CRAF) which form homo- or heterodimers to activate the mitogen activated protein kinase kinase-1 and -2 (MEK1/2). MEK1/2 thereafter phosphorylate their only known target proteins, the extracellular signal regulated kinases 1/2 (ERK1/2). ERK1/2 enters the nucleus and affects the transcription of different proliferative and pro-survival genes. It is in fact described as the kinase with the most known substrates (at least 180) (Niault and Baccarini, 2010).

Activating mutations in the BRAF kinase are the most common driver mutations (~60%) in melanoma, resulting in permanent activation of the MEK/ERK1/2 pathway (Vultur and Herlyn, 2013). Constitutive BRAF signaling profoundly changes the transcriptional and epigenetic profile of mutated tumor cells and its permanent activation leads to an around 500-fold higher signaling through the MEK/ERK1/2 pathway (Liu *et al.*, 2014). To illustrate its influence, in an analysis of 34 primary cutaneous BRAFV600E positive melanoma tumors compared with 27 wildtype BRAF samples 711 genes were regulated differentially (Guo, Xu and Zhao, 2015). BRAF mutations occur early during melanomagenesis and are also important for the initiation and development of other tumor entities (papillary thyroid carcinomas 48%, serous micropapillary ovarian carcinoma 38%, colorectal serrated polyps 60% and with a lower frequency in liver, pancreas, stomach, non-small-cell lung cancer, glioma and leukemia) (Niault and Baccarini, 2010). Over 30 single site missense mutations have been identified in this protein in different human cancers, which were mostly located in the kinase domain of BRAF (Wan *et al.*, 2004). 90% of all BRAF mutations display a valine to glutamic acid substitution (BRAFV600E). This substitution renders the MEK/ERK1/2 pathway permanently active and drives tumorigenesis, e.g. by influencing the proliferative potential of the cancer cells (Abildgaard and Guldberg, 2015) (Shtivelman *et al.*, 2014). There are other amino acid substitutions, which also stabilize the active, open state of the BRAF protein with an abundancy of 5% to 15% (V600K, V600M, V600D, V600R, V600G) (Gonzalez-Cao *et al.*, 2015). Chronically sun-damaged (CSD) melanomas as well as acral and mucosal melanomas tend to have a lower mutation rate in the oncogene BRAF than non-CSD melanomas, where mutated BRAF is found in 75% of all tumors (Curtin *et al.*, 2005).

The GTPase NRAS is the second most prevalently mutated oncogene in melanoma with a mutation rate of 20% (Abildgaard and Guldberg, 2015). Activating oncogenic mutations e.g. in its catalytic residue (NRASQ61K or NRASQ61R) are widespread, leading not only to increased signaling through the MEK/ERK1/2 pathway, but also to an activation of the PI3K/AKT signaling axis (Abildgaard and Guldberg, 2015) (Li *et al.*, 2012).

In BRAFV600E and NRAS mutated melanomas, 17% and 9% of all tumors, respectively, show additional mutations in components of the PI3K pathway, which indicates a profound role of this pathway in melanoma initiation and maintenance (Fig. 2) (Shull *et al.*, 2012). PI3K signaling regulates a vast variety of cellular processes like proliferation, survival, motility, metabolism and angiogenesis. Therefore, additional activating mutations in proteins involved in this pathway can highly increase the metastatic potential of transformed cells (Kwong and Davies, 2013). The canonical PI3K/AKT pathway under normal physiological conditions is activated through receptor tyrosine kinases, G protein coupled receptors and via integrin signals mediated through cell-cell contacts. Signaling is thereafter forwarded via RAS to the phosphoinositide 3-kinase (PI3K). This kinase phosphorylates the membrane lipid

phosphatidylinositol (PIP2 → PIP3) at the receptor, which recruits the serine-threonine kinase AKT to the membrane (Liu *et al.*, 2009). AKT is in turn phosphorylated at the residues Thr308 and Ser473 by the phosphoinosite-dependent kinase-1 (PDK1) and the mTor complex 2 (mTORC2), respectively (Brown and Toker, 2015). Only if both phosphorylation sites are activated, the three AKT isoforms (AKT1, AKT2, AKT3) can influence via different effector pathways (p53, NFκB, FoxO, VEGF, MEK/ERK1/2, mTor) cellular growth, proliferation and survival. The major antagonist of PI3K is the phosphatase PTEN that deactivates the phospholipids by removing the phosphate residue from the 3`OH group. In 10-30% of all melanoma cases PTEN is mutated, thereby preventing negative regulation of the PI3K pathway (Aguissa-Touré and Li, 2012). The importance of PTEN in melanoma progression is underlined by the fact that in mice with melanocytes expressing mutated BRAFV600E only an additional PTEN knockout triggers the occurrence of metastatic cells (Dankort *et al.*, 2009).

Moreover, mutations in the Cyclin-dependent kinase 4 pathway (CDK4) e.g. in CDK4 and cyclin-dependent kinase Inhibitor 2A (CDKN2A) and in the MITF pathway can promote melanomagenesis in neoplasia already harboring oncogenes like BRAF or NRAS.

3.2. Senescence and melanocytic nevi

The progression of BRAF-mutant melanocytes to melanoma is physiologically limited by the onset of senescence, called oncogene-induced senescence. This is supported *in vivo* by the observation that 82% of all melanocytic nevi harbor an activating BRAF mutation, but are nonetheless growth-arrested for decades (Pollock *et al.*, 2003) (Michaloglou *et al.*, 2005). Senescence is believed to act as a barrier towards further tumor progression. *In vitro*, senescence was first described by Hayflick over 40 years ago. He described replicative senescence as a process that limits the proliferative potential of fibroblasts in culture by inducing cell cycle inhibition. Strikingly, he was already able to associate this cell cycle arrest with aging and the ability to overcome this stable cellular state with the accumulation of oncogenic properties (HAYFLICK and MOORHEAD, 1961).
In general, senescence is triggered if a cell faces strong genotoxic stress. Besides telomere shortening, also oncogene expression, mitochondrial deterioration, oxidative stress, DNA damage and chromatin disruption can cause the onset of this cellular fail safe mechanism (Coppé *et al.*, 2010). Telomere degradation, DNA damage, especially double strand breaks, and chromatin relaxation caused by histone deacetylase inhibitors generate a DNA damage response (DDR), which activates the senescence induction program (Rodier and Campisi, 2011). The induced growth arrest acts as an important cellular tumor suppressor mechanism, because it hinders cells with acquired genetic instabilities to propagate. Oncogene-induced senescence can be caused by strong mitogenic oncogenes such as BRAF and NRAS. Here,

a DNA damage response is responsible for the start of the senescence program. The increased proliferation rate increases DNA replication errors in the S phase, which subsequently activate the senescence inducing p53/p21 and p16/pRb pathways.

Senescent cells are arrested in the G0/G1 or G2/M phase of the cell cycle and exhibit some characteristic properties known as hallmarks of senescence (Rodier and Campisi, 2011). Interestingly, there is no commonly shared hallmark defining all populations of senescent cells. The phenotypically most eye-catching hallmarks are the increase in cell size and the blue senescence-associated β-Gal staining at acidic pH. After initiation of the senescence program most cells increase up to twofold in size and acquire a flattened morphology. This phenotypical growth goes along with an increase of the lysosomal compartments, which is thought to be the cause for the blue senescence-associated β-Gal staining (Lee *et al.*, 2006).

A further important hallmark of senescence is the expression and secretion of different paracrine and autocrine factors. This array of different growth factors, cytokines and proteases, which is called senescence associated secretome, is able to rearrange the surrounding microenvironment of the senescent cell. It has been shown that secretion of different factors (Interleukin 6 (IL-6), Interleukin 8 (CXCL8), plasminogen activator inhibitor-1 (PAI-1)) reinforces the senescent cell cycle arrest (Ohtani *et al.*, 2012). Nonetheless, via this mechanism, senescent cells can also exert pro-tumorigenic features, e.g. by paracrine activation of cells in the vicinity or by protease-dependent remodeling of the environment (Coppé *et al.*, 2010). In melanoma cells, it has been shown that the conditioned medium of MITF silenced senescent cells, which develop a specific PARP-1 and nuclear factor kappa B (NF-κB) dependent senescence associated secretome (SASP), are able to increase the invasive capability of naive melanoma cells. Moreover, conditioned medium as well as medium containing recombinant CCL2, one of the main protagonists of the induced SASP, was able to increase tumor formation in nude mice, indicating a pro-tumorigenic effect of the induced expression program (Ohanna *et al.*, 2011).

Along the same line, the concept of senescence as an irreversible cell cycle arrest mechanism, which only acts tumor suppressive has been recently challenged, as oncogene- induced senescent multinucleated cells can serve as progenitors of highly aggressive tumor-initiating cells (Rodier and Campisi, 2011) (Leikam *et al.*, 2015). Moreover, it has been shown that mutations in genes involved in energy and stress associated pathways can lead to a reversion of the senescence phenotype. For example, cystathionase, an enzyme involved in the *de novo* synthesis of cysteine, helps to overcome senescence induction in melanocytes and melanoma cells by reducing reactive oxygen stress (Leikam *et al.*, 2014). In addition, the ribonucleotide reductase subunit M2 (RRM2), a protein responsible for the regulation of dNTP synthesis, helps cells to evade the senescent growth arrest. Oncogene induced senescence goes in hand with an reduction of RRM2 levels and can be reversed if ectopic RRM2 is expressed in human

primary fibroblasts, while knockdown of this gene increases the senescence induction of BRAFV600E expressing melanocytes (Aird *et al.*, 2013). Altogether, there is accumulating data that senescence cannot be seen as purely tumor-preventive, as it is on the one hand not entirely irreversible and on the other hand it can influence the environment in a pro-tumorigenic manner.

As stated above, senescence is triggered by stress. Therefore, the senescent phenotype can also be induced in cancer cells that are exposed to therapeutic drugs, leading to the so-called drug-induced senescence. Our group previously described that treatment with vemurafenib leads to melanoma senescence and is accompanied by heterochromatin formation, a flattened and enlarged phenotype and an increase in β-galactosidase activity (Haferkamp *et al.*, 2013).

3.3. Targeting oncogenic BRAFV600E with kinase inhibitors

3.3.1. From BRAF discovery to selective inhibition

The fact that the majority of melanomas harbor the oncogenic BRAFV600E mutation has made this protein an attractive target for therapeutic intervention. In early studies, loss of BRAF expression in BRAFV600E positive cell lines as well as artificial expression in wild type cells showed that this mutated kinase indeed could be a viable target for specific drugs (Tuveson, Weber and Herlyn, 2003). Furthermore, *in vivo* experiments demonstrated that loss of BRAF expression decreased the proliferation rate and in some cell lines also triggered cell death, thereby leading to a regression of already established tumors (Sumimoto *et al.*, 2004).

After the discovery of the mutated BRAF in melanoma, clinical trials with the multikinase inhibitor sorafenib were conducted. This small inhibitor targets besides VEGFR and PFGFR also RAF family members, but failed to show significant effects in clinical trials with melanoma patients (Hauschild *et al.*, 2009). Nonetheless, sorafenib helped to generate the first stable crystal structure that was suitable for analysis of the BRAFV600E domain (Wan *et al.*, 2004). This vital information enabled Plexxicon, an American drug-discovery company, to use a scaffold-based approach to identify novel kinase inhibitors. With insight into the three-dimensional structure of the compound bound to the kinase, chemists, computational chemists and structural biologists step by step improved the structure of the individual compounds and could in 2005 identify two BRAFV600E selective drug candidates named PLX4032 (vemurafenib) and PLX4720 (Bollag *et al.*, 2012). Both inhibitors associate with the active, V600E as well as the V600K stabilized protein and were able to effectively bind and inhibit the mutated kinase in melanoma cell lines (Bollag *et al.*, 2012). *In vivo* experiments further proved the potency of vemurafenib by inducing tumor stasis as well as tumor regression in xenograft models treated with different doses of the drug (Bollag *et al.*, 2010).

In 2006 in a dose-escalation phase 1 safety trial the first patient was treated with vemurafenib. After reformulation of the inhibitor for clinical use from a crystalline powder to an amorphous material known as microprecipitated bulk powder the bioavailability was increased and a dose of 960mg twice per day was chosen for the following clinical trials (Bollag *et al.*, 2012). Since promising results were observed, Plexxicon in cooperation with Roche filed phase 2 and 3 studies to accelerate the FDA approval process. Five years after the first screening, in August 2011, vemurafenib was approved by the FDA for clinical use followed by an approval for clinical use in the EU in February 2012.

Following the success of vemurafenib, other companies also developed specific BRAFV600E inhibitors. The second drug which was approved by the FDA was dabrafenib by GlaxoSmithKline in May 2013 (Hauschild *et al.*, 2012). Nowadays, so called pan-RAF inhibitors e.g. LY300912, which do not activate paradoxical RAF signaling, as explained in the paragraph below, are also in clinical trials (ClinicalTrials.gov. identifier: NCT02014116).

3.3.2. Efficacy and side effects of vemurafenib

For almost 3 decades, standard treatment for patients with advanced melanoma was chemotherapy with the chemotherapeutic dacarbazine. Success rates were quite limited, which was reflected by a 6-12% 3-year survival rate and a 10% 10- year survival rate (Bhatia, Tykodi and Thompson, 2009). Immunotherapeutic approaches with high doses of interleukin-2 or interferon only helped a small subset of patients, while the majority suffered from severe side effects without any beneficial effects. In 2011, after the FDA finally approved the clinical use of vemurafenib, the so-called "targeted therapy" gave medics an additional tool to fight mutated melanomas. A study published shortly after the authorization of vemurafenib in the clinics showed that 53% of all patients with BRAFV600E mutated tumors are profiting from a vemurafenib administration. Strikingly, 6% of all suitable patients lose their entire previously detected lesions and gain no additional tumor growth. This so-called total response is defined as the loss of any detectable tumors after treatment. Importantly this does not imply cure, because residual and often resistant tumor cells often start to proliferate again thereafter. A partial response, which is defined as the loss of 30% median diameter of all previously detected lesions can be seen in 47% of all patients (Sosman *et al.*, 2012). The results of a phase 3 randomized trial showed a median progression-free survival of 6,9 months, accompanied by median overall survival of 13,3 months, which is a significant increase compared to the results of a dacarbazine chemotherapy (McArthur *et al.*, 2014). The most frequent severe side effects of patients undergoing vemurafenib treatment are abnormal liver functions, cutaneous squamous-cell carcinoma and keratoacanthomas. The emergence of these lesions in up to 30% of all patients in the first few weeks after the initial drug administration is caused by a so

called paradoxical activation of the MEK/ERK1/2 pathway triggered by the drug (Su *et al.*, 2012).

This inductive effect can be observed in wild-type BRAF cells and is triggered by conformational changes induced by vemurafenib administration. In detail, binding of ATP competitive BRAF inhibitors like vemurafenib and dabrafenib to the kinase domain of wildtype RAF isoforms in the cytosol of non-BRAFV600E cells, increases dimerization of BRAF with BRAF or CRAF monomers. The drugs bind to the RAF kinase domain and induce conformational changes which favor dimer formation and mediate translocation to the plasma membrane where active RAS-GTP signals can activate the MEK/ERK1/2 pathway via the recruited RAF dimers (Arora *et al.*, 2015) (Hatzivassiliou *et al.*, 2010).

Therefore, vemurafenib in fact increases signaling through the MEK/ERK1/2 pathway in wildtype BRAF cells, e.g. with upstream activating RAS or receptor tyrosine kinase mutations via the formation of BRAF/CRAF heterodimers (Heidorn *et al.*, 2010). This paradoxical activation can lead to the growth of former subclinical cancerous lesion with RAS activating mutations (Su *et al.*, 2012).

3.3.3. Resistance development after MEK/ERK1/2 inhibition

The promising results in the first months after the start of vemurafenib treatment are usually counteracted by resistance development in month 6 or 7 after first dosage (Chapman, 2013). Tumor resistance also occurs in the same time window after dabrafenib treatment, showing that BRAF inhibitor treatment in general provokes the propagation of subpopulations of tumor cells with a resistant profile. Around 10% of these tumors are refractory and 80% of these lesions show a reactivated MEK/ERK1/2 signaling profile (Tran *et al.*, 2016). Patients treated with BRAF and MEK inhibitor in combination show higher responsiveness, but also in this situation resistance develops in the majority of patients at approximately 12 months after start of the treatment (Welsh *et al.*, 2016). Many intrinsic and acquired MEK/ERK1/2 activating resistance mechanisms have been described so far.

After the initial drug induced MEK/ERK1/2 pathway inhibition, many cells undergo apoptosis or senescence, which causes a majority of the tumor lesions to shrink (Haferkamp *et al.*, 2013) (Chapman *et al.*, 2011). This response is usually followed by the development of acquired resistance mechanisms. However, intrinsic mechanims also lead to the fact that some tumor cells survive the first therapy and thereby pave the way for the selection of clones with survival advantages under drug pressure. After BRAF inhibition, feedback regulators like SPRY2 and SPRED1/2 cease to be expressed, which increases RAS signaling again (Lito *et al.*, 2012) (Ahn, Han and Lee, 2015) (Haydn *et al.*, 2014). Generally, BRAFV600E positive melanoma

cells are less responsive towards extracellular stimulation by different receptor tyrosine kinase ligands. After BRAF inhibition, expression of these negative regulators ceases, which enables RTK ligands like EGF to stimulate their corresponsive receptors again (Lito *et al.*, 2012). The release of negative feedback mechanisms and the paradoxical activation, which is caused by the transactivation of a drug-free protomer of CRAF-CRAF and CRAF-BRAF dimers can explain why clinical responses are frequently partial responses (Chapman, 2013) (Poulikakos *et al.*, 2010).

Moreover, tumor cells or cells from the microenvironment produce several RTK ligands in auto- or paracrine manners and are therefore able to reactivate the MEK/ERK1/2 pathway in the tumor cells (Wilson *et al.*, 2012) (Straussman *et al.*, 2012). Through their individual secretomes, cells in the vicinity of the lesion, especially fibroblasts, may make the crucial difference between failure and success of a drug treatment. Fibroblast-secreted hepatocyte growth factor (HGF) is particularly potent in protecting cancer cells against therapy. In presence of BRAF inhibition, HGF is able to reactivate both MEK/ERK1/2 and PI3K/AKT pathways in melanoma cell lines (Straussman *et al.*, 2012). In patients undergoing BRAF inhibitor treatment, low HGF blood levels significantly increase the progression-free survival and overall survival. Moreover, tumor derived HGF expression is able to rescue BRAF inhibitor treated cells *in vivo* and addition of an inhibitor against the HGF receptor c-MET reverses HGF-mediated resistance in an *in vivo* xenograft model (Caenepeel *et al.*, 2017). In addition, other RTK ligands, e.g. FGF2, NRG1 and EGF can enhance cellular survival after BRAF inhibitor treatment *in vitro* (Wilson *et al.*, 2012). Moreover, a potent potential resistance promoting mechanism is the downregulation of FOSL1 after BRAF inhibition. This induces the induction of a specific secretome, which is characterized by upregulated levels of the RTK ligands IGF1, EGF, ANGPTL7 and PDGFD. These ligands, especially IGF1, increase PI3K/AKT signaling in nearby cells helping sensitive tumor cells to survive and increase the proliferation of already resistant subpopulations (Obenauf *et al.*, 2015). *In vivo* studies are needed, but if this can be seen in patient biopsies, a combination therapy of a BRAF inhibitor with an IGF-1R antibody could be a treatment option for melanoma patients (Obenauf *et al.*, 2015) (Macaulay *et al.*, 2013). These findings further underline the significance of the tumor-derived secretome and indicate that inhibition of pathways mediating adaptive resistance could be a viable option during MEK/ERK1/2 inhibitor treatment.

RTKs are frequently involved in BRAF inhibitor resistance. Increased levels of insulin-like growth factor receptor 1 (IGF-1R) could be observed *in vitro* in resistant melanoma cell lines as well as in a patient suffering a relapse after an initially successful treatment with vemurafenib. IGF-1R binds the two ligands IGF-1 and IGF-2, which could be shown *in vitro* to increase the signaling through the PI3K/AKT axis (Villanueva *et al.*, 2010). The PDGFRB receptor tyrosine kinase has also been seen to be implicated in resistance development *in*

vitro, where increased protein levels and increased MEK/ERK1/2 signaling could be observed in resistant cell lines and also *in vivo* in immunohistochemistry stainings (Nazarian *et al.*, 2010). It has been shown that BRAF inhibition selects for cells with a high expression of PDGFRB and EGFR profile (Sun *et al.*, 2014). Diminished expression of the transcription factor SOX10 leads to an increase in TGF-β signaling, which in turn elevates the expression of both RTKs. This could be validated by patient samples, where 4 out of 6 show an increase either in TGF signaling or a decrease in the SOX10 levels (Sun *et al.*, 2014). Increased expression of the EGFR family member ERBB3 via BRAF inhibitor induced elevated FOXD3 levels has also been observed to render cells resistant, proving again that an inhibition of RTK signaling could be a feasible attempt to prevent resistance development towards BRAF inhibitor resistance (Abel *et al.*, 2013).

Furthermore, there are numerous genetic alterations, which cause acquired resistance to BRAF and MEK inhibitors. Overexpression of BRAFV600E kinase as resistance mechanism was e.g. identified in 4 of 20 patients treated with vemurafenib (Shi *et al.*, 2012). Moreover elevated MEK signaling caused by mutations in the MEK1 gene were identified *in vitro* (P124L, Q56P) and also *in vivo* (C121S) in a patient (Emery *et al.*, 2009) (Wagle *et al.*, 2011). Another resistance mechanism implicated in BRAF inhibitor resistance is increased NRAS signaling. *In vitro* findings showed that isoform 2 as well as activating mutations in NRAS e.g. Q61K contribute to increased resistance under BRAF inhibition (Duggan *et al.*, 2017) (Nazarian *et al.*, 2010). Importantly, activating NRAS mutations have been found in 2 of 16 biopsy samples of patients with acquired BRAF inhibitor resistance (Nazarian *et al.*, 2010).

Altogether, a detailed understanding of the biology of BRAF/MEK inhibition in melanoma patients is of great importance to identify suitable drug combinations, which enhance the therapeutic success.

3.4. From targeted therapy to immunotherapy – Advances in melanoma treatment

Monotherapy with target inhibitors against mutated BRAF like vemurafenib has been replaced as state-of-the-art treatment by immunotherapy with ipilimumab, an anti-CTLA-4 antibody and anti-PD-1 antibodies like nivolumab and pembrolizumab (Vennepureddy, Thumallapally, & Motilal, 2016). These drugs block immune check- point receptors on T lymphocytes, thereby preventing hampering of T-cell activation and proliferation in the tumor site. They are very effective in mobilizing patient's immune system and exhibit great success in clinical trials. Pooled analysis of long-term survival data of ipilimumab showed a three-year survival rate of 22% for all patients, proving efficacy and long-term durability of this antibody (Schadendorf et al., 2015). Nonetheless targeted therapy for patients with mutated BRAF is still an important option in the clinic, since successful treatment with immunotherapy-based agents takes more time than inhibitor treatment and is only effective in 40-55% of patients (Silva and Long 2017).

Moreover, immune-related side effects in the skin and the gastrointestinal tract are common and while usually low grade and manageable, can be life threatening (Tarhini 2013). For these patients a combination therapy with a BRAF inhibitor (vemurafenib/ dabrafenib) and a MEK inhibitor (trametinib) is recommended. Therefore, understanding of emerging resistance towards MPK inhibition and possibly counteracting it, is still of great importance.

3.5. Aim of the thesis

To improve the survival rate of patients suffering from metastatic melanoma it is of utmost importance to understand the resistance mechanisms that are triggered after treatment with MEK/ERK1/2 inhibitors. Our previous findings that vemurafenib induces senescence in melanoma cells and the findings of others, that describe this cellular state as a double edged sword, both ways tumor suppressive and tumor-promoting, suggested to investigate the role of senescent cells in the resistance development towards BRAF inhibition (Haferkamp *et al.*, 2013) (Ohtani *et al.*, 2012). It has been reported that melanoma cells which were rendered senescent by MITF knockdown develop a secretome with pro-tumorigenic potential (Ohanna *et al.*, 2011). The aim of this thesis was to investigate if the senescent state after vemurafenib treatment also increases the secretion of factors that could potentially support tumor cells in their survival and their resistance development, since the identification and evaluation of potential factors in the clinical setting could pave the way for new combination therapies.

4. Material and methods

  4.1. Material

    4.1.1. Cell culture material

      4.1.1.1.   Cell lines

Table 1: Cell lines

	Supplier	**Type**
A375	ATCC, American Type Culture Collection, Manassas, USA	human melanoma cell line
SK Mel28	ATCC, American Type Culture Collection, Manassas, USA	human melanoma cell line
UACC-62	NCI/NIH, DCTD Tumor Repository, National Cancer Institute, Frederick, USA	human melanoma cell line
UACC-257	NCI/NIH, DCTD Tumor Repository, National Cancer Institute, Frederick, USA	human melanoma cell line
M14	NCI/NIH, DCTD Tumor Repository, National Cancer Institute, Frederick, USA	human melanoma cell line
MDA MB 435	NCI/NIH, DCTD Tumor Repository, National Cancer Institute, Frederick, USA	human melanoma cell line
M19 Mel	NCI/NIH, DCTD Tumor Repository, National Cancer Institute, Frederick, USA	human melanoma cell line
LoxIMVI	NCI/NIH, DCTD Tumor Repository, National Cancer Institute, Frederick, USA	human melanoma cell line
RPMI-7951	NCI/NIH, DCTD Tumor Repository, National Cancer Institute, Frederick, USA	human melanoma cell line
Malme 3M	NCI/NIH, DCTD Tumor Repository, National Cancer Institute, Frederick, USA	human melanoma cell line
MainUro	Department of Dermatology, Venereology and Allergology, Würzburg, Germany	human dermal fibroblasts
NHDF	Promocell	human dermal fibroblasts
WI-38	Department of Biochemistry and Molecular Biology, University, Würzburg, Germany	caucasian fibroblast-like fetal lung cell

4.1.1.2. Cell culture media, reagents and devices

Table 2: Cell culture media, reagents and devices

	Manufacturer	**Order number**
Dulbecco´s modified eagle medium (DMEM)	PAN	P04-03550
Fetal calf serum (FCS)	Sigma	F7524
Dialyzed FCS	Invitrogen	26400-004
OptiMEM	Invitrogen	11058-021
Penicillin/Streptomycin (P/S)	Sigma-Aldrich	P0781
Trypsin 10x	PAN	P10-024100
Dimethylsulfoxid (DMSO)	Roth	47201
0,45 µM membrane filter	Merck	SLHV004SL
Thiazolyl Blue Tetrazolium Bromide (MTT)	Sigma-Aldrich	M2128
	Composition	
Cell culture medium (D10)	DMEM containing 10% FCS and 1% P/S	
Freezing medium	DMEM containing 20% FCS and 10% DMSO	
Starvation medium (dial D2)	DMEM containing 2% dialyzed FCS and 1% P/S	
PBS	137 mM NaCl; 2,7 mM KCl; 4,3 mM Na_2HPO_4; 1,47 mM KH_2PO_4; adjusted to pH 7,4	
EDTA	3,42 mM; adjusted to pH 7,4	

4.1.1.3. Inhibitors, compounds and growth factors

Table 3: Inhibitors, compounds and growth factors

	Manufacturer	**Order number**
AZD 4547	Selleck Chem	#1035270-39-3
BEZ-235	Axon Medchem	#1281
DL-Propargylyglycine (PAG)	Selleck Chem	P78888-1G
GDC 0941	Selleck Chem	#S1065
PD 184352	Axon Medchem	#1368
Piperlongumine	Sigma-Aldrich	SML0221
Palbociclib (PD 0332991)	Selleck Chem	#S1116
Vemurafenib (PLX 4032)	Axon Medchem	#1624
FGF1 (human) Recombinant Protein	Tebu-Bio	P3456

4.1.2. Protein associated experiments

4.1.2.1.   Acrylamide gels for SDS-PAGE

Table 4: Buffers and compounds used for the casting of SDS-PAGE gels

4% Collecting gel	**per Gel (2213,2 µl)**	**Composition**	
H$_2$O	1408 µl		
Collecting gel buffer	550 µl	0,5M TrisHCl pH 6,8	
		Manufacturer	**Order number**
40% acrylamide solution (Rotiphorese Gel 40 (37,5:1)	220 µl	Roth	T802.1
10% SDS	22 µl	Sigma	75746-1kg
10% ammonium peroxodisulphate (APS)	11 µl	Merck	1201
Tetramethylethylenediamine (TEMED)	2,2 µl	Roth	2367.3

10% Separation gel	**per Gel (8551.2 µl)**	**Composition**	
H$_2$O	4152 µl		
Separation gel buffer	2125 µl	0,5M TrisHCl pH 6,8	
		Manufacturer	**Order number**
40% acrylamide solution (Rotiphorese Gel 40 (37,5:1)	2138 µl	Roth	T802.1
10% SDS	85 µl	Sigma	75746-1kg
10% APS	42,5 µl	Merck	1201
TEMED	8,5 µl	Roth	2367.3

4.1.2.2. Protein lysis, SDS polyacrylamide gel electrophoresis (SDS-PAGE) and western blot material

Table 5: Reagents and material used for protein lysis, SDS polyacrylamide gel electrophoresis (SDS-PAGE) and western blot

	Manufacturer	Order number
Bradford Reagent	Sigma-Aldrich	B6916
SuperSignal West Pico Chemiluminescent Substrat	Thermo Scientific	LH146987
Proteome Profiler Human Angiogenesis Array Kit	R&D Systems	ARY007
Nitrocellulose membrane	GE Healthcare	10600002
Marker (Page Ruler)	Thermo Scientific	26616
Bovine serum albumin (BSA)	SERVA Electrophoresis	11930
	Composition	
Laemmli	312,5 mM Tris pH 6,8; 10% SDS, 50% glycerine, 0,005% bromo-phenol-blue; 25% ß-mercaptoethanol	
NP40 lysis buffer	20 mM HEPES (pH7.8), 500 mM NaCl, 5 mM $MgCl_2$, 5 mM KCl, 0,1% deoxycholate, 0.5% Nonidet-P40, 10 µg/ml aprotinin, 10 µg/ml leupeptin, 200 µM Na3VO4, 1 mM phenylmethanesulphonyl-fluoride,100 mM NaF	
PBS	137 mM NaCl; 2,7mM KCl; 4,3 mM Na_2HPO_4; 1,47 mM KH_2PO_4; adjusted to pH 7,4	
SDS running buffer	250 mM Tris; 192 mM glycine; 0,5% SDS	
Tris-buffered saline with Tween20 (TBS-T)	10 mM Tris pH 7.9; 150 mM NaCl; 0,1% Tween	
Transfer buffer	25 mM Tris; 192 mM glycine; 20% methanol	

All kits were used according to the instruction manual provided by the manufacturer.

4.1.2.3. Antibodies

Table 6: Antibodies used for western blot

Primary Antibodies	Manufacturer	Order number
Actin β	Cell Signaling	#9272
P-ERK p42/44 (Thr202/Tyr204)	Cell Signaling	#9101
P-AKT (Ser473)	Cell Signaling	#4051
P-Rb (Ser780)	Cell Signaling	#9307
Vinculin	Sigma-Aldrich	V-9131
P-NF-κB p65 (Ser536)	Cell Signaling	#4764
Tubulin	Sigma-Aldrich	T6074
PY20	BD Transduction Lab.	#610000
MMP2	Cell Signaling	#4022
Secondary Antibodies		
Goat Anti-mouse IgG+IgM (H+L) (POD)	Thermo Scientific	3144
Goat Anti-rabbit IgG (H+L) (POD)	Bio-Rad	170-6515

4.1.2.4. Zymography material

Table 7: Buffers and compounds used for zymography

	Manufacturer	Order number
Gelatine (Porcine skin type A)	Sigma	# 9000-70-8
2.5% Triton X-100	Sigma	# 9002-93-1
	Composition	
2× loading buffer	50 mM Tris-HCl (pH 6,8), 10% glycerol, 1% SDS, 0,01% bromophenol blue	
Collagenase buffer	50 mM Tris-HCl pH 7,6, 0,2 M NaCl, 5 mM $CaCl_2$, 0,2% Brij 35	
Coomassie staining solution	40% methanol, 10% acetic acid/0,025% Coomassie brilliant blue R-250	

4.1.2.5. Senescence-associated β-galactosidase assay (SA-β-Gal) material

Table 8: Buffers and compounds used for SA-β-Gal assay

	Composition
PBS	137 mM NaCl; 2,7 mM KCl; 4,3 mM Na_2HPO_4; 1,47 mM KH_2PO_4; adjusted to pH 7,4
Fixing solution	3,7% formaldehyde in PBS
SA-β-Gal staining solution	1 mg/mL of X-gal (Stratagene, 300201), 40 mM citric acid/sodium phosphate buffer (pH 6,0), 5 mM potassium ferricyanide (Sigma, 13746-66-2), 5 mM potassium ferrocyanide (Sigma, 14459-95-1), 150 mM NaCl, and 2 mM $MgCl_2$
Citric acid/sodium phosphate buffer (0.2 M, pH 6.0)	36,85 mL of 0,1 M citric acid solution with 63,15 ml of 0,2 M sodium phosphate, pH 6

4.1.3. Nucleic acid associated experiments

4.1.3.1. RNA extraction

Table 9: Reagent used for RNA extraction

	Manufacturer	Order number
TRIzol	Life technologies	15596018

4.1.3.2. cDNA synthesis kit

Table 10: Components of the RevertAid First Strand cDNA Kit from Fermentas

	Volume used for one reaction
Template RNA	0,1 – 5 µg
Random hexamer primer	1 µl
DEPEC-treated water	to 12 µl (depending upon the volume of water in which the RNA is solved)
5x reaction buffer	4 µl
RiboLock RNase Inhibitor (20 U/µl)	1 µl
10 mM dNTP mix	2 µl
RevertAid M-MuLV Reverse Transcriptase (200 u/µl)	1 µl

4.1.3.3. Real-time PCR material

Table 11: Real-time PCR material

	Manufacturer	**Order Number**
His-Taq polymerase	Chair of developmental biochemistry (University of Würzburg)	-
SYBR Green	Life technologies	57563
96-well plates	4titude	4ti-0710/C
Cover foil for plates	4titude	4ti-0560
Ethidium bromide staining bath (1mg/l in H_2O)	Sigma-Aldrich	E1510
	Composition	
Reprofast PCR Buffer	100 mM $(NH_4)_2SO_4$; 200 mM Tris 8,8; 100 mM KCl; 20 mM $MgSO_4$; 1% Triton; 1% BSA	

4.1.3.4. Primers for real-time PCR

Table 12: Oligonucleotides used for real-time PCR

Oligo	Sequence
h_CCL2_up	5`-CAATGCCCCAGTCACCTGCTGT-3`
h_CCL2_down	5`-GGGTTTGCTTGTCCAGGTGGTCC-3`
h_Actin_up	5`-GGCATCCTGACCCTGAAGTA-3`
h_Actin_down	5`-GGGGTGTTGAAGGTCTCAAA-3`
h_CTGF_up	5`-GCGAGGAGTGGGTGTGTGACG-3`
h_CTGF_down	5`-AGCCTGCAGGAGGCGTTGTC-3`
h_FGF1_up	5`-CAGCCCTGACCGAGAAGTTT-3`
h_FGF1_down	5`-GGTTCTCCTCCAGCCTTTCC-3`
h_FGF2_up	5`-TCCCGCCCGGCCACTTCAA-3`
h_FGF2_down	5`-GCCAGGTAACGGTTAGCACACACT-3`
h_IL-6_up	5`-GCCTTCCCTGCCCCAGTACCC-3`
h_IL-6_down	5`-TGCCTCTTTGCTGCTTTCACACATG-3`
h_CXCL8_up	5`-GAGTGGACCACACTGCGCCA-3`
h_CXCL8_down	5`-TGCTTGAAGTTTCACTGGCATCTTCA-3`
h_UPAR_up	5`-GCAACGAGGGCCCAATCCTGG-3`
h_UPAR_down	5`-GCGGTTGCACAGCCTCTTACCA-3`
h_MMP2_up	5`-ACCTAGCACATGCAATACCTGAACACC-3`
h_MMP2_down	5`-CACCAGTGCCTGGGGCGAAG-3`
h_EGF_up	5`-TGACTCTACTCCACCCCCTCACCT-3`
h_EGF_down	5`-AGGTCTCGGTACTGACATCGCTCC-3`
h_FGF7_up	5`-CCCTGAGCGACACACAAGAA-3`
h_FGF7_down	5`-TTCCACCCCTTTGATTGCCA-3`
h_FGF17_up	5`-CCCAACCTCACTCTGTGCTT-3`
h_FGF17_down	5`-CAAACTTGTTGCCGTCCTCG-3`
h_FGFR1_up	5`-GACTCCGGCCTCTATGCTTG-3`
h_FGFR1_down	5`-CCAATATGGAGCTACGGGCA-3`
h_FGFR2_up	5`-CAAACGTATCCCCCTGCGG-3`
h_FGFR2_down	5`-TGCCCAGTGTCAGCTTATCTC-3`
h_FGFR3_up	5`-GGAGTTCCACTGCAAGGTGT-3`
h_FGFR3_down	5`-AAGGTGACGTTGTGCAAGGA-3`
h_FGFR4_up	5`-GGAGGAGCCAGGTGAGGA-3`
h_FGFR4_down	5`-CTGCTCTTGCTGCTCCAGG-3`

4.1.3.5. siRNAs used for transfection

Table 13: siRNAs

siRNA	Manufacturer	Order number
ON-Target plus Non-Targeting pool	Thermo Scientific	D-001810-10-20
siGENOME SMARTpool FOSL1	Thermo Scientific	M-004341-04

4.1.4. Technical equipment

Photo Image Station 4000MM (Kodak)

Mastercycler ep Realplex (Eppendorf)

Mini-PROTEAN TetraElectrophoresis System (Biorad)

Trans Blot Cell (Biorad)

Cary 50 Spectrophotometer (Varian)

NanoDrop ND-1000 Spectrophotometer (NanoDrop Technologies)

Hera Cell 150i Incubator (Thermo Scientific)

CTR 6000 inverted microscope (Leica)

4.2. Methods

4.2.1. Cell Culture methods
4.2.1.1. Cell Propagation

Cells were grown in a Hera Cell 150i incubator manufactured by Thermo Scientific. As culture medium (D10), Dulbecco's modified Eagle medium (DMEM) supplemented with 10% fetal calf serum (FCS) and 1% penicillin/streptomycin was used. The cells were cultivated at 37°C in 10 cm dishes in an atmosphere containing 5% CO_2.

Melanoma cells in culture were trypsinized at a density of 70-80% cells to maintain a suitable density for optimal cellular growth. Culture medium was removed and the cells were washed one time with EDTA and then treated with 1 x trypsin (solved in ETDA) for around 5 min depending on the attachment properties of the cell line. To solve cells from the bottom, the plate was washed with D10 and the medium containing excessive cells was aspirated. To record the time cells were in culture the passage number was noted on the dish. Only cells with a lower passage than 30 were used for experiments to avoid artifacts caused by high passaged old cells.

4.2.1.2. Freezing of cells

Freeze down of cell lines was performed by trypsinizing the cells as described above followed by solving them in 1 ml D10. The medium containing the cells was then transferred into a cryo-

vial, which thereafter was centrifuged at 1000 rpm for 5 min. The pellet eventually was solved in freezing medium and stored at -80°C or for long time storage in liquid nitrogen.

4.2.1.3. Thawing of cells

Vials with frozen cells were quickly thawed in a 37°C water bath. The freezing medium containing the cells was then transferred into a 15 ml Falcon tube (BD Bioscience) containing 10 ml of warm D10 medium. Thereafter cells were centrifuged at 1000 rpm for 5 min, the supernatant was removed and cells were solved in fresh D10 medium and put on 10 cm plates for cultivation.

4.2.1.4. Treatment of cells with inhibitors

In all experiments, in which inhibitors were used to manipulate normal cellular physiology, the compounds were always replaced after 48 h together with the medium to avoid degradation of the active agents and to ensure an optimal nutrient supply for the cells on the plates.

4.2.1.5. Generation of conditioned supernatant (CSN)

Conditioned supernatants from vemurafenib-treated M14, UACC-62 and A375 melanoma cell lines were made according to a stringent protocol depicted in Figure 3.
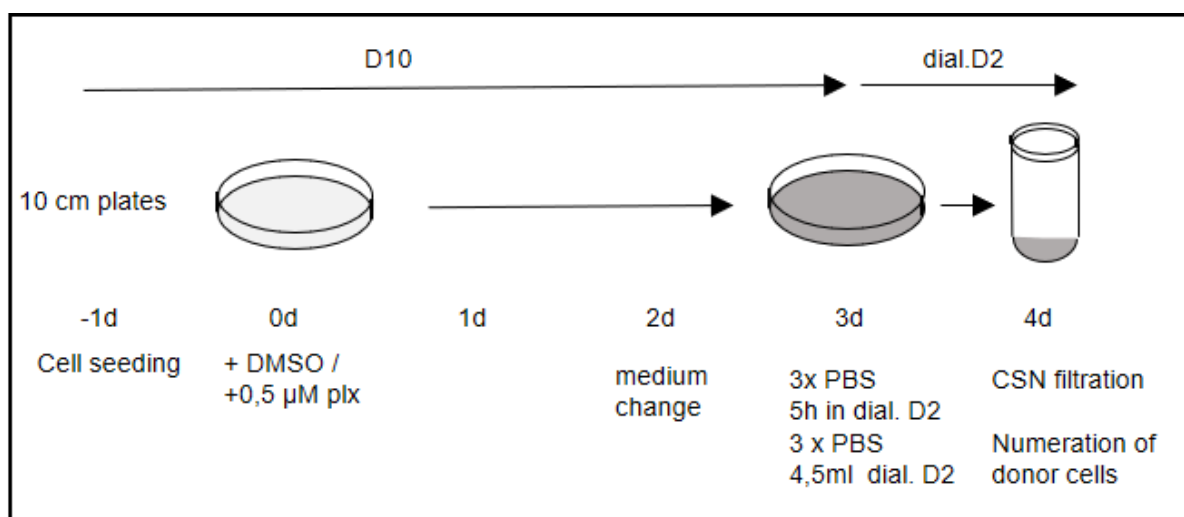
Figure 3: Schematic view of the protocol used for CSN generation. CSN was generated from melanoma cells treated for 3d with vemurafenib. After excessive washing with PBS, donor cells were incubated over night with fresh 2% starvation medium (dial D2). The medium was filtered through 0,45µm membrane filters the following morning and was termed conditioned supernatant (CSN).

Donor cells were seeded a day before the treatment with the inhibitor (-1 d). A day after seeding the medium was replaced and 0,5 µM vemurafenib or the equivalent amount of the solvent DMSO was added (day 0). To maintain constant nutrient supply and to ensure inhibitor efficacy, the medium was changed on day 2. At day 3 cells were washed three times with PBS and incubated for 5 h in dial D2. Thereafter, the medium was aspirated and the plate was washed again three times with PBS. To ensure the highest possible concentration of secreted factors in the CSN only 4,5 ml dial D2 without vemurafenib was added on the 10 cm plates, which were then incubated overnight. On the next day, CSN was filtered through a 0,45 µm membrane and used immediately in further experiments, while the donor cells were detached from the plates and counted.

For the initial experiments donor cells were seeded in a number that ensured equal density (Fig. 5, Fig. 6) at day 4 between the DMSO control and the cells under vemurafenib pressure. In later experiments involving CSN (Fig. 4 c, Fig. 7 c, Fig. 11), the donor cells were seeded to maintain the same cell number on the control plate and the vemurafenib treated plate at day 4.

Table 14: Number of donor cells seeded in experiments with equal cell number at the day of CSN harvest (Fig. 5, Fig. 6)

Donor cell line	DMSO control	vemurafenib (0,5 µM)
M14	5×10^5	$1,5 \times 10^6$
UACC-62	3×10^5	8×10^5
A375	2×10^5	$1,5 \times 10^6$

Table 15: Number of donor cells seeded in experiments with equal density at the day of CSN harvest (Fig. 4 c, Fig. 7 c, Fig. 11)

Donor cell line	DMSO control	vemurafenib (0,5 µM)
M14	8×10^5	$1,5 \times 10^6$
UACC-62	4×10^5	8×10^5
A375	3×10^5	$1,5 \times 10^6$

The acceptor cells were pre-starved for three days in dial D2 before treatment with the CSN of the different cell lines. Via this starvation step the effects of the growth factors in the D10 cell culture medium were diminished and the cells restored their responsiveness to auto- or paracrine stimulation.

4.2.1.6. Preparation of CSN for western blots

To analyze the protein levels (MMP2) secreted in the medium a western blot with CSN was performed. Donor cells in 10 cm cell culture dishes were treated for 3 days with different amounts of vemurafenib (0,5 µM, 2 µM, 5 µM), medium and inhibitor were replaced after 48 h. At the evening of day 3 after aspiration of the complete medium, 4,5 ml dial D2 without additional vemurafenib was added and cells were incubated overnight until CSN was harvested at day 4. Medium was transferred into 2 ml vials and subsequently frozen with liquid nitrogen and stored at -80°C. Thereafter the donor cells were counted to be able to normalize the probed amount of CSN according to the counted cell number. Probes were diluted to the calculated values and Lämmli buffer was added before CSN lysates were subjected to 95°C for denaturation purposes on a heating block. Thereafter, probes were loaded and Western blot was performed as described below.

4.2.1.7. Viability assay (MTT assay) with CSN

To assess possible growth promoting effects of CSN as well as to evaluate the efficacy of different combinations of compounds on melanoma cell proliferation, a viability assay based on the reagent 3-(4,5-dimethylthiazol-2-yl)-2,5-diphenyltetrazolium bromide (MTT) was used. The yellowish solution is converted into blue, water-insoluble formazan dye crystals by mitochondrial dehydrogenases of living, metabolically active cells. Photometric measurement of the absorbance of these DMSO-solved crystals shows the level of cellular metabolism in a cell population and indirectly enables the assessment of cellular proliferation and viability.

Acceptor cells were seeded 48 h before treatment in triplicates on 96 well plates in 100 µl of dial D2. After filtration of the CSN from donor cells, which was prepared as mentioned above (see 4.2.1.5.), the medium was removed from the acceptor cells, replaced by 200 µl of the respective CSN and cells were incubated for 72 h. Afterwards, 20 µl of a 5 mg/ml MTT solution was added to every well and after a 2 h incubation period the medium was removed. Crystals were solved with pure DMSO for 30 min on a rocking platform shaker. Detection of the absorption level of the DMSO-solved formazan of individual wells was performed with an ELISA reader at a wavelength of 580 nm.

In all MTT assays, cells were seeded according to Table 16 in dial D2, 96 well plates were aspirated after 48 h and CSN with the respective compounds was added. After two days the medium in every well was replaced with fresh medium with the appropriate amount of compounds.

Table 16: Number of cells seeded per 96-well according to cell line

Cell line	Number of cells seeded per 96-well
M14	3000
UACC-62	1500
A375	3000
MainUro	1500
NHDF	1500

4.2.1.8. Proliferation assay

To determine the influence of recombinant FGF1 on the survival rate of melanoma cells under vemurafenib pressure, cells were treated with the aforementioned compounds and counted manually after 5 days.

Cells were seeded in triplicates in D10 on 6 well plates (see Table 17). At the next day the medium was replaced with dial D2 supplemented with different concentrations of vemurafenib and/or recombinant FGF1. 48 h and 96 h after the initial dosage of the compounds the medium again was replaced by fresh dial D2 with the corresponding drugs. On day 5 the cells were trypsinized and resuspended in PBS and counted using a Neubauer hemacytometer.

Table 17: Number of cells seeded per 6-well according to cell line

Cell line	Number of cells seeded per 96-well
M14	8×10^4
UACC-62	1×10^5
A375	8×10^4

4.2.1.9. Senescence-associated beta-galactosidase assay

Senescent cells overexpress the lysosomal hydrolase enzyme beta-galactosidase. Its ability to cleave the chromogenic substrate X-Gal at pH 6 can lead to a blue lysosomal staining pattern, and makes it a widely used biomarker for senescent and aging cells.

Cells were incubated under different inhibitor pressures on 6 wells and were washed two times with PBS before the staining started. To fix the cells to the plates 3,7% formaldehyde in PBS was added, removed after 5 min and the cells were washed again two times with PBS. 1 ml of the SA-β -Gal staining solution was added per 6 well and the plate was incubated at 37°C with 5% CO_2 for 16 h protected from light overnight. After washing with PBS on the next day 1 ml PBS was added and the stained plates were kept at 4°C and eventually photographed.

4.2.1.10. siRNA transfection

UACC-62 cells were cultivated in 6-well plates to a confluency of approximately 70%. For transfection the manufacturers protocol was used. 5 µl of XtremeGene solution (Thermo Scientific) mixed with 10 µM of siRNA (Thermo Scientific) was used per 6-well. After preparation of the siRNA in Opti-MEM (Invitrogen) to a total volume of 100 µl, XtremeGene was dissolved in 95 µl Opti-MEM and both were mixed and incubated at room temperature for 15 min. The mixture was added dropwise to every 6 well containing 900 µl D10. After incubation at 37°C for 8 h, the medium was replaced and cells were grown for 72 h and harvested thereafter.

4.2.2. Protein methods
4.2.2.1. Cell lysate preparation

Cells were harvested with a silicon rubber and centrifugation at 13000 rpm for 2 min. Afterwards, the pellet was lysed depending on its size with 30-100 µl NP 40 lysis buffer. After a 30 min to 3 h incubation period on ice, samples were centrifuged at 13000 rpm for 15 min at 4°C. The protein concentration of the samples was measured via Bradford assay photometrically at 595 nm in a Cary 50 Spectrophotometer. The total amount of protein used per sample was between 20-50 µg, depending upon the abundancy of the proteins that could be detected. Probes were adjusted according to the concentration with lysate and NP40 buffer to a final volume of 15 µl. To break up secondary and tertiary structures 4 µl Lämmli buffer was added and the samples were heated to 95°C for 5 min before loading.

4.2.2.2. SDS polyacrylamide gel electrophoresis (SDS-PAGE)

The polyacrylamide gels which were used to separate the proteins consisted of a collecting gel and a separation gel (see 4.1.2.1.). Gels were cast between glass slides in a plastic mount. At first H_2O, buffer, acrylamide and SDS were poured into a plastic cup, before APS and TEMED were added. Both of these components were mixed in fast, because addition of these compounds starts the polymerisation process. The collecting gel is wider-pored and has a lower pH value than the separation gel to allow proteins of all sizes to enter the separation gel at the same time, which assures that all proteins are separated over the same time period. The finished gels were loaded into an electrophoresis apparatus and the samples were then pipetted into the pockets of the collecting gel together with a marker (1,5 µl) of a defined band size. The chamber is filled with SDS running buffer and after voltage is applied (25 mA/gel),

the proteins are moving towards the anode at the bottom of the gels. Approximately every two amino acids of the denatured protein bind one molecule of SDS. This induced negative charge allows for a separation according to the molecular mass along an electric field. Depending upon the protein size the separation process took 2 – 3 h.

4.2.2.3. Western blot

After separation of the proteins, they were transferred in a wet blot to a nitrocellulose membrane. The gels therefore got equilibrated in used transfer buffer for approximately 10 min and were then clamped in a plastic inlet next to the nitrocellulose membrane surrounded by a foam inlet and 3 Whatman filter papers on both sides. In a 4°C cold room together with an ice pack the gels were then put in a plastic tank filled with fresh transfer buffer. After voltage was applied with a current of 250 mA for one gel, the transfer to the nitrocellulose membrane took place for approximately 1,5 h. During that time the separated, SDS-loaded, negatively charged proteins in the gel wandered along the perpendicular electrical field towards the anode and got caught on the nitrocellulose membrane due to polar interactions.

For determination of specific proteins with different antibodies, the blots were blocked for 1 h at room temperature with 5% BSA solved in TBS-T on a rocking shaker. To probe for specific proteins attached to the membrane, antibodies dissolved in 5% BSA in TBS-T were used (see 4.1.2.3.). After incubation overnight at 4°C on a rocking platform, the blots were washed three time with TBS-T and incubated for 1 h at room temperature with a secondary antibody. Secondary antibodies coupled to horseradish peroxidase or fluorescence antibodies were used. After washing three times with TBS-T to get rid of unspecific binding, signal detection was performed using SuperSignal West Pico Chemiluminescent Substrate (Thermo Scientific) and a Photo Image Station 4000MM (Kodak).

4.2.2.4. Zymography with CSN

To assess the matrix degrading ability of the secretome of vemurafenib treated melanoma cell lines, zymography blots with CSN generated as described above were performed (see 4.2.1.5.). In contrast to the SDS-PAGE, the loading buffer contains no SDS and no reducing agents like β-mercaptoethanol. Therefore, the proteins in the probes are not denatured and are enzymatically active after the gel has run. However, since the proteins are not fully linearized, the separation according to the molecular mass is not as stringent as in an SDS-PAGE.

Probes were normalized according to the counted cell number of the DMSO control and the BRAF inhibitor treated plate. Cell supernatant was mixed with 2x loading buffer (Table 7) and resolved on an SDS-polyacrylamide gel containing 0,12 mg/ml gelatin. After the run the gel was soaked for 1 h in 2,5% Triton X-100, then washed twice with collagenase buffer and incubated at 37°C for 16 h. After washing with distilled water, the gels were incubated in Coomassie brilliant blue staining solution at room temperature for 2 h. Thereafter, gels were washed in distilled water until the excess amount of staining solution was gone.

4.2.2.5. Human angiogenesis antibody array

Differing protein levels in the CSN of A375 after vemurafenib treatment were determined with an antibody array. CSN from donor cells was generated according to the protocol described in 4.2.2. 1 ml from DMSO control CSN and vemurafenib CSN was used and incubated overnight on a rocking shaker. All steps were performed according to the manufacturers protocol (Table 5), except a Photo Image Station 4000MM was used for signal detection. Mean pixel density was calculated with the software package of the image station and analyzed with Excel.

4.2.3. DNA and RNA methods
4.2.3.1. RNA extraction

For RNA extraction the frozen cell pellets (kept at -80°C) were lysed with 300-500 µl Trizol reagent depending upon the size of the pellet by pipetting up and down. After a 5 min incubation period at room temperature, a fifth of the used amount of Trizol lysis reagent was added as chloroform. After shaking the probes for 15 seconds, another incubation period of 3 min followed. Then the probes were centrifuged for 15 min at 13.000 rpm and 4°C. The transparent upper phase, where the water-soluble RNA is located, was now transferred into another tube. Afterwards half of the amount of used Trizol lysis reagent was added as isopropanol and mixed thoroughly. Then after another 10 min at room temperature the probes were centrifuged for 15 min with 13.000 rpm and 4°C. The transparent supernatant was discarded and the pellet was then washed two times with 1 ml 75% ethanol (5 min, 13.000 rpm, 4°C). After carefully discarding the excess ethanol, the pellet was dried at 37°C in a heating block to get rid of ethanol that could impede the cDNA synthesis in later steps. Eventually the pellet was solved depending on the size in 10-20 µl RNase-free water and incubated for 10 min at 55-60°C. Finally, the concentration was measured and the RNA probes were stored till further use at -80°C. No DNase digestion has been performed.

4.2.3.2.   cDNA synthesis

The amount of extracted RNA was measured with a Nanodrop spectrophotometer and cDNA synthesis was performed with 1-4 µg RNA template with a kit from Fermentas (see 4.1.3.2.). After adding the extracted RNA, a random hexamer primer and water to a total volume of 12 µl the mixture was incubated for 5 min at 65°C to break up the secondary structures of the RNA strands. After cool down on ice, the reverse transcriptase, an RNase inhibitor, dNTPs and reaction buffer were added and the vial was incubated for 5 min at room temperature followed by 60 min at 42°C, according to the manufacturer`s instructions. The cDNA synthesis eventually was terminated by denaturing the reverse transcriptase at 70°C for 5 min.

4.2.3.3.   Real-time PCR

This method allows the quantification of a targeted DNA molecule during a PCR run. For the quantification we used in our approach the non-specific double-stranded DNA binding, fluorescent dye SYBR-Green. After excitation with the required wavelength at each PCR-cycle one can measure the number of gene copies that are generated by the reverse transcriptase. To assure that the DNA fragments of the desired genes are specifically amplified, the melting curves can later be analyzed. These curves show the intensity of the fluorescence signal against the temperature and since each generated DNA fragment has its specific, distinct fusion peak one can identify false positive results.

5 µl of diluted cDNA was used, every reaction was done in triplicates and normalized to the housekeeping gene β-actin. In a Mastercycler ep Realplex from Eppendorf, the loaded 96 well plate was subjected to a stringent PCR protocol and later analyzed. Primers which give CT values above 35 were loaded on a 2 % agarose gel and bands were visualized via UV light after ethidiumbromide staining.

Standard protocol for one reaction:

14,25 µl ddH2O

2,5 µl 10xBuffer (ReproFast)

0,75 µl forward primer (10 pmol/µl)

0,75 µl reverse primer (10 pmol/µl)

0,3 µl Taq-polymerase

0,7 µl dNTPs

0,75 µl SYBR-GREEN (1:2000)

5 µl cDNA

Step	Temperature	Time	
1	95°C	pause	
2	95°C	5'	
3	95°C	15"	40X
4	60°C	15"	
5	72°C	15"	
6	95°C	5'	
7	60°C	15"	
8	60°C-95°C gradient	20"	
9	95°C	15"	

All qPCR assays were repeated at least three times in triplicates. Significance was determined using the Student´s t-test (*:$p<0.05$; **:$p<0.01$; ***:$p<0.001$).

4.2.3.4. Real-time PCR growth factor array

To measure differences in the gene expression profile of vemurafenib treated and untreated melanoma cell lines, M14, UACC-62 and A375 cells were seeded on 10 cm plates. To get an equal count at day 3 the cell numbers depicted in Table 14 were put on plates and were cultivated and treated with DMSO and vemurafenib. Medium and inhibitor were replaced after 48 h and after treatment for 3 days cells were counted to ensure an approximately equal number of cells in the harvested probes. After RNA extraction and cDNA synthesis (see. 4.2.10.) 5 µl cDNA were used per 96 well to perform the real-time PCR according to the manufacturers protocol (Qiagen). The array was performed only once.

5. Results

5.1. Components of the vemurafenib-induced secretome

Vemurafenib treatment of melanoma cell lines induces a senescent phenotype, which is characterized by an increase in cell size, senescence-associated beta-galactosidase (SA-β-Gal) staining, as well as different other senescence associated features (Haferkamp *et al.*, 2013). Melanoma cells, like many other cell types, change their gene expression pattern and develop a characteristic senescence associated secretory phenotype (SASP) after undergoing senescent cell cycle arrest (Coppé *et al.*, 2008). Ohanna et al. could show that in response to *MITF* knockdown induced senescence, melanoma cells upregulate the expression of different growth factors, predominantly cytokines and proteinases (Ohanna *et al.*, 2011). Based on these observations, we aimed at identifying critical factors of the BRAF inhibitor induced secretome and their auto- and paracrine functions.

5.1.1. Viability promoting effects of conditioned supernatants from BRAF inhibitor induced senescent melanoma cells

To answer the question whether factors, which are secreted in vemurafenib-treated cells, have measurable effects on their surroundings, we treated naive cells with conditioned supernatant prepared from BRAF inhibitor treated melanoma cells.

To gain conditioned supernatants (CSN), a stringent protocol, as depicted in Figure 4, was used. This procedure, which comprised several washing steps, ensured that the BRAF inhibitor, that was used to treat the donor cells, was not taken over to the acceptor cells. The donor cells were incubated in medium with 0,5 µM vemurafenib for 3 days prior to the harvest of the supernatant, while the acceptor cells were primed to the starving medium over night. The filtered CSN was then used in different further experiments. In the first experiments, donor cells were seeded at conditions which reached equal cell confluence in the control and the vemurafenib-treated condition at the day of CSN harvest.
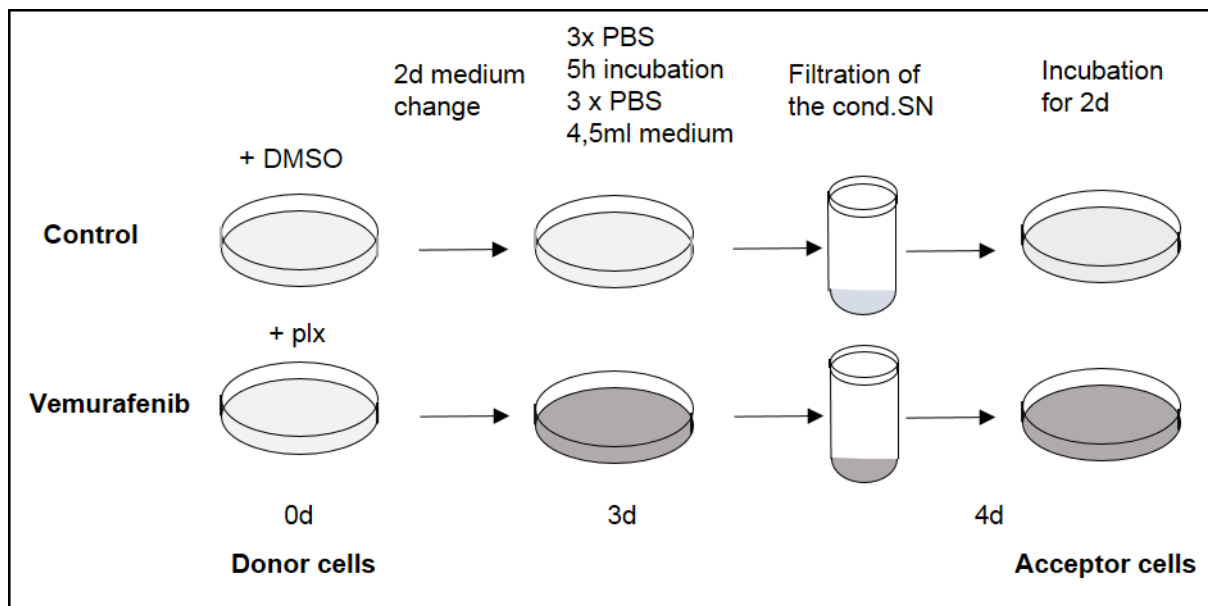
Figure 4: Schematic view of the protocol used for CSN generation. CSN was generated from melanoma cells treated for 3 d with vemurafenib. After excessive washing with PBS, donor cells were incubated over night with fresh dial D2. The medium was filtered through 0,45µm membrane filters the following morning and was termed conditioned supernatant (CSN). Subsequently, it was applied to the acceptor cells, which were prestarved for 3 d before treatment.

MTT measurements showed that the conditioned supernatant of all melanoma cells used as donors in this experiment increased the cellular viability of the acceptor cells. This was true for the melanoma cell lines M14, UACC-62 and A375 as well as the fibroblast cell line WI-38 (Fig. 5 a).

As described previously by our group, vemurafenib treated melanoma cells tend to increase their cellular size after extended treatment with vemurafenib and become senescent (Haferkamp *et al.*, 2013). In Figure 5 a, the CSN was harvested at similar cell confluency. To ensure that the stimulating effect of the BRAF inhibitor CSN was not caused by depletion of the medium in the control situation, donor cells were seeded in different numbers. In Figure 5 b seeded numbers of the control and the vemurafenib treated donor cells were chosen to acquire an approximately even cell count on the day of the CSN harvest. The cell number strongly depended upon the growth rate and the size of the three melanoma cell lines used in this experiment. As acceptor cells the human fibroblast line MainUro was used. After two days of incubation with the CSN we could also observe a proliferation stimulating effect in the fibroblasts treated with vemurafenib CSN (Fig. 5 b).

As the vemurafenib CSN had such an unexpectedly strong effect on the acceptor cells, we concluded that the supernatant contained growth-promoting factors. Many of these factors mediate their signals through receptor tyrosine kinases (RTK). To test if this could be the case,
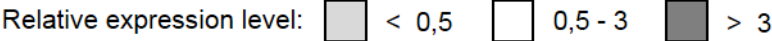
an antibody directed against phosphorylated tyrosine was used on protein lysates of vemurafenib – and control-CSN-treated acceptor cells (Fig. 5 c). Lysates from M14 cells treated with vemurafenib CSN showed an increased tyrosine phosphorylation at high molecular weight. Various RTK are in this size range, for example the EGF receptor (170kDa), PDGF receptor α (195 kDA), VEGFR 1 (180kDa) and the FGF receptor 1 (120 kDa), suggesting that the vemurafenib CSN contains an increased concentration of RTK-activating ligands.
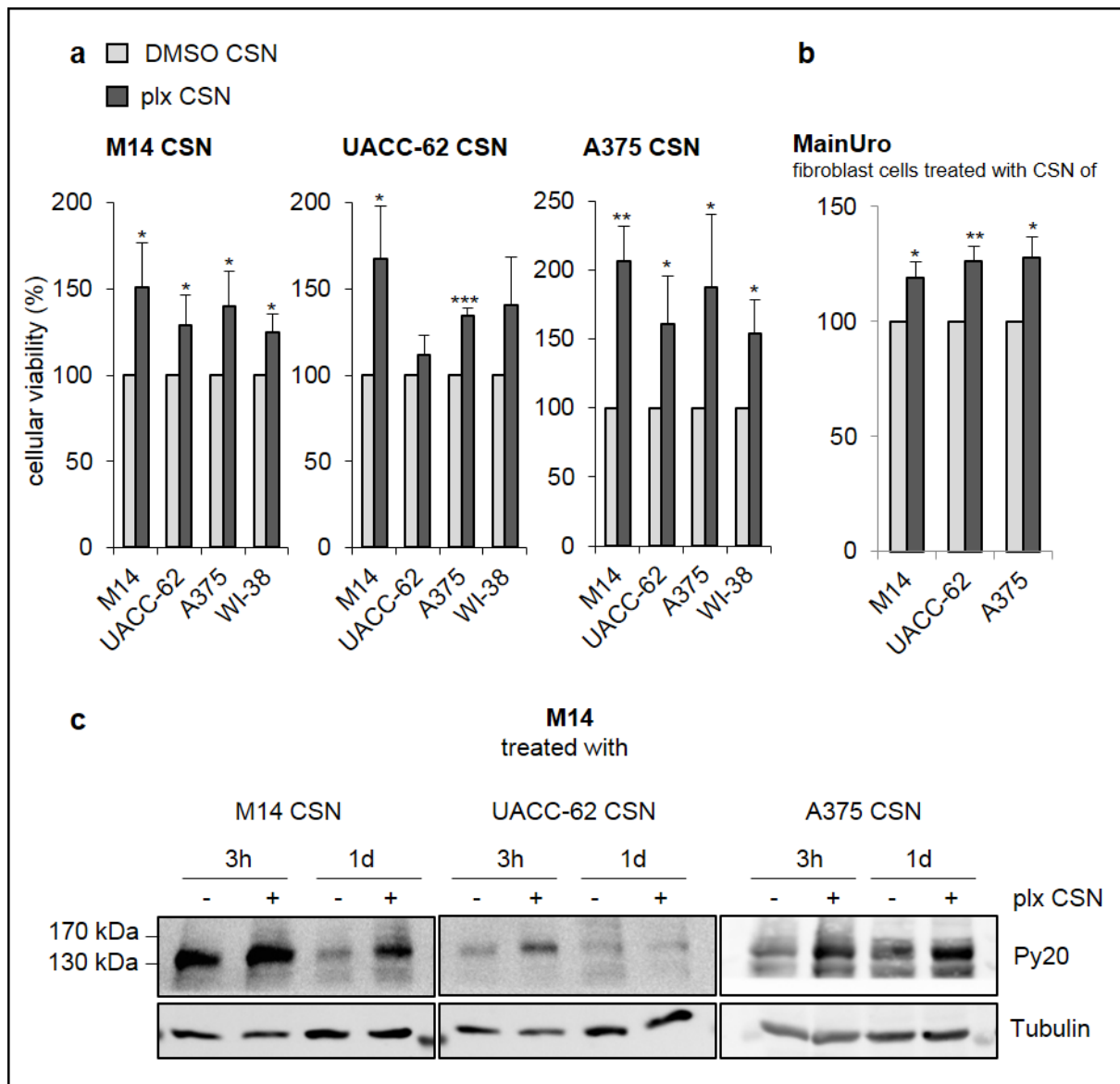
Figure 5: Treatment of melanoma cells with CSN. (a) MTT assays of the melanoma cell lines M14, UACC-62, A375 and the fibroblast cell line WI-38 treated for 48 h with DMSO and vemurafenib CSN of M14, UACC-62 and A375 cells. **(b)** MainUro fibroblasts were treated with CSN of M14, UACC-62 and A375 cells as in (a), except donor cells were seeded to ensure that the DMSO control and the vemurafenib treated cell lines have the same cell number at the day of CSN harvest. **(c)** M14 acceptor cells were pre-starved for 1 day and treated for 3 h and 1 d with CSN of different cell lines. Phosphorylation status was determined via western blot with Py20, an unspecific anti-phosphotyrosine antibody.

5.1.2. Expression of different secretome associated genes after vemurafenib treatment

Next, we wanted to identify the factors which can mediate the growth-promoting effect. The SASP factors, which are secreted in response to different senescence triggers, are often overlapping. Using several studies on stress-induced melanoma senescence, we compiled a panel of genes, which are frequently altered, and tested their expression in response to vemurafenib in three BRAFV600E mutated cell lines (Table 18) (Kuilman and Peeper, 2009) (Ohanna *et al.*, 2011). In all cases, the cytokine *CCL2* and the matrix metalloprotease 2 (*MMP2*) were upregulated, while the cytokine *CXCL8* was strongly downregulated. Furthermore, the fibroblast growth factor *FGF1* was strongly and significantly upregulated in the cell lines UACC-62 and A375. FGF1 can activate all four known FGF receptors and has strong mitogenic and angiogenic potential (Raju *et al.*, 2014). C-C Motif Chemokine Ligand 2 (*CCL2*), also known as chemokine monocyte chemoattractant protein-1 (*MCP1*) regulates inflammatory response by attracting monocytes, memory T cells and dendritic cells (Szade *et al.*, 2015). It has been shown that tumor formation of a previously poorly tumorigenic melanoma cell line increases after transfection with a CCL2 expression vector, initiating the growth of a profuse vascular network (Gazzaniga *et al.*, 2007).

Relative expression level: ☐ < 0,5 ☐ 0,5 - 3 ■ > 3

M14		UACC-62		A375	
3d 2µM vemurafenib		3d 2µM vemurafenib		3d 2µM vemurafenib	
CCL2	3,6 (+/- 1,7)	CCL2	4,6 (+/- 1,9)**	CCL2	41,2 (+/- 22,4)**
CTGF	2,6 (+/- 2,4)	CTGF	2,2 (+/- 0,8)	CTGF	0,4 (+/- 0,2)**
FGF1	1,0 (+/- 0,5)	FGF1	7,9 (+/- 2,7)**	FGF1	49,6 (+/- 16,5)**
FGF2	0,4 (+/- 0,3)**	FGF2	0,5 (+/- 0,2)**	FGF2	0,9 (+/- 0,3)
IL6	1,1 (+/- 0,5)	IL6	1,3 (+/- 0,5)	IL6	1,5 (+/- 0,4)
CXCL8	0,3 (+/- 0,2)**	CXCL8	0,0 (+/- 0,0)**	CXCL8	0,1 (+/- 0,0)**
PLAUR	0,3 (+/- 0,1)**	PLAUR	0,8 (+/- 0,5)	PLAUR	0,7 (+/- 0,4)
MMP2	16,8 (+/- 6,9)**	MMP2	10,2 (+/- 4,4)**	MMP2	7,9 (+/- 2,8)**

Table 18: Expression of different secretome associated genes after vemurafenib treatment. M14, UACC-62 and A375 were treated with vemurafenib (2 µM) or DMSO for 72 h. mRNA levels were determined by real-time PCR. Medium was once changed 48 h after the start of the experiment.

Proteinases like MMP2 are able to alter the tumor microenvironment by degrading specific substrate proteins, including those of the extracellular matrix. By targeting gelatin, MMP2 increases the invasive potential of tumor cells by enhancing their mobility through the cellular matrix (Fanjul-Fernández *et al.*, 2010). In Figure 6 a, the secreted levels of MMP2 in the vemurafenib CSN are visualized by western blot, proving that MMP2 is secreted into the medium. In the cell lines MDA-MB-435, A375 and to a lesser extent in Malme 3M, the higher MMP2 levels correlate with higher vemurafenib concentrations. Only in case of the cell line SK-MEL-28, the effect of the vemurafenib CSN on MMP2 is rather weak. To test if the secreted MMP2 is enzymatically active, I performed zymography analyses and observed that gelatin lysis was enhanced in all cell lines that were sensitive to BRAF inhibition (Fig. 6 b).
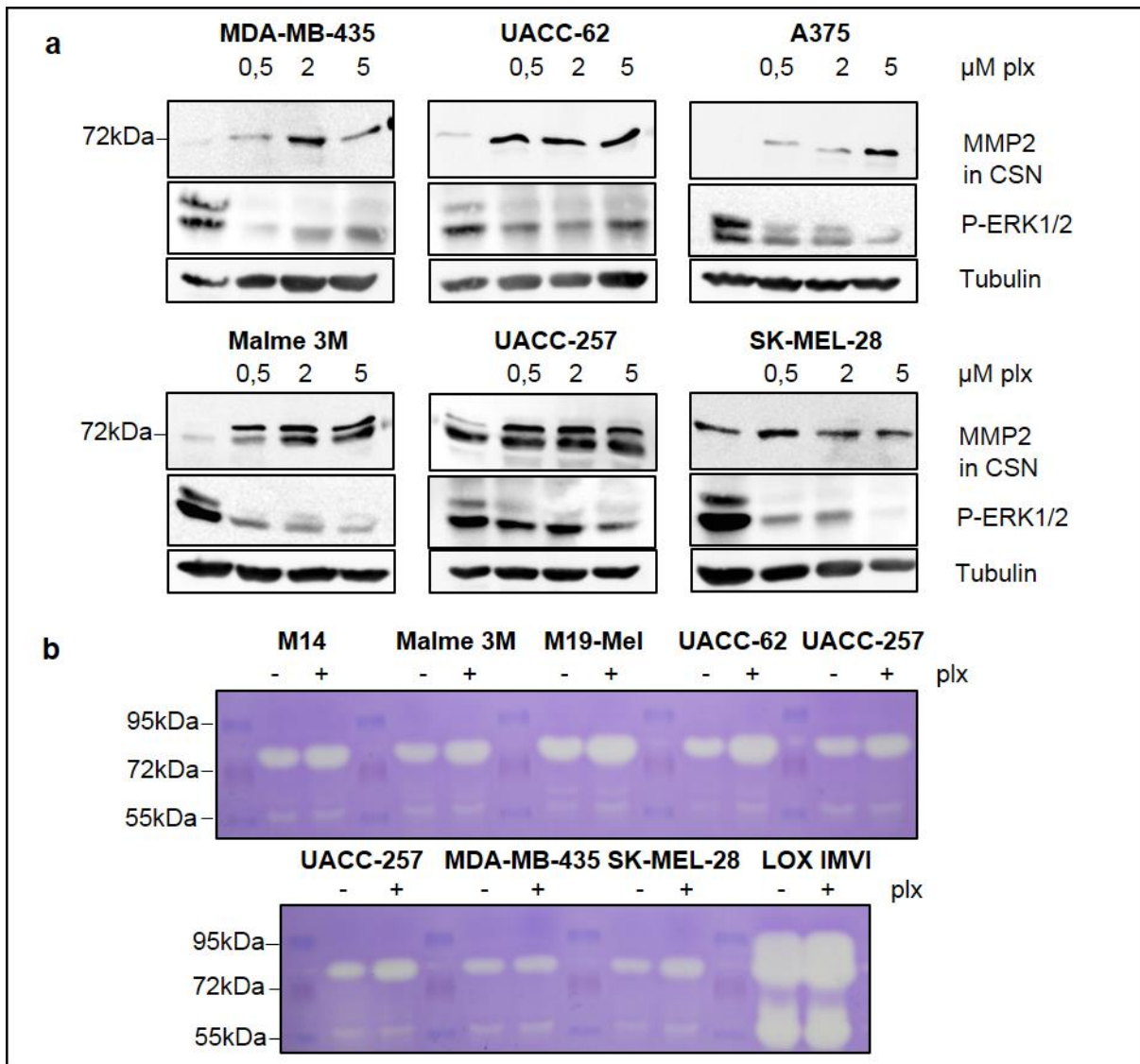
Figure 6: MMP2 in the CSN of vemurafenib treated melanoma cells. (a) The cell lines were treated with different concentrations of vemurafenib (0,5 µM, 2 µM, 5 µM) or DMSO for 72 h with a medium change after 48 h. Thereafter cells were incubated overnight in dial D2 with the respective vemurafenib concentrations, harvested on the next day, and loaded after preparation on a protein gel. Blots were probed with MMP2 and P-ERK p42/44 (Thr202/Tyr204) antibodies. **(b)** Zymogram with 15µl of the CSN prepared as described in (a). CSN were loaded on a 1% gelatin gel and seperated. Gels were then incubated over night at 37°C and stained with Coomasie Blue. LOX IMVI cells are not affected by BRAFV600E inhibition by vemurafenib (Haferkamp *et al.*, 2013).

5.1.3. FGF receptor abundance in n melanoma cells and regulation of FGF transcription after vemurafenib treatment

Since a significant transcriptional upregulation of *FGF1* could be observed in melanoma cell lines treated with vemurafenib, the FGF receptor abundancy and therefore the ability of the ligand to induce FGF signaling in the probed cell lines was examined (Fig. 7 a). RT-PCR was performed with cDNA from different melanoma cell lines and a fibroblast line and later visualized on a gel. RNA extraction and cDNA synthesis was performed simultaneously with all probes to ensure comparability. The fibroblast cell line MainUro expressed three of the four known FGF receptors. In the panel of melanoma cells, *FGFR1* seemed to be the most abundant receptor and is expressed in all three tested lines. The other FGF receptors are expressed in UACC-62 and A375 cells on a low level, while in M14 cells no noteworthy transcription takes place.

The observation of increased *FGF1* transcription after BRAF inhibitor treatment implied an influence of the FGFR signaling axis in the proliferation promoting potential of the vemurafenib CSN. We therefore checked, whether additional ligands of the FGF family are increased upon BRAF inhibition (Fig. 7 b). A more than two fold elevated transcription of *FGF1*, *FGF5*, *FGF7*, *FGF11* and *FGF17* could be observed in at least two of three vemurafenib treated cell lines (M14, UACC-62, A375), arguing for the role of FGF ligands in the stimulating effect of the vemurafenib CSN.

To further validate our findings, we performed a protein-based analysis of the vemurafenib CSN of the cell line A375 (Fig. 7 c). We could confirm the increase of CCL2 and FGF1, as well as the decrease of CXCL8 in the CSN. Interestingly, also IGFBP-2 and IGFBP-3 were found to be decreased. These two secreted proteins are able to bind and sequester insulin and the growth factors IGF1 and IGF2 in the extracellular environment (Hwa, Oh and Rosenfeld, 1999). Furthermore it has been shown recently that IGFBP-3 can reduce melanoma growth in an *in vivo* mouse model (Naspi *et al.*, 2014).
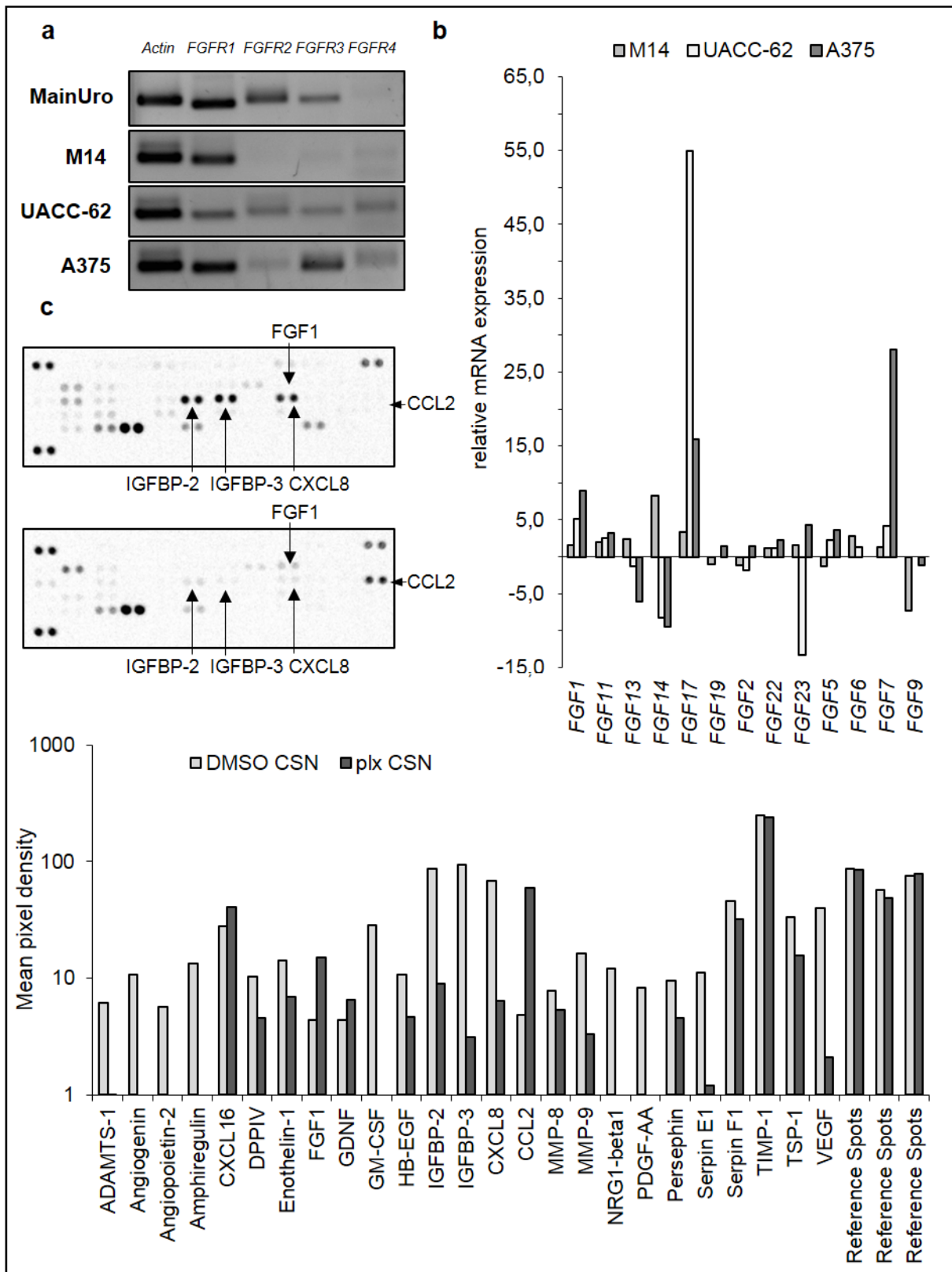
Figure 7: FGF signaling and growth factor regulation after vemurafenib treatment. (a) FGFR RT-PCR (40 cycles) was performed with cDNA of naive MainUro fibroblasts and the melanoma cell lines M14, UACC-62 and A375. RT-PCR products were run in a 1% agarose gel. **(b)** Human growth factor PCR Array was performed with cDNA from M14, UACC-62 and A375 cells, which were treated for 3 d with vemurafenib (0,5µM). Medium was changed after 48 h and the experiment was performed according to the manufacturer's protocol. **(c)** The Proteome Profiler Human Angiogenesis Antibody Array from R&D Systems was used to determine changes on protein levels of different angiogenesis related factors in A375 CSN after vemurafenib treatment for 4 d.

5.1.4. Influence of FGF1 on cellular phosphorylation status and proliferation rate

The finding that several ligands of the FGF family are induced upon BRAF inhibitor treatment is of potential high relevance for melanoma biology, as FGFs are potent mitogens with numerous pro-tumorigenic abilities. By secreting FGFs, melanoma cells might strongly affect other melanoma cells and cells from the tumor niche, thereby possibly diminishing the effect of the BRAF inhibitor. Thus, I focused on the potential effects of FGFR signaling in melanoma. To independently test whether FGF1 is able to alter signal transduction in melanoma cells, we treated different cell lines for 20 minutes or 2 h with recombinant FGF1 (Fig. 8 a). We tested alteration in P-Tyr, which indicates RTK activation, as well as an activation of the downstream components P-ERK1/2 and P-AKT. A375 and M14 cells showed a transient increase of a tyrosine-phosphorylated large molecular weight protein. Furthermore, while no significant differences could be observed in ERK phosphorylation, AKT phosphorylation was altered in the treated cell lines. In the short-term treatment A375 cells showed an increase, which was back at normal levels after 2 h. All other cell lines revealed a transient diminished P-AKT signal after 20 minutes that reversed back to normal levels after 2 h. These data indicate that all cell lines respond to FGF1, although with different effects and kinetics.

To investigate if cellular viability of human fibroblasts stimulated with recombinant FGF1 is comparable to stimulation with vemurafenib CSN, we treated two fibroblast cell lines with recombinant human FGF1. In both cell lines, viability was increased after addition of the growth factor (Fig. 8 b) to a level resembling stimulation with vemurafenib CSN (Fig. 5).
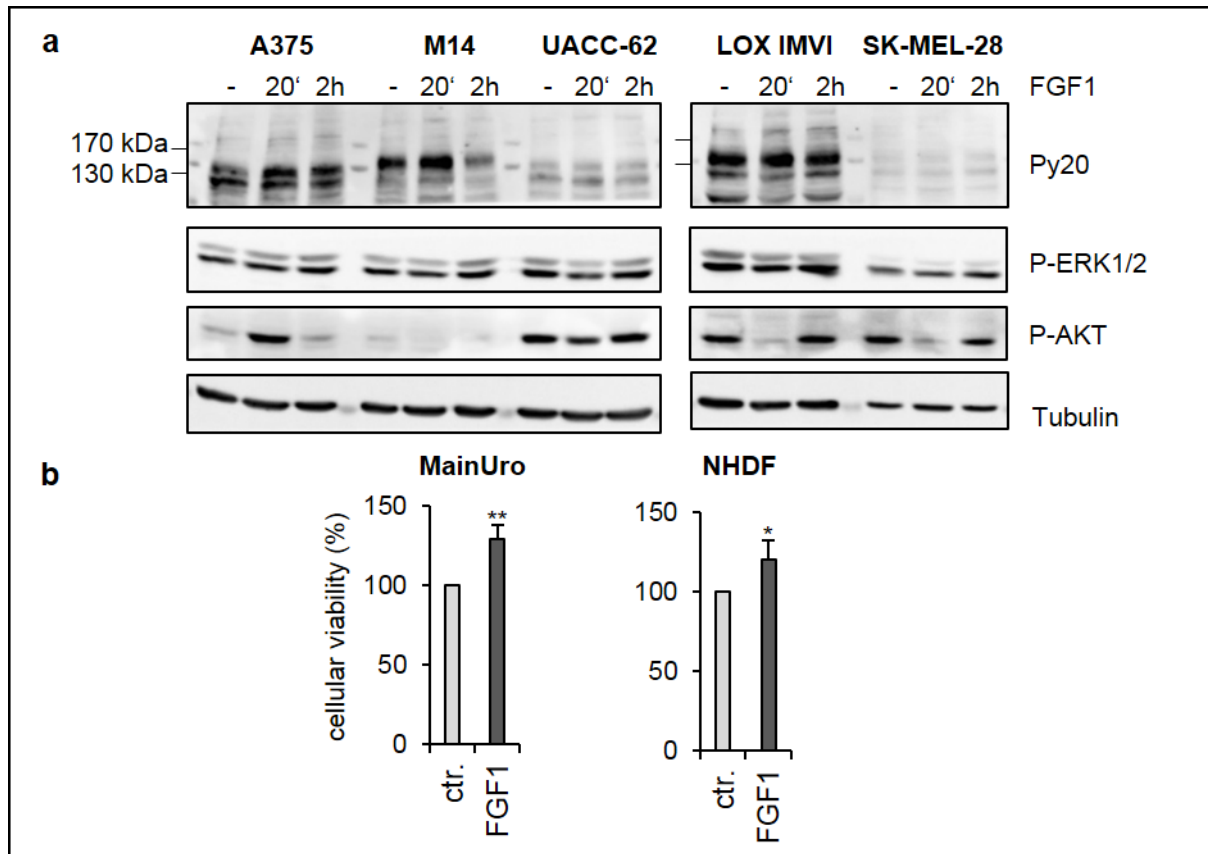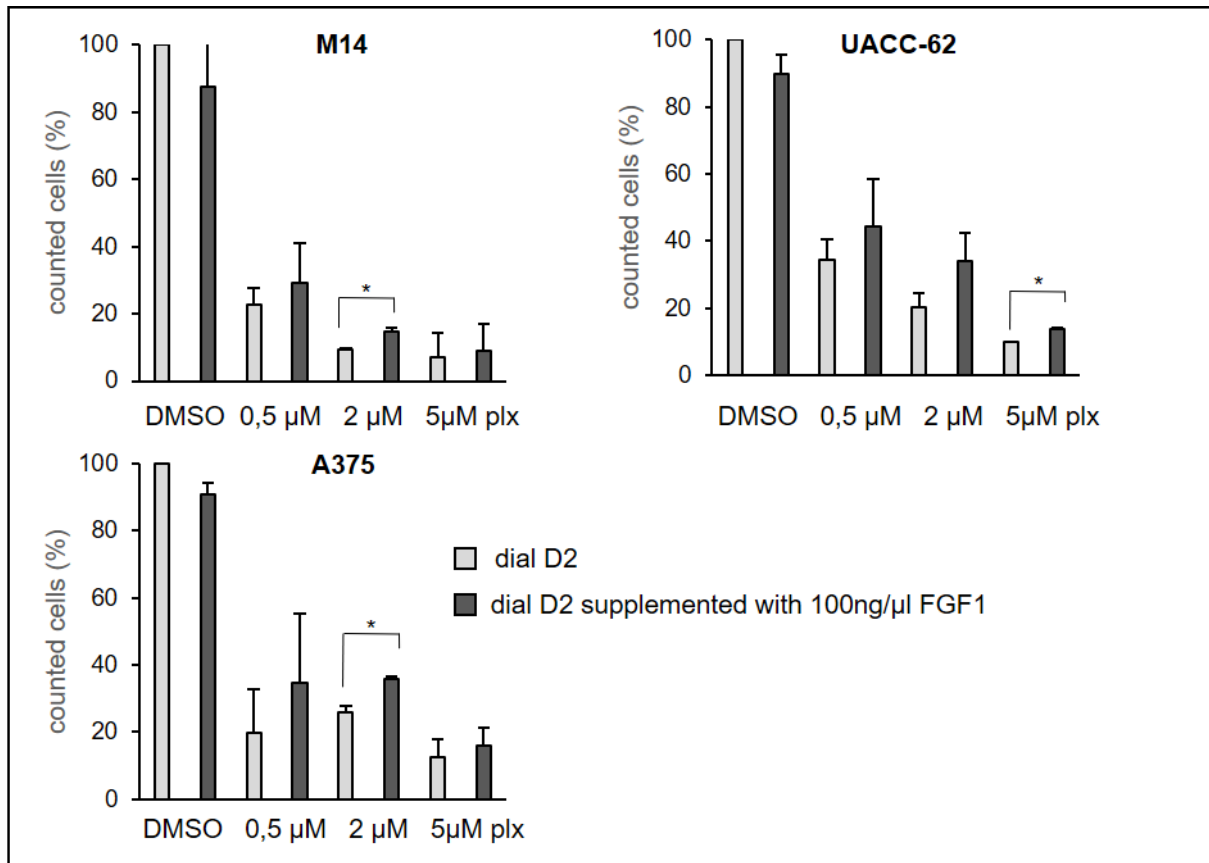
Figure 8: Effects of recombinant FGF1 treatment. **(a)** Western blot with lysates of cells, which were starved for 24h in dial D2, and were then treated for 20 minutes or 2 hours with 50 ng/ml recombinant human FGF1, respectively. Phosphorylation status was determined with antibodies against P-Tyr (Py20), P-AKT (Ser473) and P-ERK p42/44 (Thr202/Tyr204). **(b)** MTT assay of the fibroblast cell lines MainUro and NHDF in dial D2 treated for 5 d with recombinant FGF1. 1000 cells were seeded per 96 well and medium with the recombinant ligand was changed every 48 h.

5.1.5. Protective effect of FGF1 on vemurafenib treated melanoma cells

To test if FGF1 could facilitate the ability of melanoma cells to survive BRAF inhibition, FGF1 was added to vemurafenib treated melanoma cells. Addition of recombinant FGF1 did not significantly alter the proliferation of starved melanoma in absence of vemurafenib (Fig. 9). However, the addition of human FGF1 was able to enhance survival after vemurafenib treatment in all cell lines. Although the differences did not reach significance in all cases, the trend was continuously observed under all conditions. The proliferation rates of all three melanoma cell lines under vemurafenib pressure increased after FGF1 supplementation. This growth factor can save human melanoma cells from BRAF inhibition, arguing for its beneficial role in the CSN and cellular survival under MAPK inhibition.

Figure 9: Recombinant FGF1 protects melanoma cells from BRAF inhibition. Proliferation assay of M14, UACC-62 and A375 cells after 5 d treatment with vemurafenib (2 µM) and recombinant FGF1 (100 ng/ml). To only analyze the effect of recombinant FGF1 we used dial D2, because in 10% full medium the additional growth factor would meet an array of many different proliferation-stimulating proteins. Medium and compounds were changed every 48 h. Data is presented as % of cells in the untreated control.

5.1.6. FGFR inhibitor enhances the inhibitory effect of BRAF inhibition

Next, it was examined if the specific FGFR inhibitor AZD 4547 affects cellular viability of melanoma cells under vemurafenib pressure in absence or presence of recombinant FGF1 (Fig. 10). Surprisingly, addition of 100 ng/µl AZD 4547 elevated the proliferation rate of UACC-62 and A375 cells, suggesting that compensatory activation of other pathways might have taken place. A higher concentration (1000 ng/µl) effectively diminishes the viability of all cell lines. Blockade of the intrinsic BRAFV600E signal with vemurafenib decreased the viability of all cell lines, as expected. This effect was less pronounced in the presence of recombinant FGF1, but was reconstituted when AZD 4547 was added. In absence of FGF1, AZD 4547 decreased the survival of melanoma cells when vemurafenib was used at a concentration of 2 µM. This was visible at 100 and 1000 ng/ml AZZ 4547. In summary, the FGFR inhibitor was able to enhance the inhibitory effect of vemurafenib.
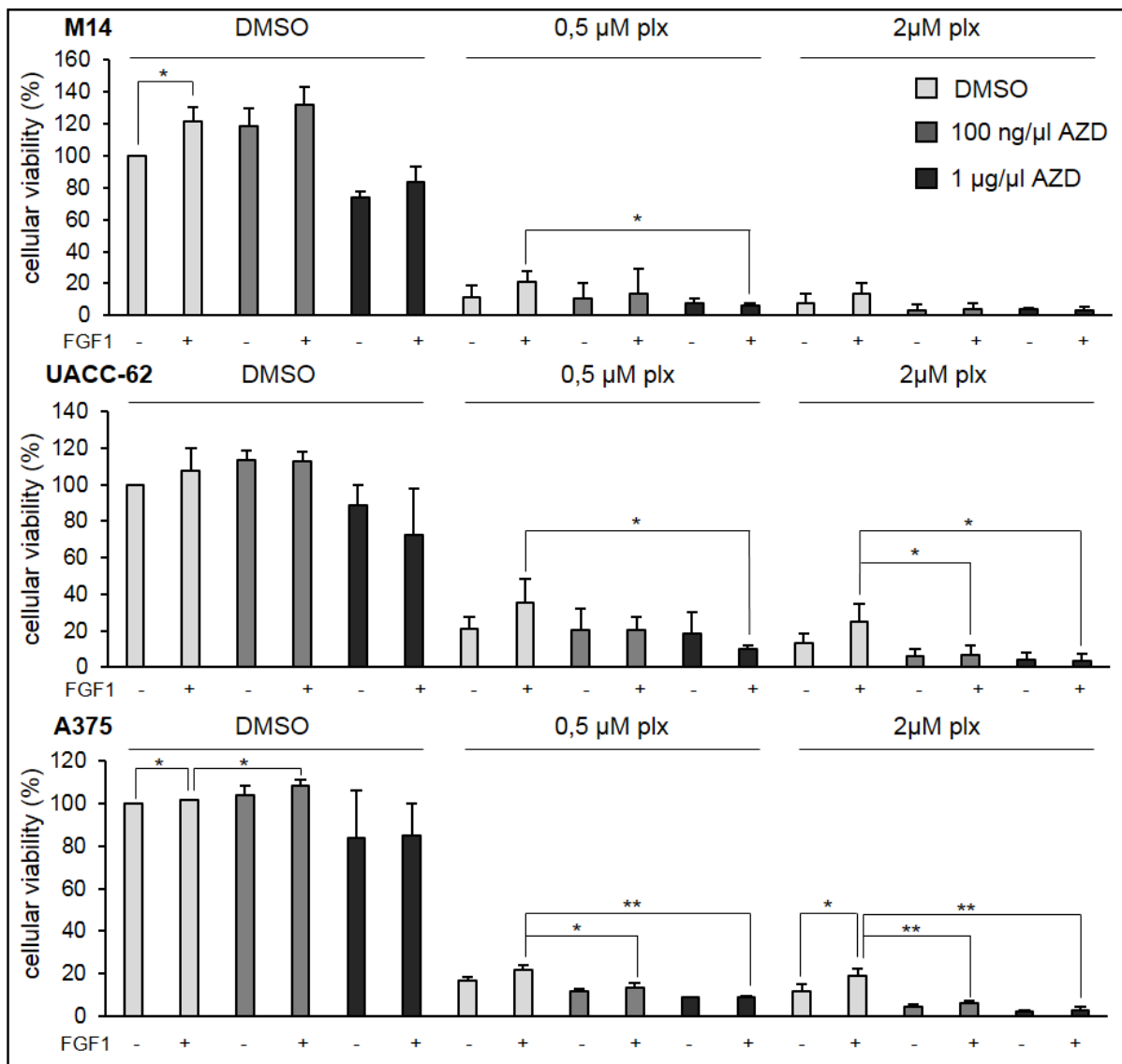
Figure 10: The specific FGFR inhibitor AZD 4547 impedes the protective effect of recombinant FGF1 on melanoma cell lines after BRAF inhibition. Cell lines in a 96 well plate in dial D2 were treated for 5 d with vemurafenib (0,5 µM, 2 µM), AZD 4547 (100 ng/µl, 1 µg/µl) and FGF1 (100 ng/ml). Medium was changed every 48 h, cellular viability was measured with an MTT test. Experiment was done three times, except AZD 4547 1µg/µl, which was done twice.

5.1.7. Relevance of FGFR signaling on the growth promoting effect of vemurafenib CSN

Next, it was tested if FGFR inhibitor affects the proliferation stimulating effects of vemurafenib CSN (Fig. 11). The vemurafenib CSN was able to enhance the viability of acceptor cells in all cases. Addition of 100 ng/µl of the FGFR inhibitor did not affect this stimulatory effect. However, at a concentration of 1000 ng/ml, the inhibitor significantly blocked the vemurafenib-mediated effect in several cell lines. The fact that AZD 4547 also inhibited viability of acceptor cells when it was added to control CSN suggests that basal FGF signaling also plays a role under control conditions. Altogether, the data indicate that FGFR signaling is involved in the

growth-promoting effect of vemurafenib CSN. However, since other growth promoting factors were also found to be elevated after vemurafenib treatment, the increased cellular viability could also be mediated by several additional ligands.
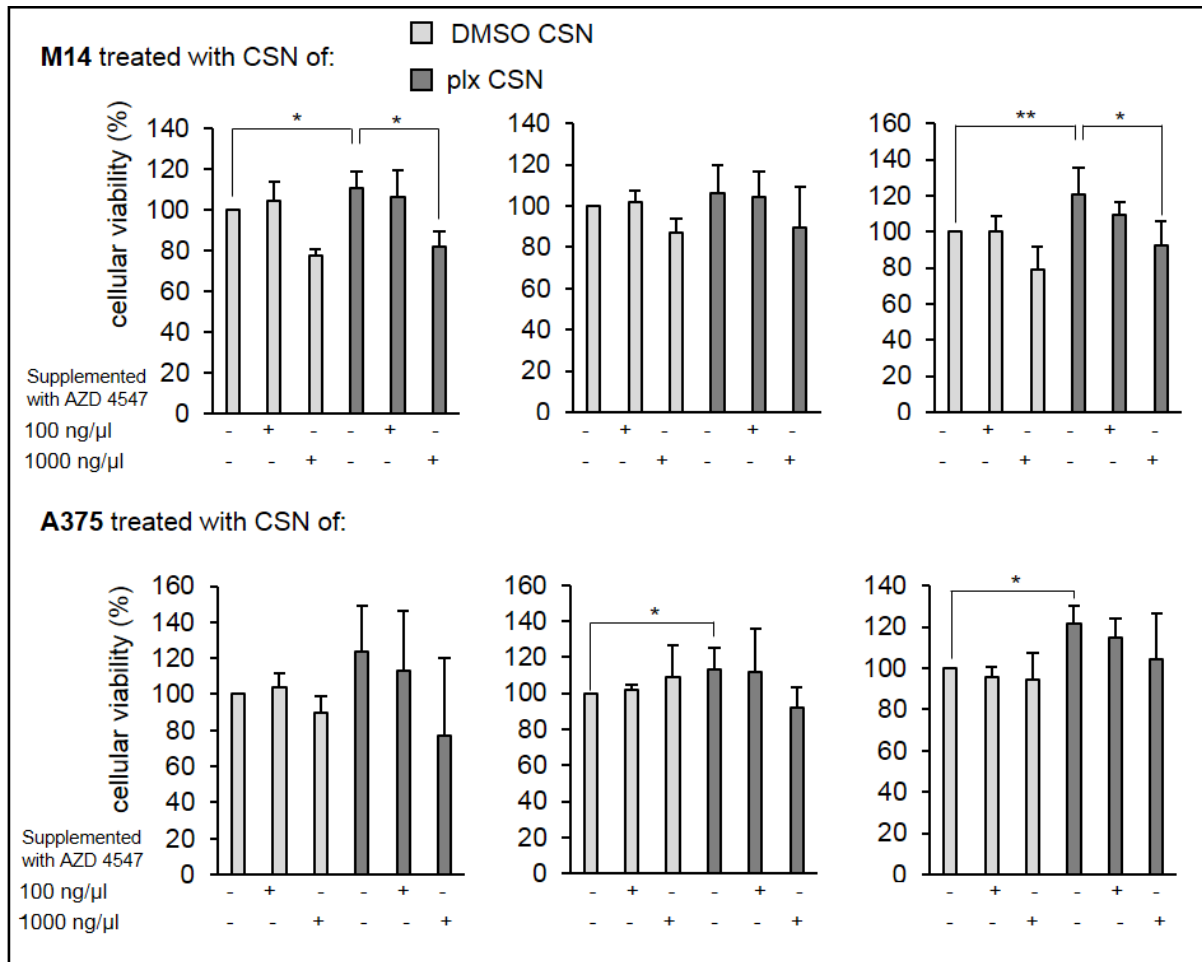
Figure 11: FGFR inhibition impedes the proliferation stimulating effect of CSN from melanoma cell lines treated with vemurafenib. CSN of M14, UACC-62 and A375 cells was produced as described in Figure 4. Acceptor cell viability (M14, A375) was measured 48 h after start of the incubation with the various CSN combined with the specific FGFR inhibitor AZD (100 ng/µl, 1000 ng/µl). UACC-62 were omitted as acceptor cells, because of their slow proliferation rate. Donor cells in the control and BRAF inhibitor treated situation were seeded to achieve an approximately even cell number at the day of CSN harvest.

5.2. Pathways resulting in the secretory phenotype of BRAF inhibitor induced senescence

5.2.1. Alteration of MAPK, PI3K and NF-κB pathways

The establishment of a BRAF inhibitor specific secretome seems to depend upon the loss of intrinsic BRAFV600E signaling through the MAPK pathway. However, as seen in other studies, a shutdown of signaling through this axis can induce the activation of other pathways responsible for cellular growth and survival. The AKT pathway for example can be activated by the downregulation of the feedback proteins SPRED1 and SPRED2 after MEK inhibition and it has been shown that vemurafenib activates AKT signaling by inducing the expression of c-Jun and RHOB (Haydn *et al.*, 2014).

Besides the signaling through this axis, we also investigated the activation of the NF-kappa B pathway by using a phospho-specific antibody, as NF-κB is a major player in the induction of immunoactive secreted factors.

Seven melanoma cell lines with mutant BRAFV600E were treated for three days with increasing concentrations of vemurafenib, as shown in Figure 12. All cell lines displayed a sustained decrease in ERK1/2 phosphorylation, indicating the efficacy of the BRAF inhibitor. Similarly, all cell lines showed a dose dependent decrease in NF-kappa B signaling after vemurafenib treatment. The P-AKT levels on the other hand were upregulated in the cell lines A375, MDA-MB-435, UACC-62, while the other melanoma lines (M14, Malme 3M, UACC-257, SK-MEL-28) showed a decrease in the overall phosphorylation status of AKT.

In conclusion, an enhanced activation of the PI3K/AKT pathway after BRAF inhibition is visible in almost half of the investigated cell lines. This might help them to survive the sudden lack of MAPK pathway stimuli. However, it is unclear whether this has implications on senescence induction and the expression of SASP genes.
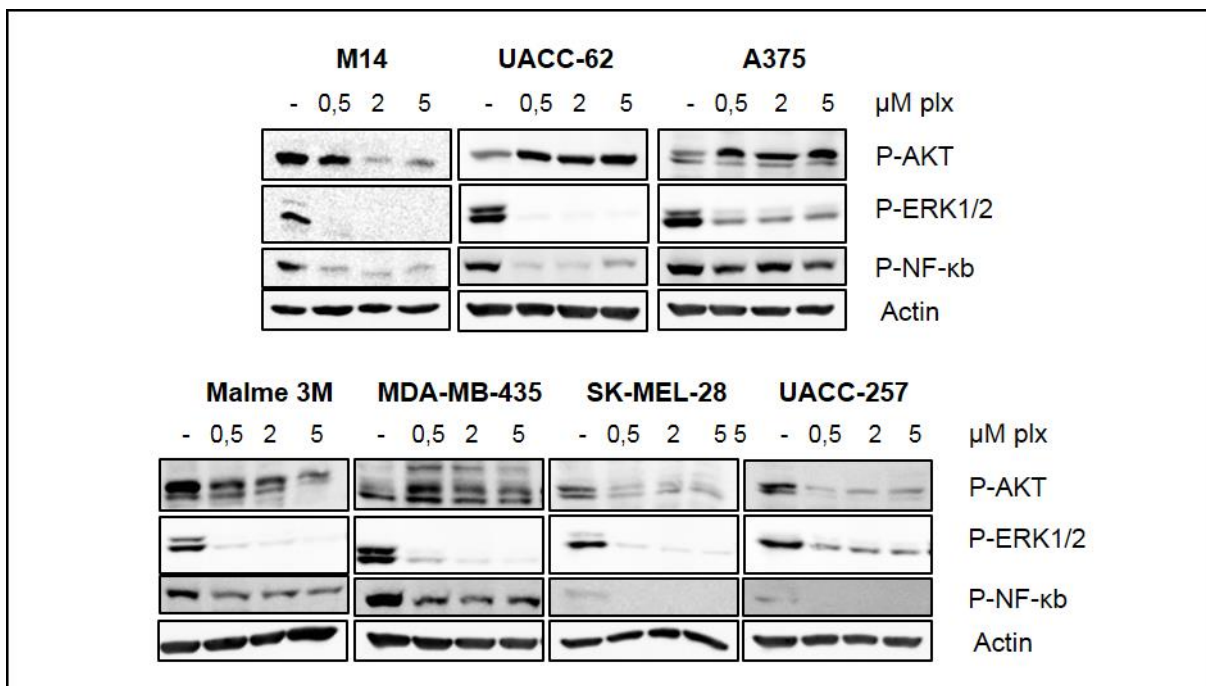
Figure 12: Phosphorylation status of different important signaling proteins after vemurafenib treatment. Cell lines were treated for 3 d with 0,5, 2, or 5 µM vemurafenib. Medium was changed and the BRAF inhibitor was replaced after 48 h. After harvest at day 3, the levels of P-AKT (Ser473), P-ERK p42/44 (Thr202/Tyr204) and P-NF-κB p65 (Ser536) were determined via western blot.

5.2.2. Effects of combined MAPK and AKT inhibition on senescence features

To analyze a potential influence of the increased P-AKT levels on the senescence phenotype after BRAF inhibition, the dual PI3K/mTOR inhibitor BEZ-235 was used to shut down signaling through the PI3K/AKT axis. First, we tested the influence of PI3K/AKT blockade on the senescence induction after vemurafenib treatment (Fig. 13 a). We used three cell lines: M14 cells (incapable of compensatory PI3K/AKT activation) and UACC-62 as well as A375 (capable of compensatory PI3K/AKT activation, as seen in Fig. 12). In all three cell lines, BEZ alone did not induce SA-β Gal staining or changes in cell morphology. Furthermore, the BRAF inhibitor mediated SA-β Gal staining was prevented in presence of BEZ. This proves that the induction of the senescent arrest depends in part upon active AKT signaling.

To test if independent inhibitors of the MAPK and PI3K pathways give similar results, the experiment was performed with the MEK inhibitor PD184352 (as MEK1/2 are located downstream of BRAFV600E) and the PI3K inhibitor GDC0941 (Fig. 13 b). Similar to vemurafenib, treatment with the MEK1/2 inhibitor strongly increased SA-β-Gal staining, indicating that senescence is caused by both BRAF and MEK inhibition. Although the PI3K inhibitor GDC0941 reduced cell numbers in presence of MEK inhibitor, SA-β Gal staining was reduced, as observed previously for vemurafenib/BEZ combination.

Next, we tested the effect of BEZ-235 on the transcription of different genes relevant for the vemurafenib-induced secretome. Since compensatory EGFR signaling was shown to be highly relevant for the initial response to BRAF inhibition, we also investigated *EGF* transcript levels (Haydn *et al.*, 2014) (Sun *et al.*, 2014). Indeed, *EGF* was significantly elevated after vemurafenib treatment in A375 cells (Fig. 14). Interestingly, the administration of BEZ-235 significantly prevented the BRAF inhibitor dependent upregulation of all investigated secretome genes. The only exception was the *CCL2* expression in UACC-62 cells. Here, the standard deviation in the BEZ-treated cells was too high to reach statistical significance.

Besides the emergence of senescent cells after alternative MAPK inhibition with PD 183452, I could furthermore identify an increased transcription of the SASP genes *FGF1*, *MMP2*, *CCL2* in the same cell lines in which their increase was shown by BRAF inhibition. PI3K inhibition had a tendency to prevent this effect (Fig. 15 a). However, this was only significant for *MMP2* transcription in M14 cells and *CCL2* in A375 cells. This suggests that pathway inhibition by BEZ-235 was more efficient than that by GDC-0941.
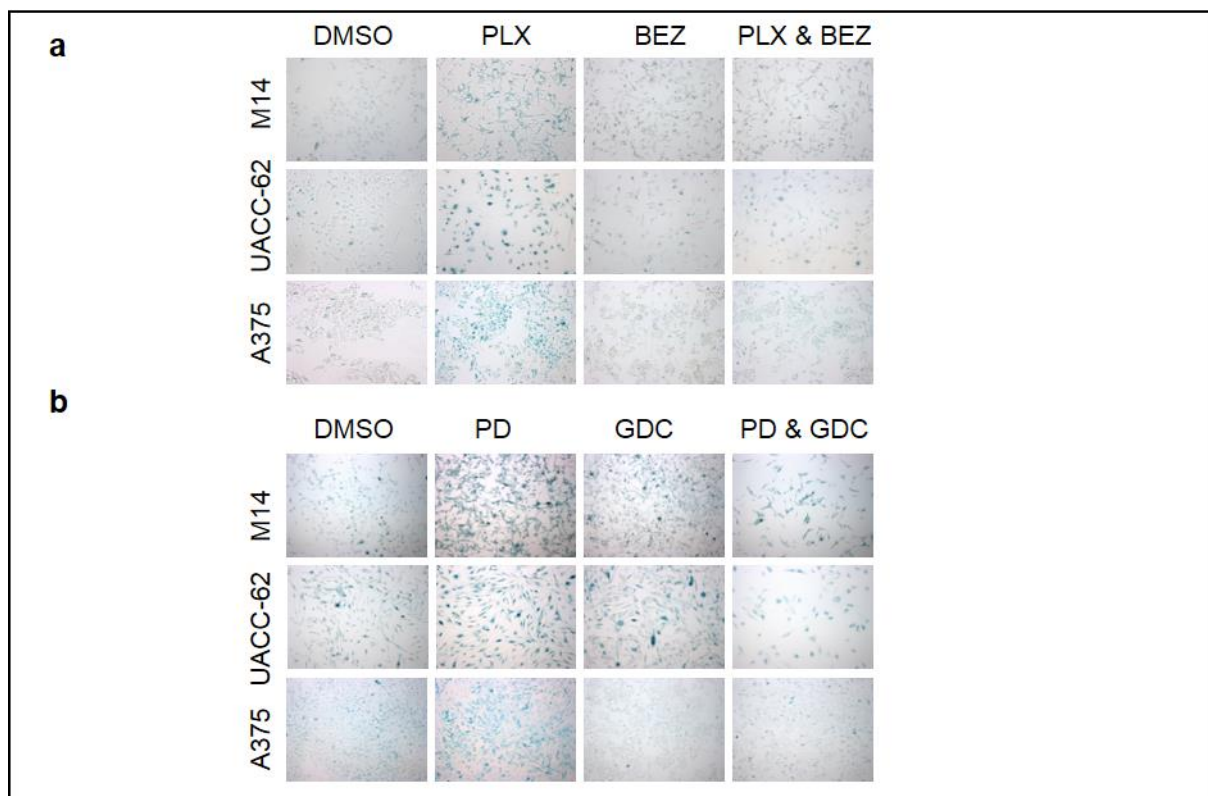
Figure 13: Senescence induction after MAPK and PI3K blockade with different inhibitors. **(a)** Cells were treated for 3 d with 0,5 µM vemurafenib and 0,5 µM of the dual PI3K/mTor inhibitor BEZ 235, as indicated. Medium and inhibitors were replaced at day 2 and cells were stained over night at day 3. **(b)** Cells were treated for 3 d with 0,5 µM PD184352 and 4 µM of the AKT inhibitor GDC 0941, as indicated. Medium and inhibitors were replaced at day 2 and cells were stained over night at day 3.
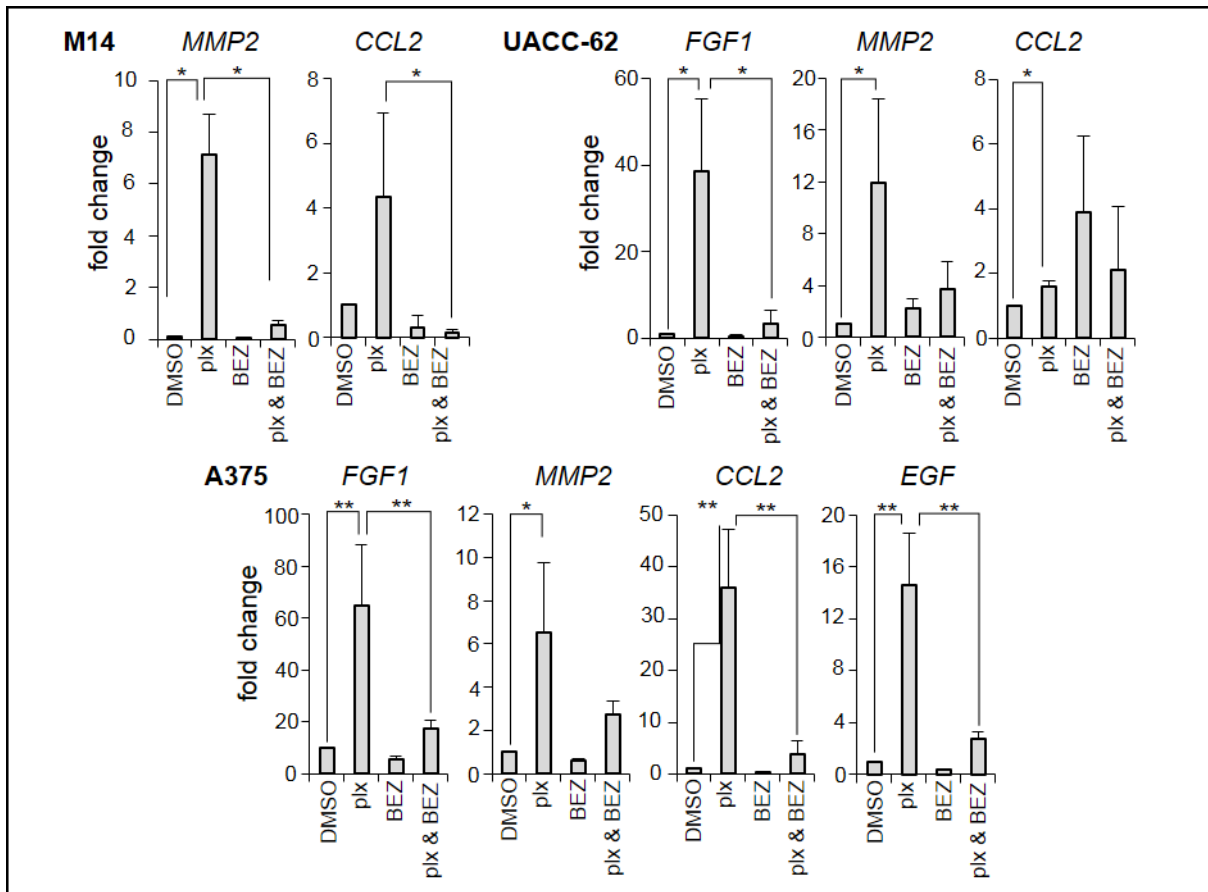
Figure 14: Expression of different SASP factors after treatment with vemurafenib and BEZ-235: Cells were treated for 3d with 0,5 µM vemurafenib and 0,5 µM of the PI3K/mTor inhibitor BEZ-235, as indicated. Medium and inhibitors were replaced after 48h and cells were harvested at day 3. mRNA expression levels were determined relative to actin.

Furthermore, I was interested in the regulation of genes downregulated by BRAF inhibition. As an example we used the gene encoding *CXCL8*, as it was consistently suppressed in all cell lines (Table 18). MEK inhibition suppressed *CXCL8* similar to BRAF inhibition. However, this effect was not dependent on PI3K (Fig. 15 b).
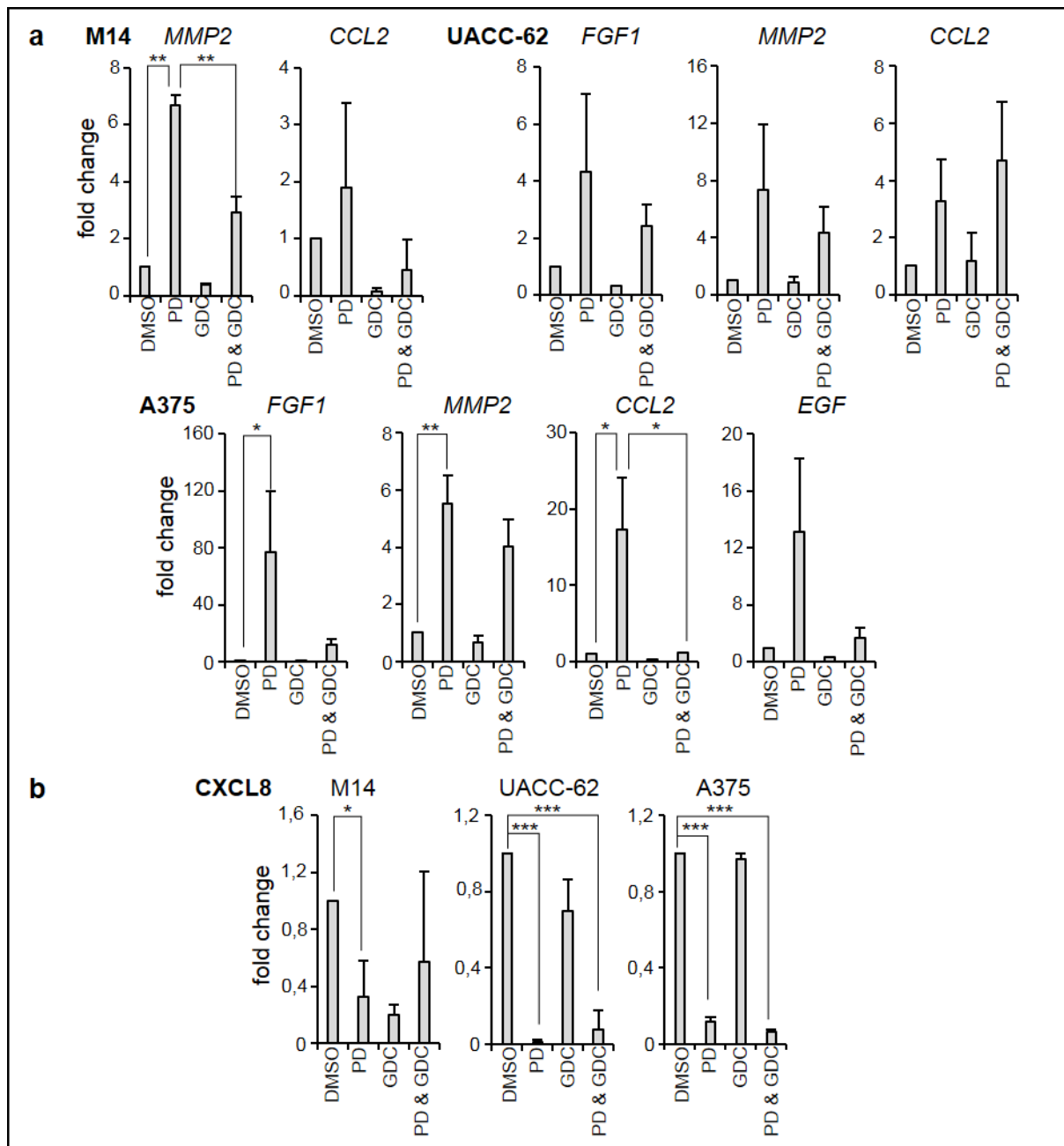
Figure 15: Expression of different SASP factors after treatment with PD 184352 and GDC-0941.
(a) Transcriptional levels of the SASP factors after alternative MAPK and PI3K inhibition. Cells were treated for 3 d with 0,5 μM vemurafenib and with 4 μM of the AKT inhibitor GDC-0941. Medium and inhibitors were replaced after 48h and cells were harvested at day 3. mRNA expression levels were determined via RT-PCR relative to actin. **(b)** Transcription of CXCL8 after MAPK and PI3K inhibition with PD 184352 and GDC-0941. Cells were treated as described in (a).

5.2.3. Therapy-induced senescence by BRAF and MEK inhibition

Inhibition of the MAPK pathway with BRAF and MEK inhibitors proved to be favorable for patients because resistance development and subsequent reactivation of MAPK signaling is impeded if both signaling nodes are inhibited. To check SASP gene induction after dual BRAF/MEK inhibition, the MEK1/2 inhibitor PD 183452 was used in combination with vemurafenib.

BRAFV600E positive melanoma cell lines with moderate or high (M14, UACC-62, A375, Malme 3M, M19-Mel) as well as weak BRAF inhibitor sensitivity (LOX IMVI) were treated with both inhibitors. This led to an induction of senescence, as indicated by the increased SA β-Gal staining pattern (Fig. 16). Only the resistant LOX IMVI cells exhibited no obvious changes in SA β-Gal staining.

To assess the transient changes in signaling during BRAF and MEK inhibition, we treated this cell panel for 1 d and 3 d with both single inhibitors or in combination and monitored P-ERK1/2 and P-AKT status (Fig. 17). In all BRAF-inhibitor sensitive cell lines, ERK1/2 phosphorylation was severely blocked in response to inhibitor treatment. An enhancement of P-AKT was visible in UACC-62, A375 and LOX IMVI cells after three days of treatment. Furthermore, we checked for FOSL1 levels in the cell lines M14, UACC-62 and A375 after 6 d of inhibitor treatment, since it has been described that the secretome establishment after vemurafenib treatment is driven by downregulation of this member of the AP1 transcription factor complex (Obenauf *et al.*, 2015). In all tested cell lines, FOSL1 levels are decreased after BRAF inhibition as well as after MEK inhibition. Next, I checked for the transcriptional levels of the secretome related genes during dual BRAF and MEK inhibition.
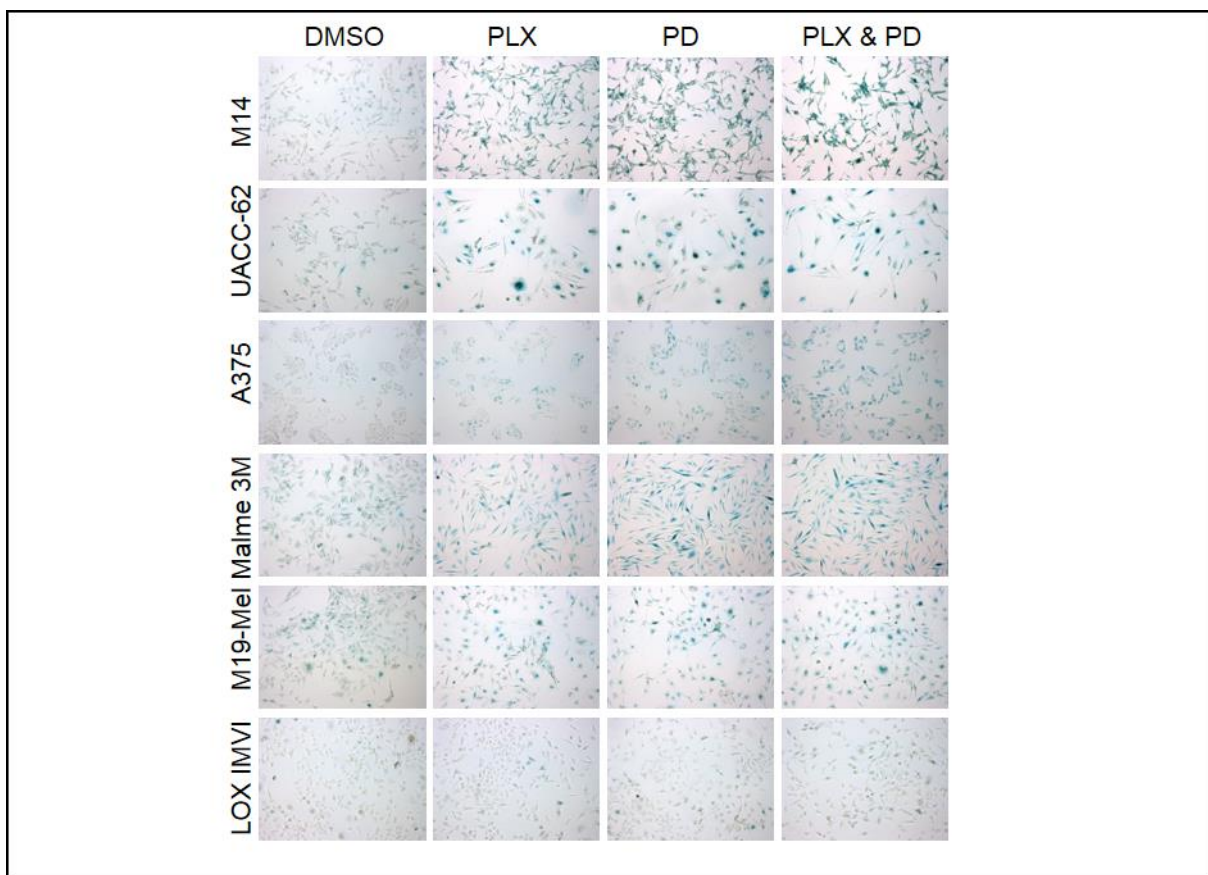
Figure 16: Senescence induction after treatment with vemurafenib and the MEK inhibitor PD 184352. Cells were treated for 3 d with 0,5 µM vemurafenib and 0,5 µM of the MEK inhibitor PD 184352. Medium and inhibitors were replaced after 48 h and cells were stained over night at day 3.
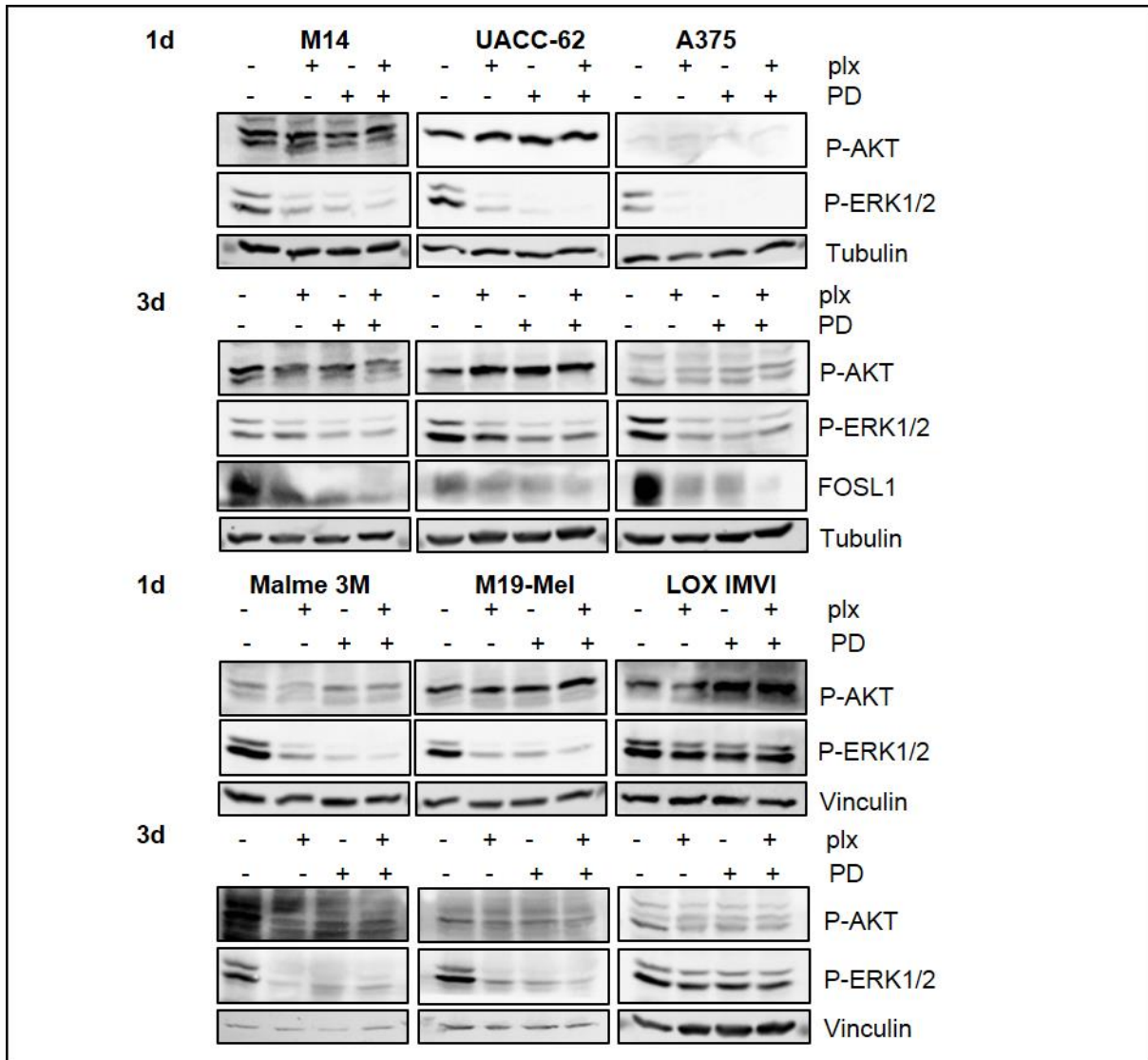
Figure 17: Phosphorylation status of different important signaling proteins after vemurafenib and MEK inhibitor treatment. Cell lines were treated for 3 d with 0,5 µM vemurafenib and 0,5 µM of the MEK inhibitor PD 184352. Medium was changed and the inhibitors were replaced after 48 h. After cell harvest and lysis at day 3, signaling status was determined via western blot with P-AKT (Ser473), P-ERK p42/44 (Thr202/Tyr204) antibodies.

Besides the gene set (*MMP2*, *FGF1*, *CCL2*) I analyzed in the previous experiments, I determined in the dual inhibition setting also the transcriptional levels of *FGF7* and *FGF17* (Fig. 18 a). Due to its absent expression under control conditions, *FGF17* was only analyzed by semiquantitative PCR and was visualized on a gel (Fig. 18 b). In the cell lines that reacted upon single inhibitor MAPK blockade with increased SASP levels, the dual inhibition had the same effect.
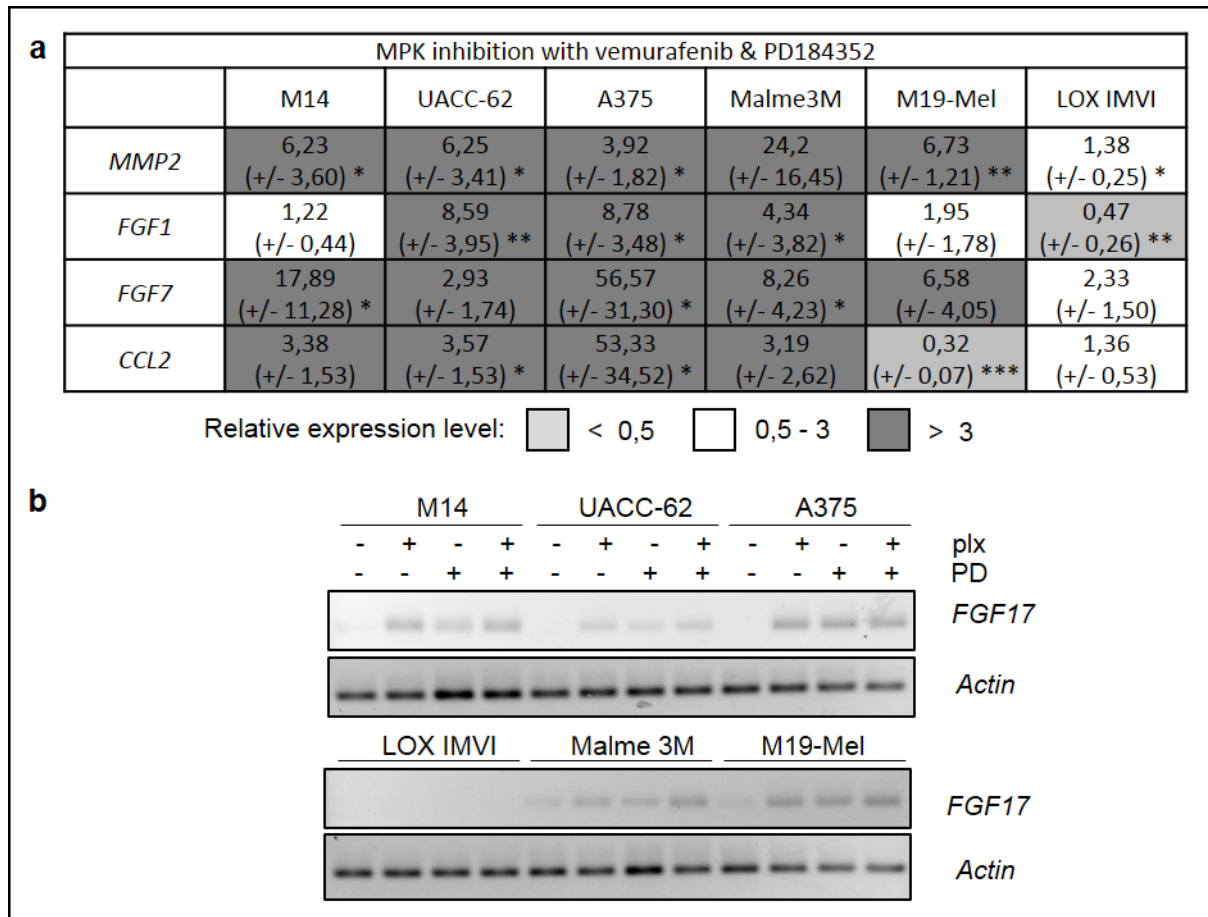
Figure 18: SASP gene expression after treatment with vemurafenib and the MEK inhibitor PD 184352. **(a)** Cells were treated for 3 d with 0,5 µM vemurafenib and 0,5 µM of the MEK inhibitor PD 184352. Medium and inhibitors were replaced after 48 h and cells were harvested at day 3. mRNA expression levels were determined via RT-PCR relative to actin. **(b)** Semiquantitative PCR products of *FGF17* primers (cycles 40) with cDNA from (a), loaded on a 1% agarose gel and stained with ethidium-bromide.

5.2.4. Regulation of SASP genes after treatment with different senescence inducing inhibitors

As seen in the previous experiments, senescence induction by MAPK pathway inhibition is accompanied by SA β-Gal staining and the expression of secreted factors. To test if these factors are specific for BRAF/MEK inhibitor induced senescence or if they represent a general senescence response, we used three agents, which are known to render melanoma cells senescent by different mechanisms. Piperlongumine (PIP) and propargylglycine (PAG) are able to induce reactive oxygen species (ROS)-mediated senescence by glutathione S transferase or cysteine synthesis inhibition, respectively (Möhler, Pfirrmann and Frei, 2014) (Thompson, Datko and Mudd, 1982). Palbociclib (Palb) is an inhibitor of CDK4 and -6, which also leads to premature senescence (Guan *et al.*, 2017). Beta Gal staining is shown after six days of treatment. The senescence induction initiated by these drugs was dependent upon the cell lines. In the cell lines M14, UACC-62 and A375, palbociclib and vemurafenib had the strongest effect on SA-β Gal activity (Fig. 19 a). A375 cells also became senescent in response to PIP and PAG. In UACC-62 cells, the senescence-inducing effect of PIP and PAG was visible, but weaker than in A375 cells, while M14 cells showed no response to ROS-induced senescence at all.

To assess changes of signaling over time we performed protein blots with cells after 3 and 6 days treated with the panel of inhibitors (Fig. 19 b). To check for cell cycle progression we examined the levels of P-Rb, since phosphorylation of this protein is an indicator for proliferating cells in S-Phase. In general P-Rb phosphorylation decreased after inhibitor treatment, while the status did not change between day 3 and day 6. In M14 cells, as in both other probed cell lines, the vemurafenib treatment exhibited the most intense decline in phosphorylated Rb followed by Palbociclib treatment. Piperlongumine hindered S-Phase progression only in A375 cells effectively, while in M4 cells, levels were comparable to the control and in UACC-62 it even increased P-Rb levels. PAG did not significantly change P-Rb levels in M14 and UACC-62 cells, only in A375 it has a major impact on the phosphorylation status of this protein. P-AKT levels in M14 declined from day 3 to day 6 under inhibitor pressure, except PAG exposure, which increased AKT phosphorylation in this cell line at day 6. UACC-62 cells decreased their P-AKT levels in general after treatment with this inhibitor panel, only the vemurafenib treated cells showed the expected increase at day 3 as well as on day 6 compared to the control. This increase after BRAF inhibitor treatment could also be seen in A375 cells. Moreover, this cell line also increased P-AKT signaling after PAG treatment. P-ERK levels were diminished as expected after vemurafenib treatment, all other agents did not affect MAPK signaling.
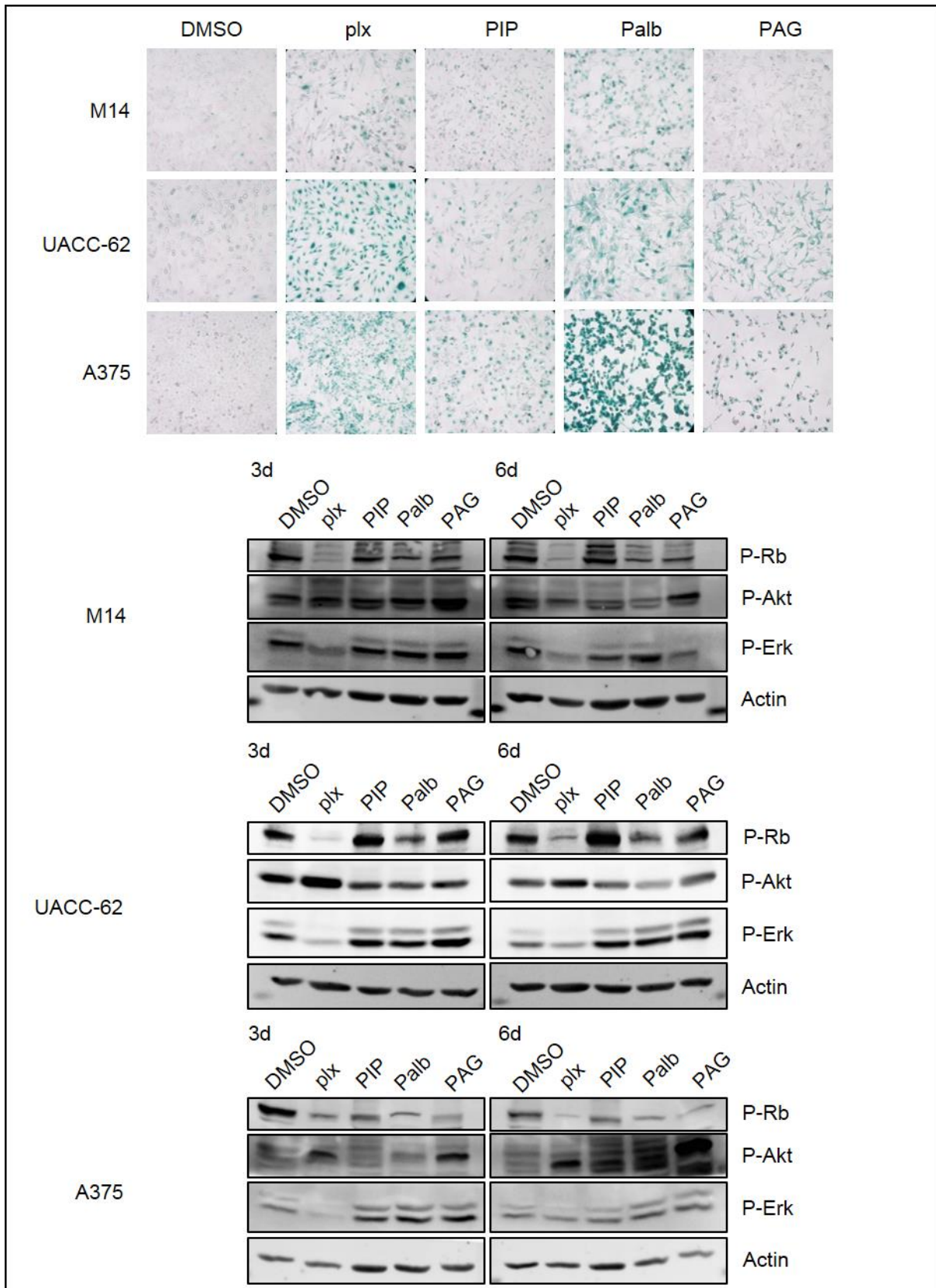
Figure 19: Beta-Gal staining after treatment with different senescence inducing inhibitors. Cell lines were treated for 6d with 2 µM vemurafenib, 2,5 µM Piperlongumine, 5 µM Palbociclib and 10 mM PAG. Medium and inhibitors were changed every 48 h. **(a)** At day 6 cells were stained over night with SA-β-Gal. **(b)** After cell harvest on day 3 and 6, signaling status was determined via western blot with P-Rb (Ser780), P-AKT (Ser473), P-ERK p42/44 (Thr202/Tyr204) antibodies.

Next, we checked which senescence inducer was able to regulate the vemurafenib associated SASP genes. Interestingly, the data indicate that the vemurafenib-induced secretome could not be reconstituted with other senescence inducers, independent of the degree of senescence that was reached (Fig. 20 a, compare with Fig. 18). Only in M14 cells, where vemurafenib failed to induce *FGF1* expression, palbociclib treatment increased *FGF1* levels after 6 days. Furthermore, A375 showed a weak induction of *CCL2* after PIP and of *FGF1* and *CCL2* after PAG treatment, but this was much lower compared to the vemurafenib treatment. Taken together these results implicate that the SASP found after vemurafenib treatment is not caused by senescence induction in general, but the blockade of the MAPK pathway seems to be the trigger for the establishment of the potential pro-tumorigenic secretome.

As mentioned above, it has been described that the secretome establishment after vemurafenib treatment is driven by downregulation of *FOSL1* (Obenauf *et al.*, 2015). I therefore checked for the transcriptional levels of the SASP genes in the cell line UACC-62 after *FOSL1* knockdown (Fig. 20 b). Notably, *FGF1* transcription is significantly increased after the knockdown, arguing for the influence of FOSL1 loss in the upregulation of this growth factor during BRAF inhibition. *CCL2* levels are also elevated, but this effect is caused by a strong upregulation in only one probe of the three tested. Therefore, the *FOSL1* dependency of *CCL2* upregulation needs to be elucidated with additional experiments. The transcription of *MMP2* is not altered after loss of FOSL1. According to these results, which need to be confirmed in other cell lines, *FGF1* could be part of the *FOSL1* regulated secretome under MAPK inhibition.
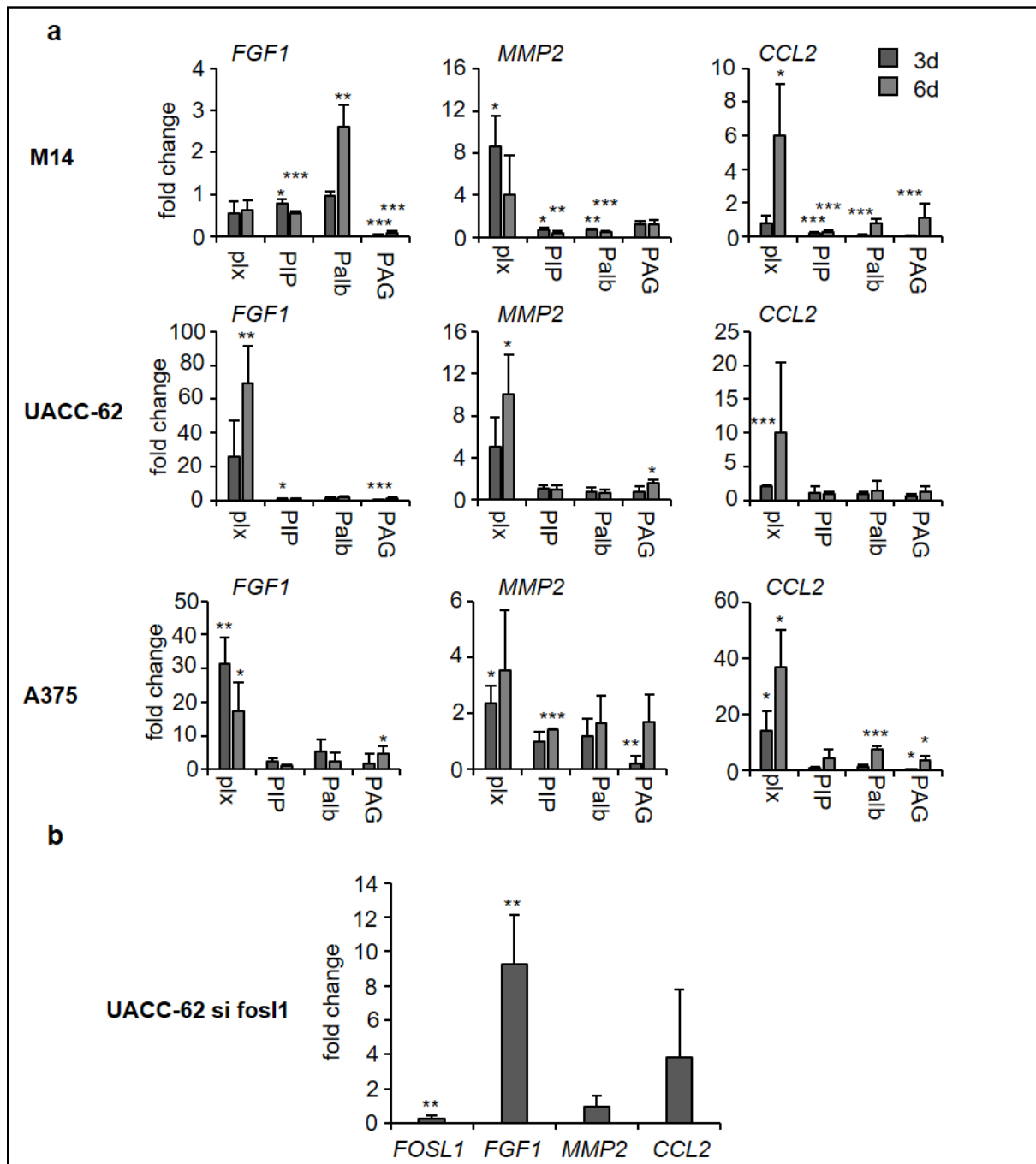
Figure 20: SASP gene expression after treatment with different senescence inducers and while FOSL1 knockdown. (a) Transcriptional levels of *FGF1*, *MMP2* and *CCL2*. Cell lines were treated for 3 d and 6 d with 2 µM vemurafenib, 2,5 µM Piperlongumine, 5 µM Palbociclib and 10 mM PAG. Medium was changed and the inhibitors were replaced every 48h. After cell harvest, mRNA expression levels were determined via RT-PCR relative to actin. **(b)** Transcriptional levels of *FGF1*, *MMP2* and *CCL2* 3 d after *FOSL1* knockdown in UACC62 cells.

6. Discussion

6.1. Components of the vemurafenib-induced secretome

This study describes the induction of various pro-tumorigenic secreted factors, including CCL2, FGF1 and MMP2 by targeted BRAF or MEK inhibition. These factors help melanoma cells to survive and acquire a resistant phenotype towards the inhibitor induced MAPK signaling deprivation. The identified factors are able to influence the melanoma cells via stimulation of different cellular processes. Modulation of the immune system (CCL2), stimulation of proliferative as well as anti-apoptotic pathways (FGF1) and increased invasiveness (MMP2) are all involved in helping melanoma cells to tolerate MAPK inhibition. Previously, Obenauf and colleagues also observed a therapy-induced secretome of melanoma cells treated with the BRAF inhibitor vemurafenib (Obenauf *et al.*, 2015). While the general observation, that BRAF inhibitor treated cells secrete survival-relevant factors, was also observed in my study, I could furthermore show that FGF signaling contributes to the stimulating effect and that MAPK inhibition in general invokes the establishment of the aforementioned secretome. The BRAF/MEK inhibitor-induced pro-tumorigenic factors and their influence on cellular survival, pro-tumorigenic microenvironment and senescence induction are discussed in detail in the following.

6.1.1. C-C motif chemokine ligand 2 – CCL2

CCL2 or Monocyte chemoattractant protein-1 plays an important role in the immune response by recruiting and activating macrophages during acute inflammation. Usually the expression of this chemokine is triggered via active NF-κB and HIF1 signaling (Hasegawa *et al.*, 2014). In melanoma cells it has been shown that senescence induction due to MITF depletion, oxidative stress and chemotherapeutic drugs increases the expression of CCL2 (Ohanna *et al.*, 2011). I could show that unlike the secretome described by Ohanna et al., which is associated with increased PARP-1 and NF-κB signaling, the secretome we observe after BRAF inhibition is not dependent on signaling through this pathway, since we could monitor a drastic decline of NF-κB phosphorylation levels after vemurafenib treatment.

The influence of secreted CCL2 on tumor cells is described both as tumor-promoting and as tumor-suppressing (Li *et al.*, 2013). For melanoma, it has been reported that it influences tumor cells depending on its concentration in the cellular microenvironment. Whereas high levels of CCL2 in the medium prevent growth, low to intermediate levels seem to stimulate tumor cell proliferation (Gazzaniga et al. 2007). In general, CCL2 attracts, as it name implies, immune cells like tumor-associated lymphocytes and monocytes to the site of the lesion (Lanca et al. 2013) (Rollins et al. 1991). In three-dimensional organotypic melanoma culture it has been

shown that CCL2 attracts cytotoxic T lymphocytes towards melanoma cells, which results in tumor cell apoptosis (Zhang *et al.*, 2006) .

Nonetheless it is speculated that the negative effects of an increased CCL2 level at the tumor site exceed the positive effects (Li *et al.*, 2013). Concerning its immune modulating role, it has been shown that CCL2 recruits monocytes to the tumor site, which differentiate into macrophages (Mizutani *et al.*, 2009) (Loberg *et al.*, 2007). Especially so called tumors-associated macrophages of the M2 phenotype secrete several growth factors that promote tumor growth (Allavena *et al.*, 2008). Moreover, high CCL2 levels are associated with poor prognosis in breast carcinoma patients (Lebrecht *et al.*, 2004). Furthermore, it has been reported to increase the tumor cell migration of mammary carcinoma cell lines and the recruitment of specific monocytes that enhance the metastatic potential of breast carcinoma cells (Youngs *et al.*, 1997) (Qian *et al.*, 2011).

For melanoma the pro-tumorigenic properties of CCL2 could be observed *in vivo* as the secretome from senescent melanoma cells and recombinant CCL2 conferred metastatic properties to 501mel human melanoma cells, which usually do not grow as xenografts in nude mice (Ohanna *et al.*, 2011). Furthermore, elevated CCL2 levels after BRAF inhibition have also been reported in melanoma cell lines as well as in tumor tissues and in plasma acquired from patients during treatment with vemurafenib (Vergani *et al.*, 2016). It acts as an autocrine growth factor, stimulating the proliferation and resistance to apoptosis of drug treated cells *in vitro* by inducing the expression of three miRNAs (miR-34a, miR-100, miR-125). Upregulated levels of these three miRNAs could also be found in resistant cell lines and tumor biopsies of patients undergoing BRAF inhibitor treatment, indicating a protective role after loss of BRAFV600E signaling (Vergani *et al.*, 2016). Interestingly miR-34a has also been described to regulate senescence in Type II alveolar epithelial cells as well as in colon cancer cells (Tazawa *et al.*, 2007) (Disayabutr *et al.*, 2016). It is activated by DNA damage and successive p53 activation, leading to increased miR-34a, miR-34b and miR-34c levels. These miRNAs inhibit the translation of an array of cell cycle and apoptosis relevant genes including BCL-2, CCND1, CDK4, MYCN. Specifically miR34a downregulates the E2F signaling pathway and upregulates the p53/p21 pathway, which is accompanied by an increase in cellular size and a positive SA-β-Gal staining pattern (Tazawa *et al.*, 2007) (Hermeking, 2010). For all its effects miR-34 can be considered as a tumor suppressor gene and has been described as target of CpG methylation in a broad range of tumor specimens (Lodygin *et al.*, 2008). Taken together, DNA damage and subsequent p53 activation after MAPK inhibition accompanied by elevated CCL2 levels might increase the expression of miR-34a and might induce or intensify the senescence features, we observe after BRAF and MEK inhibitor treatment.

6.1.2. Matrix metalloprotease 2 - MMP2

The matrix metalloproteinase MMP2, which is transcriptionally upregulated after vemurafenib inhibition and which I found in higher amounts in the CSN of BRAF inhibitor treated cells, is a protease, mainly responsible for the degeneration and the remodeling of the extracellular matrix (Pytliak et al. 2012). I could show the degrading proteolytic activity in a zymogram, proving efficient cleavage of gelatin by MMP2 present in the CSN. Besides gelatin as substrate, this enzyme has also the ability to degrade collagens, rendering it an effective remodeler of the extracellular matrix. Increased expression has been investigated in many human tumors and is correlated with a higher metastatic potential. In the context of a proliferation stimulating effect, it has been shown that MMP2 can cleave the membrane-anchored form of the heparin-binding EGF-like growth factor (pro-HB-EGF) in the plasma membrane, thereby transactivating EGFR in gonadotropic cells (Roelle *et al.*, 2003). Moreover, MMP2 can release VEGF, which could lead to increased VEGFR signaling (Dean *et al.*, 2007). This angiogenic growth factor often forms inhibitory complexes with Connective Tissue Growth Factor (CTGF) and Pleiotrophin (PTN) in the extracellular matrix. In this complexed form VEGF´s bioavailability is reduced, which abrogates neovascularization. MMP2 can release VEGF by cleavage of its binding partners, thereby it increases the abundance of this potent growth factor. Moreover, it has also been postulated that secreted MMP2 induces a αvβ5 integrin and a PI3K dependent increase of VEGF-A expression in highly invasive melanoma cells, which enhances the VEGF secretion and the angiogenetic potential of the tumor microenvironment (Desch *et al.*, 2012). In melanoma cells, an interaction between MMP2 and αvβ3 integrin has been observed at the leading edge of migrating tumor cells. Through cleaving of fibronectin, MMP2 together with αvβ3 integrin is able to increase the adhesion, invasion and migration of melanoma cells *in vitro* (Jiao *et al.*, 2012). Furthermore, in matrigel experiments, CSN from hypoxia- induced senescent melanoma cells, which showed increased MMP2 expression, augmented the invasiveness of naive melanoma cells. It is, however, not shown if MMP2 was the major player facilitating these process (Mo *et al.*, 2013).

In terms of immunomodulation, it has been shown that matrix metalloproteinases can affect the susceptibility of melanoma cells to NK-mediated lysis. MMP2 secreted by cancer-associated fibroblasts decreases the abundance of two NK-activating receptor ligands MHC class I chain-related protein A and B (MICA/B) on the surface of melanoma cells leading to a reduced anti-tumor immune response (Ziani *et al.*, 2017). In line with my observation of elevated MMP2 levels after MAPK inhibition, other groups also reported increased levels of this protease after vemurafenib and MEK inhibitor treatment. BRAF inhibition was performed in 3D culture with A375 cells and it could be observed that, additionally to increased MMP2 levels in the supernatant, the motility of the treated melanoma cells also increased (Leight *et al.*, 2015). In A375 and WM266-4 cells it was shown that after MEK inhibition with PD 184352,

the CSN exhibited an increased collagen degrading potential (Ferguson *et al.*, 2013). In 2004 Zhang et al. proposed a model elucidating the regulatory process behind different MMP2 expression profiles. They worked with a lung carcinoma cell line, which they treated with different concentrations of recombinant IGF-1 and could show that MMP2 levels depend on an interplay between PI3K and MAPK signaling. The proposed model differentiates between a low dose (10ng/ml) and high dose (100ng/ml) IGF signaling cascade. Lower levels of IGF-1 activate AKT signaling and increase *MMP2* transcription and translation via a mTOR-dependent mechanism, while MAPK signaling remains only on a low level. If the ligand availability is increased, MAPK signaling is increased and *MMP2* transcription is suppressed (Zhang *et al.*, 2004). In my setting after vemurafenib inhibition, signaling through the MAPK cascade is almost abolished, therefore paracrine or autocrine stimulation with IGF1 could possibly trigger the PI3K pathway and *MMP2* transcription. Since I could also observe a decrease in the IGF binding proteins IGFBP2 and IGFBP 3, availability of this growth factor and therefore stimulation of IGFR1 receptors might also be increased and could contribute to the increased P-AKT levels seen in different cell lines.

6.1.3. Fibroblast growth factor 1 - FGF1

FGF1 is a member of the fibroblast growth factor family and it binds and activates all five members of the FGFR family (FGFR1, FGFR2, FGFR3, FGFR4, FGFRL1). FGF1 activates FGFR signaling and affects development, angiogenesis, wound healing, adipogenesis and neurogenesis. Moreover, if deregulated through activating mutations or excessive ligand abundancy, FGFR signaling is also reported to be involved in tumorigenic processes including tumor invasion and metastasis (Nies *et al.*, 2015). As FGF1 lacks a signal peptide, it is not transported via the classical endoplasmic reticulum- and Golgi-mediated secretion mechanism. Its secretion is facilitated by a copper-dependent multiprotein complex, which is activated by different cellular stresses like heat shock, hypoxia and serum starvation (Prudovsky *et al.*, 2008). In the extracellular environment, FGF1 can bind and activate FGFRs in an autocrine and paracrine manner. Polysulfated polysaccharides like heparan sulfate proteoglycan (HSPG) are needed on the cell membrane as cofactors to form a stable signaling complex between FGFR and FGF1 (Nies *et al.*, 2015). Phosphorylated FGF receptors initiate signaling of various intracellular pathways like the MAPK, AKT/PI3K and PLC-□-pathways (Rodriguez-Enfedaque *et al.*, 2009). Besides initiating signaling by direct binding to FGFRs, FGF1 can also be endocytosed and translocated across the plasma membrane (Wiedłocha *et al.*, 2005). After FGFR receptor-mediated endocytosis, the growth factor can be translocated to the nucleus, which is initiated by its nuclear translocation sequence (Imamura *et al.*, 1990) (Bober *et al.*, 2016). Survival and apoptosis protection have been reported to be mediated by

nuclear FGF1, which binds directly to p53, thereby inhibiting its phosphorylation. This prevents the transcription of pro-apoptotic genes after DNA damages and decreases the mitochondrial apoptotic pathway and impedes caspase-3 cleavage (Rodriguez-Enfedaque *et al.*, 2009). Furthermore, FGF1 has also been described to enhance epithelial-to-mesenchymal transition (EMT), a process in which epithelial cancer cells acquire a motile mesenchymal phenotype, thereby facilitating cancer metastasis. In mammary epithelial cells, EMT can be initiated by TGF-β1 induced increased levels of integrin αvβ3 and FGFR1. After binding of FGF1, EMT is augmented (Mori *et al.*, 2015). Since BRAF inhibition has been reported to increase TGF-β1 expression in melanoma cell lines, accompanied FGF1 expression and secretion might also lead to EMT-like processes (Fedorenko *et al.*, 2015). Moreover, in co-culture experiments with fibroblasts it has been shown that this phenotype switch, which is accompanied by an increase of PI3K/mTOR signaling in melanoma cells, renders them more resistant towards BRAF inhibitor induced apoptosis (Seip *et al.*, 2016). A strong protective effect could also be seen in head and neck squamous cell carcinoma cells co-treated with an EGFR inhibitor and recombinant FGF1. Combined treatment almost completely rescued the significant loss of viability seen after EGFR inhibition (Tepper *et al.*, 2016). Furthermore, it has been shown in esophageal squamous-cell carcinoma cell lines that addition of FGF1 can stimulate the proliferation of 6 of 22 cell lines and that supernatants from esophageal fibroblasts expressing FGF ligands can rescue the growth inhibition by the EGFR inhibitor lapatinib (Saito *et al.*, 2015). This resembles the results I observed after treating melanoma cell lines with CSN and recombinant FGF1. The addition of CSN induced cell proliferation in the majority of tested cell lines and the addition of FGF1 into the medium mimicked the stimulating effect and furthermore helped melanoma cells tolerate the BRAF inhibition. Secreted FGF1 could help tumor cells to compensate the loss of MAPK signaling. In order to prevent that mechanism, it is of vital importance to understand the signaling behind that increased expression. In A375 cells it has been reported that expression and release of FGF1 into the extracellular environment is negatively regulated by active NOTCH signaling (Kacer *et al.*, 2011). Interestingly, miRNA-34a, which has been reported to be upregulated after vemurafenib expression, suppressed the invasiveness of cervical and choriocarcinoma cell lines by downregulation of *NOTCH1* and *JAG1* (Vergani *et al.*, 2016) (Pang *et al.*, 2010). Furthermore, in pancreatic cancer cell lines miRNA-34a initiates, besides *NOTCH1* downregulation, also a post-transcriptional decrease of NOTCH2 (Ji *et al.*, 2009). I could show that transcription of *FGF1* depends on an active PI3K/AKT signaling pathway, nonetheless downregulated Notch signaling might potentiate the expression and release of FGF1 in the CSN. In the clinical situation, as part of a non-small cell lung cancer (NSCLC) study, patients were treated with sorafenib, a multitargeted inhibitor against KDR, RAF-kinases, PDGFRB and KIT. A gene expression signature associated with sorafenib´s clinical benefit was observed. Increased expression of FGF1, together with

increased signaling through NF-kB, and the hypoxia pathways were identified as potential drivers of this increased kinase inhibitor resistance profile (Blumenschein *et al.*, 2013). In another study, where 113 primary human NSCLC tissues were examined for the immunohistochemical expression of FGF1, high expression was associated with a significantly lower overall survival rate, larger tumor size and vascular invasion (Li *et al.*, 2015). Taken together, FGF1 expression seems to increase tumorigenicity and can facilitate tumor survival under MAPK inhibition in melanoma, but also targeted inhibition in other cancer types, supporting the idea of a beneficial effect of increased FGF1 expression in BRAF inhibited melanoma specimen.

6.2. Resistance mechanisms to vemurafenib based on elevated FGFR signaling

I could show that after MAPK inhibition transcription of several FGF ligands such as FGF1, FGF7, and FGF17 is increased and could validate elevated FGF1 protein levels in the CSN of vemurafenib treated A375 cells. Interestingly, it has been reported that in vemurafenib resistant M14 and A375 cells enhanced activation of FGFR3 reactivated MAPK signaling and conferred resistance towards BRAF inhibition (Yadav *et al.*, 2012). This is in accordance with our findings that recombinant FGF1 was able to increase the viability of melanoma cell lines under vemurafenib pressure, which could be prevented by FGFR inhibitor induced blockade of the FGF signaling axis.

Notably, addition of recombinant FGF1 resembled the viability stimulating effect of the vemurafenib treated conditioned supernatant. When fibroblasts were grown with supplemented growth factor in the medium, they showed a comparable viability stimulation as when they were kept in presence of vemurafenib CSN. In melanoma cells, I observed a similar effect: here, addition of recombinant FGF1 was able to increase proliferation and enhance survival of melanoma cell lines under vemurafenib pressure. This effect was averted in presence of a FGFR inhibitor.

Many receptor tyrosine kinase dependent resistance mechanisms have been described so far. In a panel of 12 treatment-naive BRAFV600E mutant melanoma cell lines, the expression of many ERBB family members were found to be upregulated after vemurafenib treatment, which conveyed increased resistance in response to BRAF inhibition (Capaldo *et al.*, 2015). IGF-1R and PDGFRβ have also been shown to mediate resistance towards BRAF inhibition, illustrating that a variety of elevated RTKs can sustain viability under vemurafenib pressure (Villanueva *et al.*, 2010) (Shi *et al.*, 2011). FGFR signaling seems to play an important role in adaptive resistance. The increased FGF ligand production I could observe after vemurafenib treatment could help MAPK inhibited cells to tolerate the drug pressure during patient treatment, thereby

supporting resistance development. In xenotransplantation experiments, it has been shown that expression of dominant-negative (dn) FGF receptors, especially with dnFGFR1, decreased the tumor volume significantly. Moreover, inhibition of FGF signaling in combination with the multikinase inhibitor sorafenib significantly reduced growth of xenograft tumors (Metzner *et al.*, 2011). This further supports the importance for FGF signaling after BRAF inhibition and combined with my findings, that melanoma cells secrete FGF ligands, could make it a viable therapeutic option in the clinics. In fact, many FGFR inhibitors are already in Phase 1 trials and demonstrated a manageable toxicity profile (Chae *et al.*, 2017). As Phase 2 trials emerge, especially with selective drugs that specifically target FGF receptors, a combination with MAPK inhibition could be an option for certain patients (Saka *et al.*, 2017).

6.3. Regulation of the BRAF inhibitor induced secretome

Human melanoma cells acquire a therapy induced secretome after treatment with BRAF, ALK or EGFR kinase inhibitors and it has been shown that the secretome induction is accompanied by increased P-AKT signaling in naive and resistant melanoma cell lines (Obenauf *et al.*, 2015). Moreover, in tumor biopsies dissected early after the start of vemurafenib treatment increased P-AKT levels could be detected (Shi *et al.*, 2014). In fact, our group reported previously that after MAPK inhibition a feedback loop is triggered by downregulated SPRED family members and increased EGFR signaling, which in turn activates protective P-AKT signaling. Due to increased RAS signals, because of the lack of SPRED proteins, P-AKT signaling prevents the induction of the apoptosis promotor PUMA (Haydn *et al.*, 2014). These findings show that in the clinical situation, during BRAF inhibitor treatment, upregulated AKT levels could induce a pro-tumorigenic microenvironment in which resistant subpopulations could thrive.

In my studies, increased P-AKT levels were detected in two of seven melanoma cell lines treated for three days with vemurafenib. This could be explained by the MAPK inhibition induced downregulation of SPRED family members, as stated above (Haydn *et al.*, 2014). Loss of the negative feedback proteins controlling RAS signaling in combination with an abundance of BRAF inhibitor induced secreted factors like e.g. different FGF ligands, which could trigger the signaling through RTKs, might contribute to the increased P-AKT levels in A375 and UACC-62 cells. Furthermore, in the cell line UACC-62 the tumor suppressor gene PTEN is disrupted, resulting in elevated PI3K/AKT signaling (Ikediobi *et al.*, 2006). All other tested melanoma cell lines harbour wildtype PTEN and showed no increase in P-AKT levels after three days.

Since AKT signaling is crucial for cell survival, proliferation and migration, upregulation of this pathway should support melanoma cell lines to tolerate BRAF inhibition (Prasad et al. 2015).

Especially for patients with PTEN deficient tumors, BRAF inhibition and the subsequent increased AKT activation correlates with worse outcome (Shi *et al.*, 2014). If the increased AKT levels are caused by the development of a BRAF inhibitor induced stimulatory secretome or intracellular crosstalk mechanisms between the MAPK and AKT pathways disturbed by the MAPK blockade remains to be elucidated. Many groups have reported that the pharmacologic inhibition of one of the pathways can lead to dynamic and complex signal propagation, in a positive or negative manner (Pappalardo *et al.*, 2016). For instance, MEK inhibition increases PI3K/AKT signaling in EGFR and HER2 driven cancers via hyperactivation of ERBB3 (Turke *et al.*, 2012). In the MEK inhibitor driven scenario, where increased P-AKT levels where observed by our group due to downregulation of SPRED family members, increased EGFR signaling also plays a role in the crosstalk between the AKT and MAPK pathway (Haydn *et al.*, 2014). Also, Elevated FGF and CCL2 levels as well as the decrease in IGFBP2 and IGFBP3 protein could cause increased RTK activation through higher IGF abundancy and subsequent triggering of AKT signaling. The elevated P-AKT levels after MAPK inhibition therefore are probably triggered on one hand by the loss of intracellular negative regulation mechanisms and on the other hand by an enhanced stimulation due to an increased growth factor abundancy in the extracellular environment.

To assess if the upregulated P-AKT levels have an influence on senescence induction I used the inhibitor BEZ-235. This dual pan class PI3K and mTor inhibitor blocks both crucial signaling nodes of the PI3K/AKT pathway effectively. In my cell panel (M14, UACC-62, A375) treatment with vemurafenib and BEZ-235 reduced the SA-β-Gal staining, that can be observed after BRAF inhibition. Moreover, cell density was decreased in the co-treatment situation as described by other groups (Penna *et al.*, 2016). MEK inhibitor (PD184352) treatment in combination with specific PI3K inhibition by the inhibitor GDC0941 also showed decreased SA-β-Gal staining, but the reduction was not as distinct as seen with the dual inhibitor BEZ-235. Taken together, this indicates that active PI3K/mTOR signaling is involved in senescence induction and survival under BRAF inhibitor pressure. Along the same lines, senescence caused by other factors is frequently dependent on mTOR signaling (Pani, 2011) (Tomimatsu and Narita, 2015). Besides growth factor induced signaling via the PI3K/AKT axis, the mTOR pathway is also activated by nutrients like glucose and amino acids. If a cell has been forcefully arrested e.g. via administration of different chemotherapeutic agents, active signaling through this pathway converts reversible cell-cycle-arrested, quiescent cells into senescent cells (Leontieva, Demidenko and Blagosklonny, 2015). This process is called geroconversion and can be suppressed or decelerated by mTOR inhibitors like rapamycin. It has been shown that fibrosarcoma cells, fibroblasts and breast adenocarcinoma cells, if treated with a mTOR inhibitor, maintain their proliferative potential after senescence induction. Ectopic p21 expression and treatment with etoposide and doxorubicin under mTOR inhibition hinders cells

to undergo geroconversion and impedes the establishment of the typical senescent morphology (Leontieva, Demidenko and Blagosklonny, 2015). In multiple myeloma cells mTOR inhibition prevents senescence and the accompanied pro-inflammatory secretome, if the cells were faced with genotoxic stresses like C-ion or X-ray irradiation and doxocubicin (Coudre *et al.*, 2016). The AKT pathway as the primary stimulus is essential for active mTOR signaling. Blockade of the PI3K signaling node as well as the downstream S6K protein kinase, which has been shown to be crucial for geroconversion, could make dual mTOR/PI3K inhibitors like BEZ-235 very effective in preventing senescence induction after BRAF inhibition (Leontieva, Demidenko and Blagosklonny, 2013).

Analysis of the transcriptional levels of *CCL2*, *MMP2* and *FGF1* revealed that not only cellular senescence, but also transcriptional induction of these genes is dependent on PI3K/AKT/mTOR signaling. This was best observed with the usage of the PI3K/mTOR inhibitor. Similar effects were seen with a specific PI3K inhibitor, but to a lesser degree. Notably, MAPK blockade with a MEK inhibitor also increased the transcription of the gene set and the transcriptional levels were comparable to the changes seen in vemurafenib treated cells. These findings show that the upregulation of the secretome genes induced via PI3K/mTOR signaling is a general answer of melanoma cells towards MAPK inhibition.

Different clinical trials combining MAPK inhibition with PI3K/AKT inhibition are currently ongoing. For example, the AKT inhibitor GSK2141795 is used in combination with the BRAF inhibitor dabrafenib and the MEK inhibitor trametinib. In another trial vemurafenib is administered with the mTOR inhibitors everolimus and temsirolimus (ClinicalTrials.gov. identifier: NCT01902173/ NCT01596140). Many agents have been developed to target the AKT/PI3K pathway, including PI3K inhibitors, (e.g. buparlisib, alpelisib), PI3K/mTOR inhibitors (e.g. BEZ235), or AKT inhibitors (e.g. GSK2141795, BKM120), but many showed unfavorable pharmaceutical activities, toxicity, and crossover inhibition of other lipid and protein kinases (Ebrahimi *et al.*, 2017) (Massacesi *et al.*, 2016) (Johnson and Puzanov, 2015). Combined with other drugs, these side effects could be even more problematic, as a clinical trial with prostate cancer patients showed. Combination therapy of abiraterone acetate, a androgen synthesis inhibitor, with BEZ-235 has been terminated early because 50% of all patients showed severe side effects (Wei *et al.*, 2017). Several other clinical trials in phase I/II with BEZ-235 as single agent or in combination are currently ongoing. A clinical trial in phase I has been canceled preliminarily in patients with advanced renal cell carcinoma due to grade 3–4 adverse effects in 50% of patients without objective responses (Pongas and Fojo, 2016). Interestingly, for treatment of metastatic melanoma the phase 1 escalation study mentioned above, where MAPK inhibition, either with dabrafenib and/or trametinib, was combined with the AKT inhibitor GSK2141795 reported that the inhibition of both pathways was well tolerated and durable objective responses were seen in patients with metastatic melanoma (Algazi *et al.*, 2017).

Another clinical study is currently ongoing, where BRAF and MEK inhibition is combined with a third compound. The genetic analysis of tumor biopsies of patients who were treated with the BRAF inhibitor LGX818 and the MEK inhibitor MEK162 until disease progression are screened and receive, according to the genetic profile, a third inhibitory agent (ClinicalTrials.gov. identifier NCT02159066). Notably, one of the four drugs administered after disease progression is the PI3K inhibitor BKM120 for patients with genomic alterations in the PI3K/AKT pathway. Even more interesting in the light of my work is the administration of the specific FGFR inhibitor BGJ398 as third agent. Since I could observe increased transcription of different FGF ligands after BRAF inhibition and blockade of FGFR signaling combined with sorafenib showed synergistic effects, I speculate that the sub-group of patients with an increased FGF signaling profile could profit from this treatment (Metzner *et al.*, 2011).

6.4. Conclusion

With my work I could show that vemurafenib treatment induces the development of a pro-tumorigenic secretome in different melanoma cell lines. The factors I could identify are potentially able to increase the metastatic as well as the proliverative potential (FGFs, CCL2) of tumor cells and could also be able to modify the immune response (CCL2). Others could show the *in vivo* induction of a secretome after BRAF inhibitor treatment, therefore especially the FGF expression could be a viable target for a combination therapy in the clinics. If increased FGF expression can be observed in patient tumor samples, the treatment of this patient subgroup with vemurafenib in hand with an FGF inhibitor could help to reinforce the impact of the BRAF inhibition as well as hinder the emergence of resistant tumor cells.

7.   Bibliography

Abel, E. V *et al.* (2013) 'Melanoma adapts to RAF/MEK inhibitors through FOXD3-mediated upregulation of ERBB3.', *The Journal of clinical investigation*, 123(5), pp. 2155–68. doi: 10.1172/JCI65780.

Abildgaard, C. and Guldberg, P. (2015) 'Molecular drivers of cellular metabolic reprogramming in melanoma.', *Trends in molecular medicine*. Elsevier Ltd, 21(3), pp. 164–71. doi: 10.1016/j.molmed.2014.12.007.

Aguissa-Touré, A. H. and Li, G. (2012) 'Genetic alterations of PTEN in human melanoma', *Cellular and Molecular Life Sciences*, pp. 1475–1491. doi: 10.1007/s00018-011-0878-0.

Ahn, J., Han, B. and Lee, M. (2015) 'Induction of Resistance to BRAF Inhibitor Is Associated with the Inability of Spry2 to Inhibit BRAF-V600E Activity in BRAF Mutant Cells.', *Biomolecules & therapeutics*, 23(4), pp. 320–6. doi: 10.4062/biomolther.2015.007.

Aird, K. M. *et al.* (2013) 'Suppression of nucleotide metabolism underlies the establishment and maintenance of oncogene-induced senescence.', *Cell reports*. The Authors, 3(4), pp. 1252–65. doi: 10.1016/j.celrep.2013.03.004.

Algazi, A. P. *et al.* (2017) 'SWOG S1221: A phase 1 dose escalation study co-targeting MAPK-dependent and MAPK-independent BRAF inhibitor resistance in BRAF mutant advanced solid tumors with dabrafenib, trametinib, and GSK2141795 (ClinicalTrials.gov NCT01902173).', *Journal of Clinical Oncology*, 35(15_suppl), p. 2578. doi: 10.1200/JCO.2017.35.15_suppl.2578.

Allavena, P. *et al.* (2008) 'The inflammatory micro-environment in tumor progression: the role of tumor-associated macrophages.', *Critical reviews in oncology/hematology*, 66(1), pp. 1–9. doi: 10.1016/j.critrevonc.2007.07.004.

American Cancer Society (2017) 'Cancer Facts and Figures 2017', *Genes and Development*, 21(20), pp. 2525–2538. doi: 10.1101/gad.1593107.

Arora, R. *et al.* (2015) 'Structural investigation of B-Raf paradox breaker and inducer inhibitors.', *Journal of medicinal chemistry*, 58(4), pp. 1818–31. doi: 10.1021/jm501667n.

Baade, P. *et al.* (2012) 'Time trends and latitudinal differences in melanoma thickness distribution in Australia, 1990-2006', *International Journal of Cancer*, 130(1), pp. 170–178. doi: 10.1002/ijc.25996.

Bataille, V. and de Vries, E. (2008) 'Melanoma--Part 1: epidemiology, risk factors, and prevention.', *BMJ (Clinical research ed.)*, 337, p. a2249. doi: 10.1136/bmj.a2249.

Bhatia, S., Tykodi, S. S. and Thompson, J. A. (2009) 'Treatment of metastatic melanoma: an overview.', *Oncology (Williston Park, N.Y.)*, 23(6), pp. 488–96. Available at: http://www.ncbi.nlm.nih.gov/pubmed/19544689.

Blumenschein, G. R. *et al.* (2013) 'Comprehensive biomarker analysis and final efficacy results of sorafenib in the BATTLE trial.', *Clinical cancer research : an official journal of the American Association for Cancer Research*, 19(24), pp. 6967–75. doi: 10.1158/1078-0432.CCR-12-1818.

Bober, J. *et al.* (2016) 'Identification of new FGF1 binding partners - Implications for its intracellular function', *IUBMB Life*, 68(3), pp. 242–251. doi: 10.1002/iub.1480.

Bollag, G. *et al.* (2010) 'Clinical efficacy of a RAF inhibitor needs broad target blockade in BRAF-mutant melanoma.', *Nature*, 467(7315), pp. 596–9. doi: 10.1038/nature09454.

Bollag, G. *et al.* (2012) 'Vemurafenib: the first drug approved for BRAF-mutant cancer.', *Nature reviews. Drug discovery*. Nature Publishing Group, 11(11), pp. 873–86. doi:

10.1038/nrd3847.

Brenner, M. and Hearing, V. J. (2008) 'The protective role of melanin against UV damage in human skin', *Photochemistry and Photobiology*, 84(3), pp. 539–549. doi: 10.1111/j.1751-1097.2007.00226.x.

Brown, K. K. and Toker, A. (2015) 'The phosphoinositide 3-kinase pathway and therapy resistance in cancer.', *F1000prime reports*, 7(February), p. 13. doi: 10.12703/P7-13.

Bulliard, J. L. and Cox, B. (2000) 'Cutaneous malignant melanoma in New Zealand: trends by anatomical site, 1969-1993.', *International journal of epidemiology*, 29(3), pp. 416–423.

Caenepeel, S. *et al.* (2017) 'MAPK pathway inhibition induces MET and GAB1 levels , priming BRAF mutant melanoma for rescue by hepatocyte growth factor', *Oncotarget*, 8(11), p. doi: 10.18632/oncotarget.14855. doi: 10.18632/oncotarget.14855.

Cancer Genome Atlas Network (2015) 'Genomic Classification of Cutaneous Melanoma.', *Cell*, 161(7), pp. 1681–96. doi: 10.1016/j.cell.2015.05.044.

Capaldo, B. J. *et al.* (2015) 'Systems Analysis of Adaptive Responses to MAP Kinase Pathway Blockade in BRAF Mutant Melanoma.', *PloS one*, 10(9), p. e0138210. doi: 10.1371/journal.pone.0138210.

Chae, Y. K. *et al.* (2017) 'Inhibition of the fibroblast growth factor receptor (FGFR) pathway: the current landscape and barriers to clinical application', *Oncotarget*, 8(9), pp. 16052–16074. doi: 10.18632/oncotarget.14109.

Chapman, P. B. *et al.* (2011) 'Improved survival with vemurafenib in melanoma with BRAF V600E mutation.', *The New England journal of medicine*, 364(26), pp. 2507–16. doi: 10.1056/NEJMoa1103782.

Chapman, P. B. (2013) 'Mechanisms of Resistance to RAF Inhibition in Melanomas Harboring a BRAF Mutation.', *American Society of Clinical Oncology educational book / ASCO. American Society of Clinical Oncology. Meeting*, pp. 80–82. doi: 10.1200/EdBook_AM.2013.33.e80.

Cichorek, M. *et al.* (2013) 'Skin melanocytes: Biology and development', *Postepy Dermatologii i Alergologii*, 30(1), pp. 30–41. doi: 10.5114/pdia.2013.33376.

Coppé, J.-P. *et al.* (2008) 'Senescence-associated secretory phenotypes reveal cell-nonautonomous functions of oncogenic RAS and the p53 tumor suppressor.', *PLoS biology*, 6(12), pp. 2853–68. doi: 10.1371/journal.pbio.0060301.

Coppé, J.-P. *et al.* (2010) 'The senescence-associated secretory phenotype: the dark side of tumor suppression.', *Annual review of pathology*, 5, pp. 99–118. doi: 10.1146/annurev-pathol-121808-102144.

Coudre, C. *et al.* (2016) 'HIF-1α and rapamycin act as gerosuppressant in multiple myeloma cells upon genotoxic stress', *Cell Cycle*. Taylor & Francis, 15(16), pp. 2174–2182. doi: 10.1080/15384101.2016.1196302.

Curtin, J. a *et al.* (2005) 'Distinct sets of genetic alterations in melanoma.', *The New England journal of medicine*, 353(20), pp. 2135–2147. doi: 10.1056/NEJMoa050092.

D'Orazio, J. and Fisher, D. E. (2011) 'Central role for cAMP signaling in pigmentation and UV resistance', *Cell Cycle*, 10(1), pp. 8–9. doi: 10.4161/cc.10.1.14292.

Damsky, W. E., Theodosakis, N. and Bosenberg, M. (2013) 'Melanoma metastasis: new concepts and evolving paradigms.', *Oncogene*. Nature Publishing Group, (April), pp. 1–10. doi: 10.1038/onc.2013.194.

Dankort, D. *et al.* (2009) 'Braf(V600E) cooperates with Pten loss to induce metastatic

melanoma.', *Nature genetics*, 41(5), pp. 544–52. doi: 10.1038/ng.356.

Dean, R. a *et al.* (2007) 'Identification of candidate angiogenic inhibitors processed by matrix metalloproteinase 2 (MMP-2) in cell-based proteomic screens: disruption of vascular endothelial growth factor (VEGF)/heparin affin regulatory peptide (pleiotrophin) and VEGF/Connective ', *Molecular and cellular biology*, 27(24), pp. 8454–8465. doi: 10.1128/MCB.00821-07.

Desch, A. *et al.* (2012) 'Highly invasive melanoma cells activate the vascular endothelium via an MMP-2/integrin αvβ5-induced secretion of VEGF-A.', *The American journal of pathology*. Elsevier Inc., 181(2), pp. 693–705. doi: 10.1016/j.ajpath.2012.04.012.

Disayabutr, S. *et al.* (2016) 'miR-34 miRNAs Regulate Cellular Senescence in Type II Alveolar Epithelial Cells of Patients with Idiopathic Pulmonary Fibrosis', *Plos One*, 11(6), p. e0158367. doi: 10.1371/journal.pone.0158367.

Duggan, M. C. *et al.* (2017) 'Identification of NRAS isoform 2 overexpression as a mechanism facilitating BRAF inhibitor resistance in malignant melanoma.', *Proceedings of the National Academy of Sciences of the United States of America*, 114(36), pp. 9629–9634. doi: 10.1073/pnas.1704371114.

Ebrahimi, S. *et al.* (2017) 'Targeting the Akt/PI3K Signaling Pathway as a Potential Therapeutic Strategy for the Treatment of Pancreatic Cancer.', *Current medicinal chemistry*, 24(13), pp. 1321–1331. doi: 10.2174/0929867324666170206142658.

Emery, C. M. *et al.* (2009) 'MEK1 mutations confer resistance to MEK and B-RAF inhibition.', *Proceedings of the National Academy of Sciences of the United States of America*, 106(48), pp. 20411–20416. doi: 10.1073/pnas.0905833106.

Fanjul-Fernández, M. *et al.* (2010) 'Matrix metalloproteinases: evolution, gene regulation and functional analysis in mouse models.', *Biochimica et biophysica acta*. Elsevier B.V., 1803(1), pp. 3–19. doi: 10.1016/j.bbamcr.2009.07.004.

Fedorenko, I. V *et al.* (2015) 'BRAF Inhibition Generates a Host-Tumor Niche that Mediates Therapeutic Escape.', *The Journal of investigative dermatology*. Nature Publishing Group, 135(12), pp. 3115–3124. doi: 10.1038/jid.2015.329.

Ferguson, J. *et al.* (2013) 'Combination of MEK and SRC inhibition suppresses melanoma cell growth and invasion.', *Oncogene*. Nature Publishing Group, 32(1), pp. 86–96. doi: 10.1038/onc.2012.25.

Gazzaniga, S. *et al.* (2007) 'Targeting tumor-associated macrophages and inhibition of MCP-1 reduce angiogenesis and tumor growth in a human melanoma xenograft.', *The Journal of investigative dermatology*, 127(8), pp. 2031–41. doi: 10.1038/sj.jid.5700827.

Gonzalez-Cao, M. *et al.* (2015) 'BRAF mutation analysis in circulating free tumor DNA of melanoma patients treated with BRAF inhibitors.', *Melanoma research*, 25(6), pp. 486–95. doi: 10.1097/CMR.0000000000000187.

Guan, X. *et al.* (2017) 'Stromal Senescence By Prolonged CDK4/6 Inhibition Potentiates Tumor Growth.', *Molecular cancer research : MCR*, 15(3), pp. 237–249. doi: 10.1158/1541-7786.MCR-16-0319.

Guo, X., Xu, Y. and Zhao, Z. (2015) 'In-depth genomic data analyses revealed complex transcriptional and epigenetic dysregulations of BRAFV600E in melanoma.', *Molecular cancer*, 14, p. 60. doi: 10.1186/s12943-015-0328-y.

Haferkamp, S. *et al.* (2013) 'Vemurafenib induces senescence features in melanoma cells.', *The Journal of investigative dermatology*, 133(6), pp. 1601–9. doi: 10.1038/jid.2013.6.

Hasegawa, Y. *et al.* (2014) 'CCL2 enhances pluripotency of human induced pluripotent stem

cells by activating hypoxia related genes.', *Scientific reports*, 4, p. 5228. doi: 10.1038/srep05228.

Hatzivassiliou, G. *et al.* (2010) 'RAF inhibitors prime wild-type RAF to activate the MAPK pathway and enhance growth.', *Nature*. Nature Publishing Group, 464(7287), pp. 431–5. doi: 10.1038/nature08833.

Hauschild, A. *et al.* (2009) 'Results of a phase III, randomized, placebo-controlled study of sorafenib in combination with carboplatin and paclitaxel as second-line treatment in patients with unresectable stage III or stage IV melanoma', *Journal of Clinical Oncology*, 27(17), pp. 2823–2830. doi: 10.1200/JCO.2007.15.7636.

Hauschild, A. *et al.* (2012) 'Dabrafenib in BRAF-mutated metastatic melanoma: a multicentre, open-label, phase 3 randomised controlled trial.', *Lancet (London, England)*, 380(9839), pp. 358–65. doi: 10.1016/S0140-6736(12)60868-X.

Haydn, J. M. *et al.* (2014) 'The MAPK pathway as an apoptosis enhancer in melanoma.', *Oncotarget*, 5(13), pp. 5040–53. doi: 10.18632/oncotarget.2079.

HAYFLICK, L. and MOORHEAD, P. S. (1961) 'The serial cultivation of human diploid cell strains.', *Experimental cell research*, 25, pp. 585–621. Available at: http://www.ncbi.nlm.nih.gov/pubmed/13905658.

Heidorn, S. J. *et al.* (2010) 'Kinase-Dead BRAF and Oncogenic RAS Cooperate to Drive Tumor Progression through CRAF', *Cell*. Elsevier Ltd, 140(2), pp. 209–221. doi: 10.1016/j.cell.2009.12.040.

Hermeking, H. (2010) 'The miR-34 family in cancer and apoptosis.', *Cell death and differentiation*. Nature Publishing Group, 17(2), pp. 193–9. doi: 10.1038/cdd.2009.56.

Hwa, V., Oh, Y. and Rosenfeld, R. G. (1999) 'The insulin-like growth factor-binding protein (IGFBP) superfamily.', *Endocrine reviews*, 20(6), pp. 761–87. doi: 10.1210/edrv.20.6.0382.

Ikediobi, O. N. *et al.* (2006) 'Mutation analysis of 24 known cancer genes in the NCI-60 cell line set.', *Molecular cancer therapeutics*, 5(11), pp. 2606–12. doi: 10.1158/1535-7163.MCT-06-0433.

Imamura, T. *et al.* (1990) 'Recovery of mitogenic activity of a growth factor mutant with a nuclear translocation sequence.', *Science (New York, N.Y.)*, 249(4976), pp. 1567–70. Available at: http://www.ncbi.nlm.nih.gov/pubmed/1699274.

Ji, Q. *et al.* (2009) 'MicroRNA miR-34 inhibits human pancreatic cancer tumor-initiating cells.', *PloS one*, 4(8), p. e6816. doi: 10.1371/journal.pone.0006816.

Jiao, Y. *et al.* (2012) 'Matrix metalloproteinase-2 promotes αvβ3 integrin-mediated adhesion and migration of human melanoma cells by cleaving fibronectin.', *PloS one*, 7(7), p. e41591. doi: 10.1371/journal.pone.0041591.

Johnson, D. B. and Puzanov, I. (2015) 'Treatment of NRAS-mutant melanoma.', *Current treatment options in oncology*, 16(4), p. 15. doi: 10.1007/s11864-015-0330-z.

Kacer, D. *et al.* (2011) 'Regulation of non-classical FGF1 release and FGF-dependent cell transformation by CBF1-mediated notch signaling.', *Journal of cellular physiology*, 226(11), pp. 3064–75. doi: 10.1002/jcp.22663.

Kuilman, T. and Peeper, D. S. (2009) 'Senescence-messaging secretome: SMS-ing cellular stress.', *Nature reviews. Cancer*, 9(2), pp. 81–94. doi: 10.1038/nrc2560.

Kwong, L. N. and Davies, M. a. (2013) 'Navigating the therapeutic complexity of PI3K pathway inhibition in melanoma.', *Clinical cancer research : an official journal of the American Association for Cancer Research*, 19(19), pp. 5310–9. doi: 10.1158/1078-0432.CCR-13-0142.

Lawrence, M. S. *et al.* (2013) 'Mutational heterogeneity in cancer and the search for new cancer-associated genes.', *Nature*, 499(7457), pp. 214–218. doi: 10.1038/nature12213.

Lebrecht, A. *et al.* (2004) 'Monocyte chemoattractant protein-1 serum levels in patients with breast cancer.', *Tumour biology : the journal of the International Society for Oncodevelopmental Biology and Medicine*, 25(1–2), pp. 14–7. doi: 10.1159/000077718.

Lee, B. Y. *et al.* (2006) 'Senescence-associated beta-galactosidase is lysosomal beta-galactosidase.', *Aging cell*, 5(2), pp. 187–95. doi: 10.1111/j.1474-9726.2006.00199.x.

Leight, J. L. *et al.* (2015) 'Multifunctional bioscaffolds for 3D culture of melanoma cells reveal increased MMP activity and migration with BRAF kinase inhibition.', *Proceedings of the National Academy of Sciences of the United States of America*, 112(17), pp. 5366–71. doi: 10.1073/pnas.1505662112.

Leikam, C. *et al.* (2014) 'Cystathionase mediates senescence evasion in melanocytes and melanoma cells.', *Oncogene*, 33(6), pp. 771–82. doi: 10.1038/onc.2012.641.

Leikam, C. *et al.* (2015) 'In vitro evidence for senescent multinucleated melanocytes as a source for tumor-initiating cells.', *Cell death & disease*, 6(4), p. e1711. doi: 10.1038/cddis.2015.71.

Leontieva, O. V., Demidenko, Z. N. and Blagosklonny, M. V. (2013) 'S6K in geroconversion.', *Cell cycle (Georgetown, Tex.)*, 12(20), pp. 3249–52. doi: 10.4161/cc.26248.

Leontieva, O. V, Demidenko, Z. N. and Blagosklonny, M. V (2015) 'Dual mTORC1/C2 inhibitors suppress cellular geroconversion (a senescence program).', *Oncotarget*, 6(27), pp. 23238–48. doi: 10.18632/oncotarget.4836.

Li, A. *et al.* (2012) 'Activated mutant NRas(Q61K) drives aberrant melanocyte signaling, survival, and invasiveness via a Rac1-dependent mechanism.', *The Journal of investigative dermatology*. Nature Publishing Group, 132(11), pp. 2610–21. doi: 10.1038/jid.2012.186.

Li, J. *et al.* (2015) 'Clinicopathological significance of fibroblast growth factor 1 in non-small cell lung cancer.', *Human pathology*, 46(12), pp. 1821–8. doi: 10.1016/j.humpath.2015.07.022.

Li, M. *et al.* (2013) 'A role for CCL2 in both tumor progression and immunosurveillance.', *Oncoimmunology*, 2(7), p. e25474. doi: 10.4161/onci.25474.

Linos, E. *et al.* (2009) 'Increasing burden of melanoma in the United States.', *The Journal of investigative dermatology*. Nature Publishing Group, 129(7), pp. 1666–74. doi: 10.1038/jid.2008.423.

Lito, P. *et al.* (2012) 'Relief of profound feedback inhibition of mitogenic signaling by RAF inhibitors attenuates their activity in BRAFV600E melanomas.', *Cancer cell*. Elsevier, 22(5), pp. 668–82. doi: 10.1016/j.ccr.2012.10.009.

Liu, J. *et al.* (2014) 'Developmental pathways activated in melanocytes and melanoma.', *Archives of biochemistry and biophysics*. Elsevier Inc., 563, pp. 13–21. doi: 10.1016/j.abb.2014.07.023.

Liu, J. J. and Fisher, D. E. (2010) 'Lighting a path to pigmentation: mechanisms of MITF induction by UV.', *Pigment cell & melanoma research*, 23(6), pp. 741–5. doi: 10.1111/j.1755-148X.2010.00775.x.

Liu, P. *et al.* (2009) 'Targeting the phosphoinositide 3-kinase pathway in cancer.', *Nature reviews. Drug discovery*, 8(8), pp. 627–44. doi: 10.1038/nrd2926.

Loberg, R. D. *et al.* (2007) 'CCL2 as an important mediator of prostate cancer growth in vivo through the regulation of macrophage infiltration.', *Neoplasia (New York, N.Y.)*, 9(7), pp. 556–62. doi: 10.1593/neo.07307.

Lodygin, D. *et al.* (2008) 'Inactivation of miR-34a by aberrant CpG methylation in multiple types of cancer.', *Cell cycle (Georgetown, Tex.)*, 7(16), pp. 2591–600. doi: 10.4161/cc.7.16.6533.

Lopez-Bergami, P. (2011) 'The role of mitogen- and stress-activated protein kinase pathways in melanoma.', *Pigment cell & melanoma research*, 24(5), pp. 902–21. doi: 10.1111/j.1755-148X.2011.00908.x.

Macaulay, V. M. *et al.* (2013) 'Phase I study of humanized monoclonal antibody AVE1642 directed against the type 1 insulin-like growth factor receptor (IGF-1R), administered in combination with anticancer therapies to patients with advanced solid tumors.', *Annals of oncology : official journal of the European Society for Medical Oncology*, 24(3), pp. 784–91. doi: 10.1093/annonc/mds511.

Massacesi, C. *et al.* (2016) 'PI3K inhibitors as new cancer therapeutics: implications for clinical trial design.', *OncoTargets and therapy*, 9, pp. 203–10. doi: 10.2147/OTT.S89967.

Mayor, R. and Theveneau, E. (2013) 'The neural crest', *Development*, 140(11), pp. 2247–2251. doi: 10.1242/dev.091751.

McArthur, G. A. *et al.* (2014) 'Safety and efficacy of vemurafenib in BRAF(V600E) and BRAF(V600K) mutation-positive melanoma (BRIM-3): extended follow-up of a phase 3, randomised, open-label study.', *The Lancet. Oncology*, 15(3), pp. 323–32. doi: 10.1016/S1470-2045(14)70012-9.

McCubrey, J. A. *et al.* (2012) 'Mutations and deregulation of Ras/Raf/MEK/ERK and PI3K/PTEN/Akt/mTOR cascades which alter therapy response.', *Oncotarget*, 3(9), pp. 954–87. doi: 10.18632/oncotarget.652.

Metzner, T. *et al.* (2011) 'Fibroblast growth factor receptors as therapeutic targets in human melanoma: synergism with BRAF inhibition.', *The Journal of investigative dermatology*, 131(10), pp. 2087–95. doi: 10.1038/jid.2011.177.

Michaloglou, C. *et al.* (2005) 'BRAFE600-associated senescence-like cell cycle arrest of human naevi.', *Nature*, 436(7051), pp. 720–4. doi: 10.1038/nature03890.

Mizutani, K. *et al.* (2009) 'The chemokine CCL2 increases prostate tumor growth and bone metastasis through macrophage and osteoclast recruitment.', *Neoplasia (New York, N.Y.)*, 11(11), pp. 1235–42. doi: 10.1593/neo.09988.

Mo, J. *et al.* (2013) 'Hypoxia-induced senescence contributes to the regulation of microenvironment in melanomas.', *Pathology, research and practice*. Elsevier GmbH., 209(10), pp. 640–7. doi: 10.1016/j.prp.2013.07.004.

Möhler, H., Pfirrmann, R. W. and Frei, K. (2014) 'Redox-directed cancer therapeutics: Taurolidine and Piperlongumine as broadly effective antineoplastic agents (review).', *International journal of oncology*, 45(4), pp. 1329–36. doi: 10.3892/ijo.2014.2566.

Mori, S. *et al.* (2015) 'Enhanced Expression of Integrin αvβ3 Induced by TGF-β Is Required for the Enhancing Effect of Fibroblast Growth Factor 1 (FGF1) in TGF-β-Induced Epithelial-Mesenchymal Transition (EMT) in Mammary Epithelial Cells.', *PloS one*, 10(9), p. e0137486. doi: 10.1371/journal.pone.0137486.

Mort, R. L., Jackson, I. J. and Patton, E. E. (2015) 'The melanocyte lineage in development and disease.', *Development (Cambridge, England)*, 142(7), p. 1387. doi: 10.1242/dev.123729.

Naspi, A. *et al.* (2014) 'Insulin-like-growth-factor-binding-protein-3 (IGFBP-3) contrasts melanoma progression in vitro and in vivo.', *PloS one*, 9(6), p. e98641. doi: 10.1371/journal.pone.0098641.

Nazarian, R. *et al.* (2010) 'Melanomas acquire resistance to B-RAF(V600E) inhibition by RTK or N-RAS upregulation.', *Nature*, 468(7326), pp. 973–7. doi: 10.1038/nature09626.

Niault, T. S. and Baccarini, M. (2010) 'Targets of Raf in tumorigenesis.', *Carcinogenesis*, 31(7), pp. 1165–74. doi: 10.1093/carcin/bgp337.

Nies, V. J. M. *et al.* (2015) 'Fibroblast Growth Factor Signaling in Metabolic Regulation.', *Frontiers in endocrinology*, 6(January), p. 193. doi: 10.3389/fendo.2015.00193.

Obenauf, A. C. *et al.* (2015) 'Therapy-induced tumour secretomes promote resistance and tumour progression.', *Nature*, 520(7547), pp. 368–72. doi: 10.1038/nature14336.

Ohanna, M. *et al.* (2011) 'Senescent cells develop a PARP-1 and nuclear factor-{kappa}B-associated secretome (PNAS).', *Genes & development*, 25(12), pp. 1245–61. doi: 10.1101/gad.625811.

Ohtani, N. *et al.* (2012) 'Cellular senescence: a double-edged sword in the fight against cancer.', *Experimental dermatology*, 21 Suppl 1, pp. 1–4. doi: 10.1111/j.1600-0625.2012.01493.x.

Palmer, J. S. *et al.* (2000) 'Melanocortin-1 receptor polymorphisms and risk of melanoma: is the association explained solely by pigmentation phenotype?', *American journal of human genetics*, 66(1), pp. 176–86. doi: 10.1086/302711.

Pang, R. T. K. *et al.* (2010) 'MicroRNA-34a suppresses invasion through downregulation of Notch1 and Jagged1 in cervical carcinoma and choriocarcinoma cells.', *Carcinogenesis*, 31(6), pp. 1037–44. doi: 10.1093/carcin/bgq066.

Pani, G. (2011) 'From growing to secreting: new roles for mTOR in aging cells.', *Cell cycle (Georgetown, Tex.)*, 10(15), pp. 2450–3. doi: 10.4161/cc.10.15.16886.

Pappalardo, F. *et al.* (2016) 'Computational Modeling of PI3K/AKT and MAPK Signaling Pathways in Melanoma Cancer.', *PloS one*, 11(3), p. e0152104. doi: 10.1371/journal.pone.0152104.

Penna, I. *et al.* (2016) 'Primary cross-resistance to BRAFV600E-, MEK1/2- and PI3K/mTOR-specific inhibitors in BRAF-mutant melanoma cells counteracted by dual pathway blockade.', *Oncotarget*, 7(4), pp. 3947–65. doi: 10.18632/oncotarget.6600.

Pollock, P. M. *et al.* (2003) 'High frequency of BRAF mutations in nevi.', *Nature genetics*, 33(1), pp. 19–20. doi: 10.1038/ng1054.

Pongas, G. and Fojo, T. (2016) 'BEZ235: When Promising Science Meets Clinical Reality.', *The oncologist*, 21(9), pp. 1033–4. doi: 10.1634/theoncologist.2016-0243.

Poulikakos, P. I. *et al.* (2010) 'RAF inhibitors transactivate RAF dimers and ERK signalling in cells with wild-type BRAF.', *Nature.* Nature Publishing Group, 464(7287), pp. 427–30. doi: 10.1038/nature08902.

Prasad, C. P., Mohapatra, P. and Andersson, T. (2015) 'Therapy for BRAFi-Resistant Melanomas: Is WNT5A the Answer?', *Cancers*, 7(3), pp. 1900–24. doi: 10.3390/cancers7030868.

Prudovsky, I. *et al.* (2008) 'Secretion without Golgi.', *Journal of cellular biochemistry*, 103(5), pp. 1327–43. doi: 10.1002/jcb.21513.

Pytliak, M., Vargová, V. and Mechírová, V. (2012) 'Matrix metalloproteinases and their role in oncogenesis: a review.', *Onkologie*, 35(1–2), pp. 49–53. doi: 10.1159/000336304.

Qian, B.-Z. *et al.* (2011) 'CCL2 recruits inflammatory monocytes to facilitate breast-tumour metastasis.', *Nature*, 475(7355), pp. 222–5. doi: 10.1038/nature10138.

Raju, R. *et al.* (2014) 'A Network Map of FGF-1/FGFR Signaling System.', *Journal of signal*

transduction. Hindawi Publishing Corporation, 2014, p. 962962. doi: 10.1155/2014/962962.

Rodier, F. and Campisi, J. (2011) 'Four faces of cellular senescence.', *The Journal of cell biology*, 192(4), pp. 547–56. doi: 10.1083/jcb.201009094.

Rodriguez-Enfedaque, A. *et al.* (2009) 'FGF1 nuclear translocation is required for both its neurotrophic activity and its p53-dependent apoptosis protection.', *Biochimica et biophysica acta*. Elsevier B.V., 1793(11), pp. 1719–27. doi: 10.1016/j.bbamcr.2009.09.010.

Roelle, S. *et al.* (2003) 'Matrix metalloproteinases 2 and 9 mediate epidermal growth factor receptor transactivation by gonadotropin-releasing hormone.', *The Journal of biological chemistry*, 278(47), pp. 47307–18. doi: 10.1074/jbc.M304377200.

Saito, S. *et al.* (2015) 'The role of HGF/MET and FGF/FGFR in fibroblast-derived growth stimulation and lapatinib-resistance of esophageal squamous cell carcinoma.', *BMC cancer*, 15(1), p. 82. doi: 10.1186/s12885-015-1065-8.

Saka, H. *et al.* (2017) 'Safety, tolerability and pharmacokinetics of the fibroblast growth factor receptor inhibitor AZD4547 in Japanese patients with advanced solid tumours: a Phase I study.', *Investigational new drugs*, 35(4), pp. 451–462. doi: 10.1007/s10637-016-0416-x.

Schadendorf, D. and Hauschild, A. (2014) 'Melanoma in 2013: Melanoma--the run of success continues.', *Nature reviews. Clinical oncology*. Nature Publishing Group, a division of Macmillan Publishers Limited. All Rights Reserved., 11(2), pp. 75–6. doi: 10.1038/nrclinonc.2013.246.

Seip, K. *et al.* (2016) 'Fibroblast-induced switching to the mesenchymal-like phenotype and PI3K/mTOR signaling protects melanoma cells from BRAF inhibitors.', *Oncotarget*, 7(15), pp. 19997–20015. doi: 10.18632/oncotarget.7671.

Shi, H. *et al.* (2011) 'Combinatorial treatments that overcome PDGFRβ-driven resistance of melanoma cells to V600EB-RAF inhibition.', *Cancer research*, 71(15), pp. 5067–74. doi: 10.1158/0008-5472.CAN-11-0140.

Shi, H. *et al.* (2012) 'Melanoma whole-exome sequencing identifies (V600E)B-RAF amplification-mediated acquired B-RAF inhibitor resistance.', *Nature communications*. Nature Publishing Group, 3, p. 724. doi: 10.1038/ncomms1727.

Shi, H. *et al.* (2014) 'A novel AKT1 mutant amplifies an adaptive melanoma response to BRAF inhibition.', *Cancer discovery*, 4(1), pp. 69–79. doi: 10.1158/2159-8290.CD-13-0279.

Shtivelman, E. *et al.* (2014) 'Pathways and therapeutic targets in melanoma.', *Oncotarget*, 5(7), pp. 1701–52. doi: 10.18632/oncotarget.1892.

Shull, A. Y. *et al.* (2012) 'Novel somatic mutations to PI3K pathway genes in metastatic melanoma.', *PloS one*, 7(8), p. e43369. doi: 10.1371/journal.pone.0043369.

Sneyd, M. J. and Cox, B. (2009) 'Melanoma in Maori, Asian, and Pacific peoples in New Zealand.', *Cancer epidemiology, biomarkers & prevention : a publication of the American Association for Cancer Research, cosponsored by the American Society of Preventive Oncology*, 18(6), pp. 1706–13. doi: 10.1158/1055-9965.EPI-08-0682.

Sosman, J. A. *et al.* (2012) 'Survival in BRAF V600-mutant advanced melanoma treated with vemurafenib.', *The New England journal of medicine*, 366(8), pp. 707–14. doi: 10.1056/NEJMoa1112302.

Straussman, R. *et al.* (2012) 'Tumour micro-environment elicits innate resistance to RAF inhibitors through HGF secretion.', *Nature*. Nature Publishing Group, 487(7408), pp. 500–4. doi: 10.1038/nature11183.

Su, F. *et al.* (2012) 'RAS mutations in cutaneous squamous-cell carcinomas in patients treated with BRAF inhibitors.', *The New England journal of medicine*, 366(3), pp. 207–15.

doi: 10.1056/NEJMoa1105358.

Sumimoto, H. *et al.* (2004) 'Inhibition of growth and invasive ability of melanoma by inactivation of mutated BRAF with lentivirus-mediated RNA interference.', *Oncogene*, 23(36), pp. 6031–9. doi: 10.1038/sj.onc.1207812.

Sun, C. *et al.* (2014) 'Reversible and adaptive resistance to BRAF(V600E) inhibition in melanoma.', *Nature*. Nature Publishing Group, 508(7494), pp. 118–22. doi: 10.1038/nature13121.

Szade, A. *et al.* (2015) 'Cellular and molecular mechanisms of inflammation-induced angiogenesis.', *IUBMB life*, 67(3), pp. 145–59. doi: 10.1002/iub.1358.

Takata, M., Murata, H. and Saida, T. (2010) 'Molecular pathogenesis of malignant melanoma: a different perspective from the studies of melanocytic nevus and acral melanoma.', *Pigment cell & melanoma research*, 23(1), pp. 64–71. doi: 10.1111/j.1755-148X.2009.00645.x.

Tazawa, H. *et al.* (2007) 'Tumor-suppressive miR-34a induces senescence-like growth arrest through modulation of the E2F pathway in human colon cancer cells.', *Proceedings of the National Academy of Sciences of the United States of America*, 104(39), pp. 15472–7. doi: 10.1073/pnas.0707351104.

Tepper, S. R. *et al.* (2016) 'Growth factor expression mediates resistance to EGFR inhibitors in head and neck squamous cell carcinomas.', *Oral oncology*, 56, pp. 62–70. doi: 10.1016/j.oraloncology.2016.03.008.

Thompson, G. a, Datko, a H. and Mudd, S. H. (1982) 'Methionine Synthesis in Lemna: Inhibition of Cystathionine gamma-Synthase by Propargylglycine.', *Plant physiology*, 70(5), pp. 1347–52. doi: 10.1104/pp.70.5.1347.

Tomimatsu, K. and Narita, M. (2015) 'Translating the effects of mTOR on secretory senescence.', *Nature cell biology*. Nature Publishing Group, 17(10), pp. 1230–2. doi: 10.1038/ncb3244.

Tran, K. A. *et al.* (2016) 'MEK inhibitors and their potential in the treatment of advanced melanoma: the advantages of combination therapy.', *Drug design, development and therapy*, 10, pp. 43–52. doi: 10.2147/DDDT.S93545.

Turke, A. B. *et al.* (2012) 'MEK inhibition leads to PI3K/AKT activation by relieving a negative feedback on ERBB receptors.', *Cancer research*, 72(13), pp. 3228–37. doi: 10.1158/0008-5472.CAN-11-3747.

Tuveson, D. A., Weber, B. L. and Herlyn, M. (2003) 'BRAF as a potential therapeutic target in melanoma and other malignancies.', *Cancer cell*, 4(2), pp. 95–8. Available at: http://www.ncbi.nlm.nih.gov/pubmed/12957284.

Vergani, E. *et al.* (2016) 'Overcoming melanoma resistance to vemurafenib by targeting CCL2-induced miR-34a, miR-100 and miR-125b.', *Oncotarget*, 7(4), pp. 4428–41. doi: 10.18632/oncotarget.6599.

Villanueva, J. *et al.* (2010) 'Acquired resistance to BRAF inhibitors mediated by a RAF kinase switch in melanoma can be overcome by cotargeting MEK and IGF-1R/PI3K.', *Cancer cell*. Elsevier Inc., 18(6), pp. 683–95. doi: 10.1016/j.ccr.2010.11.023.

de Vries, E. and Coebergh, J. W. (2004) 'Cutaneous malignant melanoma in Europe.', *European journal of cancer (Oxford, England : 1990)*, 40(16), pp. 2355–66. doi: 10.1016/j.ejca.2004.06.003.

Vultur, A. and Herlyn, M. (2013) 'SnapShot: melanoma.', *Cancer cell*. Elsevier, 23(5), p. 706–706.e1. doi: 10.1016/j.ccr.2013.05.001.

Wagle, N. *et al.* (2011) 'Dissecting therapeutic resistance to RAF inhibition in melanoma by tumor genomic profiling.', *Journal of clinical oncology : official journal of the American Society of Clinical Oncology*, 29(22), pp. 3085–96. doi: 10.1200/JCO.2010.33.2312.

Wan, P. T. C. *et al.* (2004) 'Mechanism of activation of the RAF-ERK signaling pathway by oncogenic mutations of B-RAF.', *Cell,* 116(6), pp. 855–67. doi: 10.1016/S0092-8674(04)00215-6.

Wei, X. X. *et al.* (2017) 'A Phase I Study of Abiraterone Acetate Combined with BEZ235, a Dual PI3K/mTOR Inhibitor, in Metastatic Castration Resistant Prostate Cancer.', *The oncologist*, 22(5), pp. 503-e43. doi: 10.1634/theoncologist.2016-0432.

Wellbrock, C. and Arozarena, I. (2015) 'Microphthalmia-associated transcription factor in melanoma development and MAP-kinase pathway targeted therapy.', *Pigment cell & melanoma research*, 28(4), pp. 390–406. doi: 10.1111/pcmr.12370.

Welsh, S. J. *et al.* (2016) 'Resistance to combination BRAF and MEK inhibition in metastatic melanoma: Where to next?', *European journal of cancer (Oxford, England : 1990)*, 62, pp. 76–85. doi: 10.1016/j.ejca.2016.04.005.

Wiedłocha, A. *et al.* (2005) 'Phosphorylation-regulated nucleocytoplasmic trafficking of internalized fibroblast growth factor-1.', *Molecular biology of the cell*, 16(2), pp. 794–810. doi: 10.1091/mbc.e04-05-0389.

Wilson, T. R. *et al.* (2012) 'Widespread potential for growth-factor-driven resistance to anticancer kinase inhibitors.', *Nature.* Nature Publishing Group, 487(7408), pp. 505–9. doi: 10.1038/nature11249.

Yadav, V. *et al.* (2012) 'Reactivation of Mitogen-activated Protein Kinase (MAPK) pathway by FGF Receptor 3 (FGFR3)/Ras mediates resistance to vemurafenib in human B-RAF V600E mutant melanoma', *Journal of Biological Chemistry*, 287(33), pp. 28087–28098. doi: 10.1074/jbc.M112.377218.

Youngs, S. J. *et al.* (1997) 'Chemokines induce migrational responses in human breast carcinoma cell lines.', *International journal of cancer*, 71(2), pp. 257–66. Available at: http://www.ncbi.nlm.nih.gov/pubmed/9139852.

Zentrum für Krebsregisterdaten (2019). Available at: http://www.krebsdaten.de/Krebs/DE/Content/Krebsarten/Melanom/melanom_node.html.

Zhang, D. *et al.* (2004) 'Dual regulation of MMP-2 expression by the type 1 insulin-like growth factor receptor: the phosphatidylinositol 3-kinase/Akt and Raf/ERK pathways transmit opposing signals.', *Journal of Biological Chemistry*, 279(19), pp. 19683–19690. doi: 10.1074/jbc.M313145200.

Zhang, T. *et al.* (2006) 'Migration of cytotoxic T lymphocytes toward melanoma cells in three-dimensional organotypic culture is dependent on CCL2 and CCR4.', *European journal of immunology*, 36(2), pp. 457–67. doi: 10.1002/eji.200526208.

Ziani, L. *et al.* (2017) 'Melanoma-associated fibroblasts decrease tumor cell susceptibility to NK cell-mediated killing through matrix-metalloproteinases secretion.', *Oncotarget*, 8(12), pp. 19780–19794. doi: 10.18632/oncotarget.15540.

8. Acknowledgments